SEISMIC ANALYSIS OF THE WESTBOUND LANES OF THE I-90 BRIDGES CROSSING MERCER SLOUGH

WA-RD 299.1

Final Technical Report
February 1994

Washington State Department of Transportation

Washington State Transportation Commission
Transit, Research, and Intermodal Planning (TRIP) Division
in cooperation with the U.S. Department of Transportation
Federal Highway Administration

TECHNICAL REPORT STANDARD TITLE PAGE

1. REPORT NO.	2. GOVERNMENT ACCESSION NO.	3. RECIPIENT'S CATALOG NO.
WA-RD 299.1		

4. TITLE AND SUBTITLE	5. REPORT DATE
Seismic Analysis of the Westbound Lanes of the I-90 Bridges Crossing Mercer Slough	February 1994
	6. PERFORMING ORGANIZATION CODE
7. AUTHOR(S)	8. PERFORMING ORGANIZATION REPORT NO.
Authors: David I. McLean and Ian B.S. Cannon	
9. PERFORMING ORGANIZATION NAME AND ADDRESS	10. WORK UNIT NO.
Washington State Transportation Center (TRAC) Civil and Environmental Engineering; Sloan Hall, Room 101 Washington State University Pullman, Washington 99164	11. CONTRACT OR GRANT NO. GC8720-11, Task 09
12. SPONSORING AGENCY NAME AND ADDRESS	13. TYPE OF REPORT AND PERIOD COVERED
Washington State Department of Transportation Transportation Building, MS 7370 Olympia, Washington 98504-7370	Final Technical Report
	14. SPONSORING AGENCY CODE

15. SUPPLEMENTARY NOTES

This study was conducted in cooperation with the U.S. Department of Transportation, Federal Highway Administration.

16. ABSTRACT

This study investigated the seismic response of the westbound lanes of I-90 crossing Mercer Slough. Mercer Slough is filled with a very soft, thick peat deposit. Both linear and nonlinear dynamic analyses were performed, including spectral analyses, linear time-history analyses and nonlinear time-history analyses. Variables considered in the analyses included different column and foundation stiffnesses, different seismic input, different simultaneous seismic input, and nonlinear joint behavior.

The response of the bridge was found to be extremely sensitive to seismic input and, to a lesser extent, foundation stiffness. Consideration of nonlinear effects tended to lessen the bridge response. The analyses also indicated that a long, loosely connected bridge, such as that crossing Mercer Slough, can be adequately analyzed using a fairly short section of the bridge.

All of the different analyses indicated that elements in the bridge would probably be close to or exceed their capacity during an earthquake. Problem areas which were identified included the inability of the expansion joints to sustain large relative displacements and the possible overloading of the columns in flexure.

17. KEY WORDS	18. DISTRIBUTION STATEMENT
Key words: Seismic responses, bridges, peat, dynamic analysis.	No restrictions. This document is available to the public through the National Technical Information Service, Springfield, VA 22616

19. SECURITY CLASSIF. (of this report)	20. SECURITY CLASSIF. (of this page)	21. NO. OF PAGES	22. PRICE
None	None	122	

Technical Report

Research Project GC 8720-11
Seismic Behavior of Structures in Soft Soils

SEISMIC ANALYSIS OF THE WESTBOUND LANES OF THE I-90 BRIDGES CROSSING MERCER SLOUGH

by

David I. McLean
Associate Professor

Ian B.S. Cannon
Graduate Student

Washington State Transportation Center (TRAC)
Department of Civil and Environmental Engineering
Washington State University
Pullman, Washington 99164-2910

Washington State Department of Transportation
Technical Monitors

Richard B. Stoddard
Bridge Engineer

Alan P. Kilian
Chief Geotechnical Engineer

Prepared for

Washington State Transportation Commission
Department of Transportation
and in cooperation with
U.S. Department of Transportation
Federal Highway Administration

February 1994

DISCLAIMER

The contents of this report reflect the views of the authors, who are responsible for the facts and the accuracy of the data presented herein. The contents do not necessarily reflect the official views or policies of the Washington State Transportation Commission, Department of Transportation, or the Federal Highway Administration. This report does not constitute a standard, specification, or regulation.

TABLE OF CONTENTS

Section Page

LIST OF FIGURES

SUMMARY

Interstate 90 crosses Mercer Slough near Bellevue, Washington. Mercer Slough is filled with a very soft, thick peat deposit. Very little is currently known about the dynamic behavior of such soils or the seismic response of bridges supported on peaty soils. Coordinated projects were initiated by the Washington State Department of Transportation to address both of these areas by examining the soil and foundation characteristics and by performing a structural evaluation of the bridges at Mercer Slough.

This study investigated the seismic response of the westbound lanes of I-90 crossing Mercer Slough. Both linear and nonlinear dynamic analyses were performed, including spectral analyses, linear time-history analyses and nonlinear time-history analyses. Variables considered in the analyses included different column and foundation stiffnesses, different seismic input, different simultaneous seismic input, and nonlinear joint behavior. The response of the bridge was found to be extremely sensitive to seismic input and, to a lesser extent, foundation stiffness. Consideration of nonlinear effects tended to lessen the bridge response. The analyses also indicated that a long, loosely connected bridge, such as that crossing Mercer Slough, can be adequately analyzed using a fairly short section of the bridge.

All of the different analyses indicated that elements in the bridge would probably be close to or exceed their capacity during an earthquake. Problem areas which were identified included the inability of the expansion joints to sustain large relative displacements and the possible overloading of the columns in flexure.

INTRODUCTION AND RESEARCH APPROACH

INTRODUCTION AND BACKGROUND

The Puget Sound area of Washington State is well known as a seismically active area that is likely to be subjected to both small and possibly very large earthquakes in the near future. The Washington State Department of Transportation (WSDOT) is responsible for a large number of critical bridge structures, some of which may be at risk during a major earthquake. Many of these bridges represent lifelines whose successful performance during and after earthquakes will be critical to rescue, repair and rehabilitation efforts.

Many bridges cross, and have foundations extending through, deposits of soft to very soft soils. Soft soils have been known to frequently amplify the effects of earthquake ground shaking while providing little resistance to lateral bridge movement. A number of bridges in Washington state cross extremely soft soils found in sloughs. Sloughs are generally filled to some depth with peat, an organic material in varying stages of decomposition. The recent failure of the Struve Slough bridge (1) in the 1989 Loma Prieta earthquake illustrated the potential vulnerability of pile-supported highway bridges crossing substantial peat deposits.

A site very similar to the Struve Slough is where Interstate 90 (I-90) crosses Mercer Slough in south Belleview, Washington, as shown in Figure 1. Mercer Slough is filled with a very soft, thick peat deposit. Previous research (2) has shown that the soft, peaty soils at this site provide little resistance to static lateral bridge movement. However, very little is currently known about the dynamic behavior of such soils or

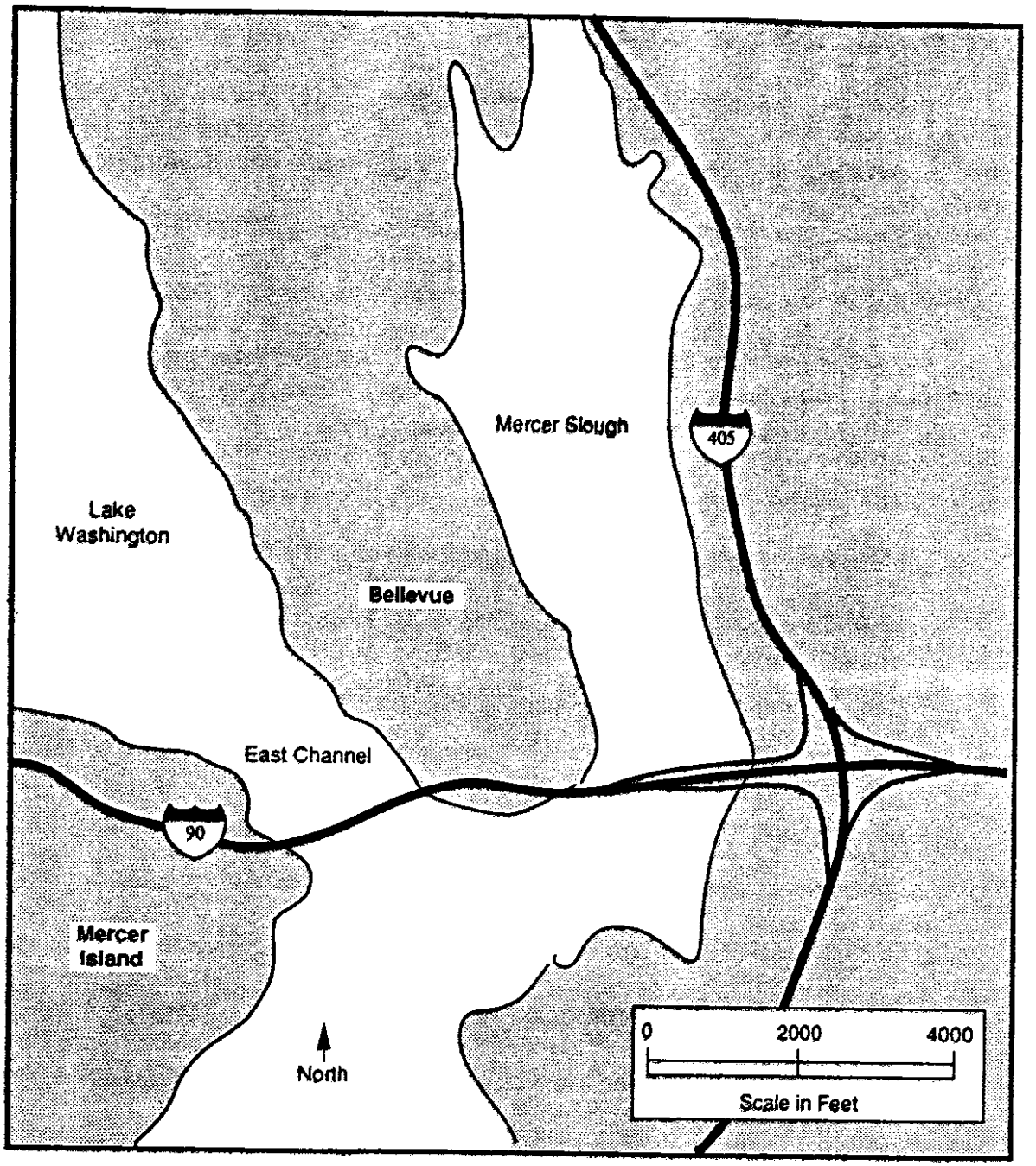

Figure 1. Location of Mercer Slough in Bellevue, Washington

the response of bridge structures supported on peaty soils during earthquakes. In response to these areas of lack of knowledge, and to develop seismic rehabilitation alternatives for bridges on peaty soils, the Washington State Department of Transportation initiated research to define the dynamic properties of peaty soil and to evaluate the seismic response of bridge structures supported on such soils.

RESEARCH OBJECTIVES

The objectives of this research were as follows:

1. to evaluate the dynamic properties of the peaty soils and to determine the anticipated ground response at the Mercer Slough site;
2. to evaluate the seismic behavior of the I-90 bridge foundations at Mercer Slough for the purpose of providing geotechnical input for structural analyses of the existing bridge structures;
3. to evaluate the adequacy of the existing bridge structures crossing Mercer Slough by performing detailed dynamic analyses, both linear and nonlinear; and
4. to identify the most vulnerable elements of the bridges in the event of a major earthquake and target possible retrofit measures for improving the seismic performance of the bridges.

The first two objectives were performed by Dr. Steven L. Kramer of the University of Washington in a related research effort and are documented in reference 3. The remaining two objectives define the scope of the research presented in this report.

DESCRIPTION OF THE BRIDGES

SITE CONDITIONS

Mercer Slough is a peat-filled extension of Lake Washington that covers several square miles in Bellevue, Washington. The surface of the slough is flat and heavily overgrown with horsetails, grasses and small trees. Lake Washington water levels are maintained at a nearly constant level at the Hiram Chittenden Locks in Seattle; consequently, the groundwater level in Mercer Slough is generally within 1 foot of the ground surface.

The thickness of the Mercer Slough peat is variable across the slough, with a maximum thickness of approximately 60 feet along the alignment of Interstate 90, which crosses Mercer Slough by means of four pile-supported bridge structures. The peat is underlain by very soft to medium stiff silty clay and occasional loose to dense sand, which is in turn underlain by heavily overconsolidated, dense glacial till. Tertiary bedrock in the area is about 1000 feet down. A subsurface profile of Mercer Slough along the I-90 alignment is shown in Figure 2.

From the figure, it can be seen that the soil profile varies across the site. Because of these variations, it can be expected that the surface seismic response would also vary across the site. Therefore, the site was broken into five sections, numbered from east to west, as shown in Figure 2. The assumed soil profiles for each section are also shown in Figure 2.

The response of each of the five different soil profiles was analyzed by Dr. Steven L. Kramer for three different earthquake input motions: Castaic, El Centro

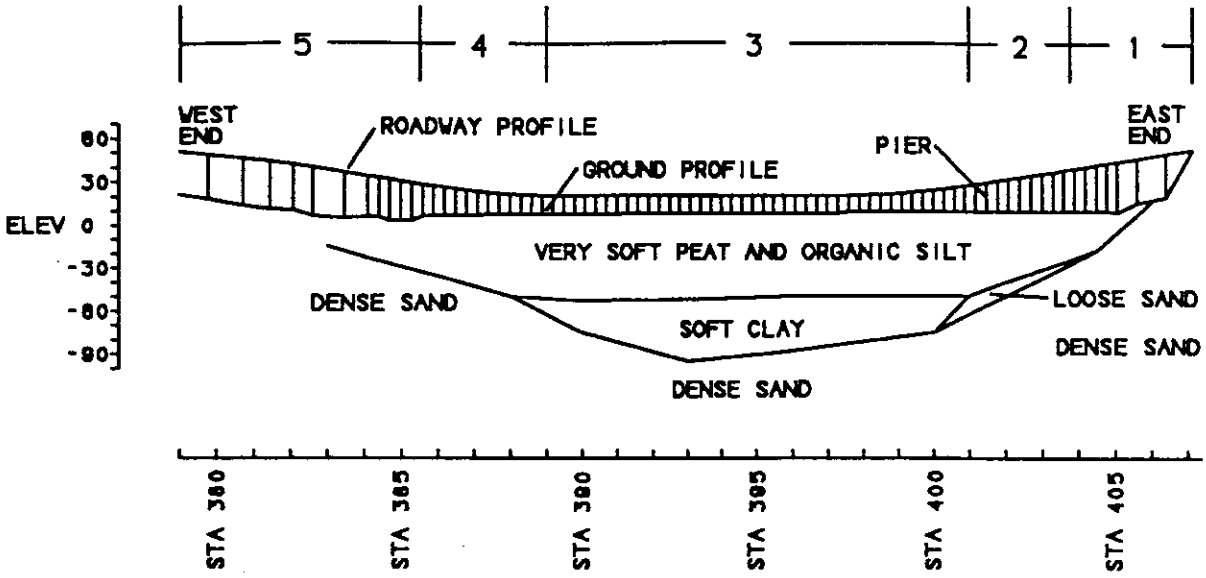

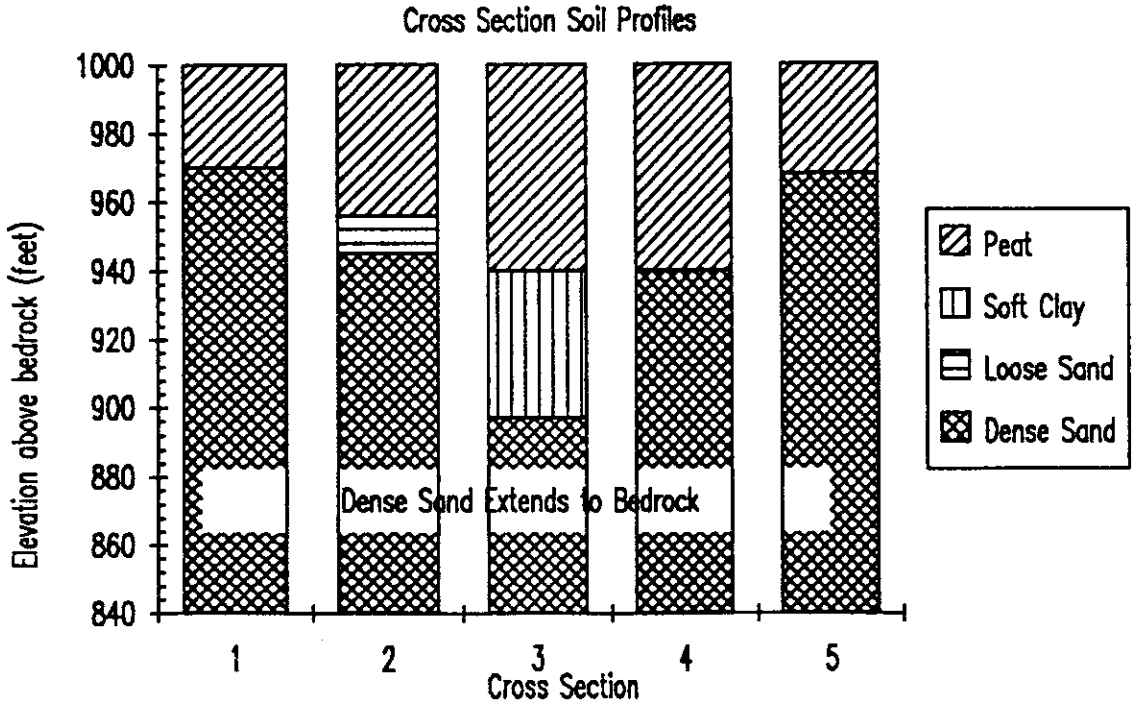

Figure 2 Profile of Mercer Slough and Assumed Soil Profiles

and Lake Hughes. Each input motion was scaled to a peak bedrock acceleration of 0.25g and a predominant period of 0.36 sec. These values correspond to the range of input motion that might be expected from a magnitude 7.5 earthquake with an epicenter near the Mercer Slough site. This level of shaking was determined in consultation with WSDOT personnel and is consistent with the criteria used for other important WSDOT structures in the area. A detailed description of the procedures used to determine the soil profile responses is given in reference (3). Acceleration time histories and acceleration response spectra for each of the five soil profiles for each of the three input motions are given in Appendix A. These soil responses were used as the input for the structural analyses portion of this research effort.

BRIDGE STRUCTURES

The bridge structures consist of two major roadways, one eastbound and one westbound, and several ancillary collectors and distributers, as shown in Figure 3. The westbound lanes (which are the darker lanes in the photograph) were originally constructed in the 1930's as part of the old US Highway 10. The rest of the bridge structures were constructed in the early 1970's as part of the Interstate 90 system. At the same time, the westbound bridge was widened to add an additional lane. The structural analyses focused on the westbound bridge as this structure is the oldest design and likely to be the most vulnerable in a seismic event.

Geometry

The westbound bridge consists of T-girders which are continuous over four

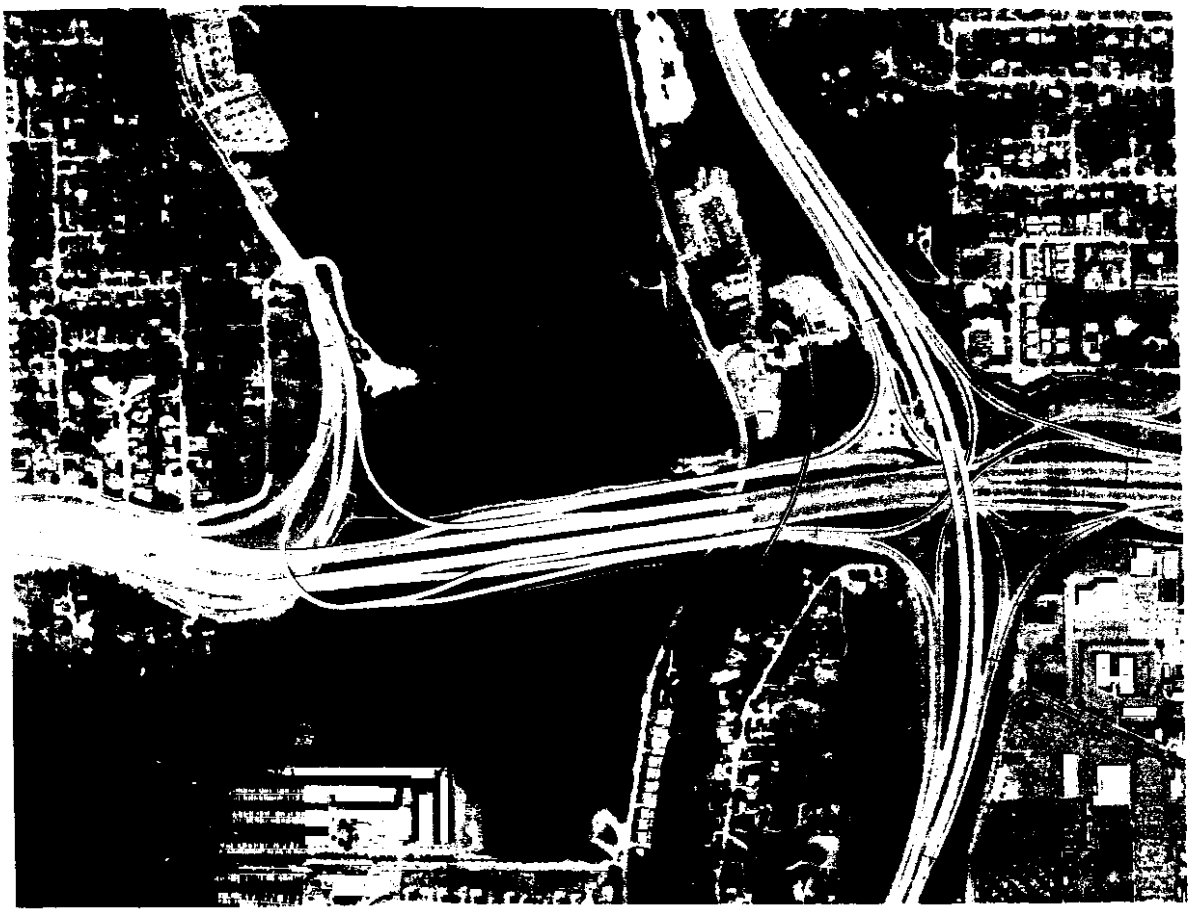

Figure 3. Aerial View of Bridges

spans. The length of the bridge is approximately 2800 feet and contains 85 spans. The spans are 30 feet long, except for the spans near each end of the bridge which are longer. There is an expansion joint at every fourth span. The bent caps are monolithic with the bridge superstructure except at the bents where there is an expansion joint. The bents typically consist of five square columns, each of which is supported on a concrete pile cap. The pile cap is supported on timber piles which were driven through the peaty soil to refusal at the dense layer below. The piles vary in length depending on soil profile, but are as long as 80 to 90 feet in places.

Spans

The spans are typically 30-feet long T-girders. Most of the spans are 60 feet wide. The spans have a 6-inch thick slab and nine 16-inch wide webs at approximately 7.5 feet centers. The section is typically 2 feet 9 inches deep from the bottom of the web to the top of the slab. The bent caps form diaphragms between the T-girder webs. Figure 4 shows the side elevation and cross-section of the typical span section.

Joints

There is typically a joint at every fourth bent. One span is connected to the bent cap, and the other span rests on top of a rocker, allowing for rotation around a vertical axis and for longitudinal joint translation. Figure 5 shows the expansion joint. The gap between the spans is approximately one inch. Over a sixty-foot width, this allows for only a small amount of rotation before adjacent spans contact each other. Further, the ledge and rocker dimensions limit the safe longitudinal

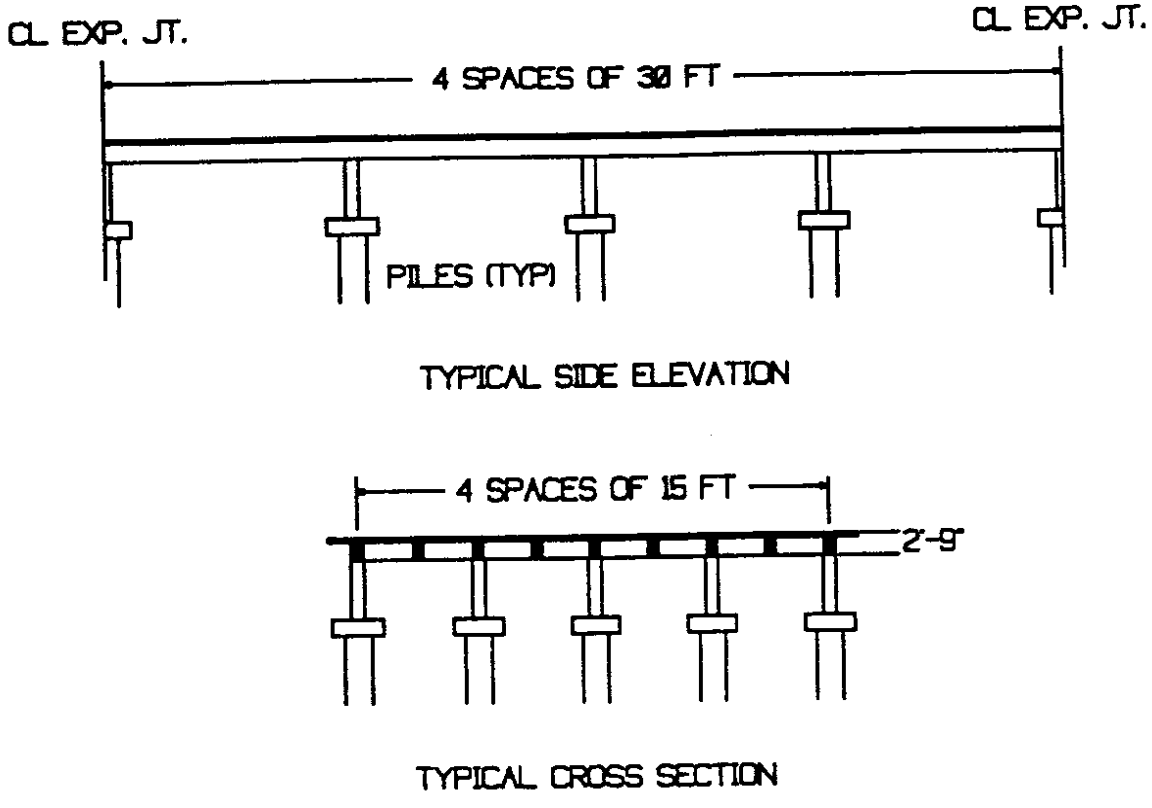

Figure 4. Bridge Elevation and Cross-section

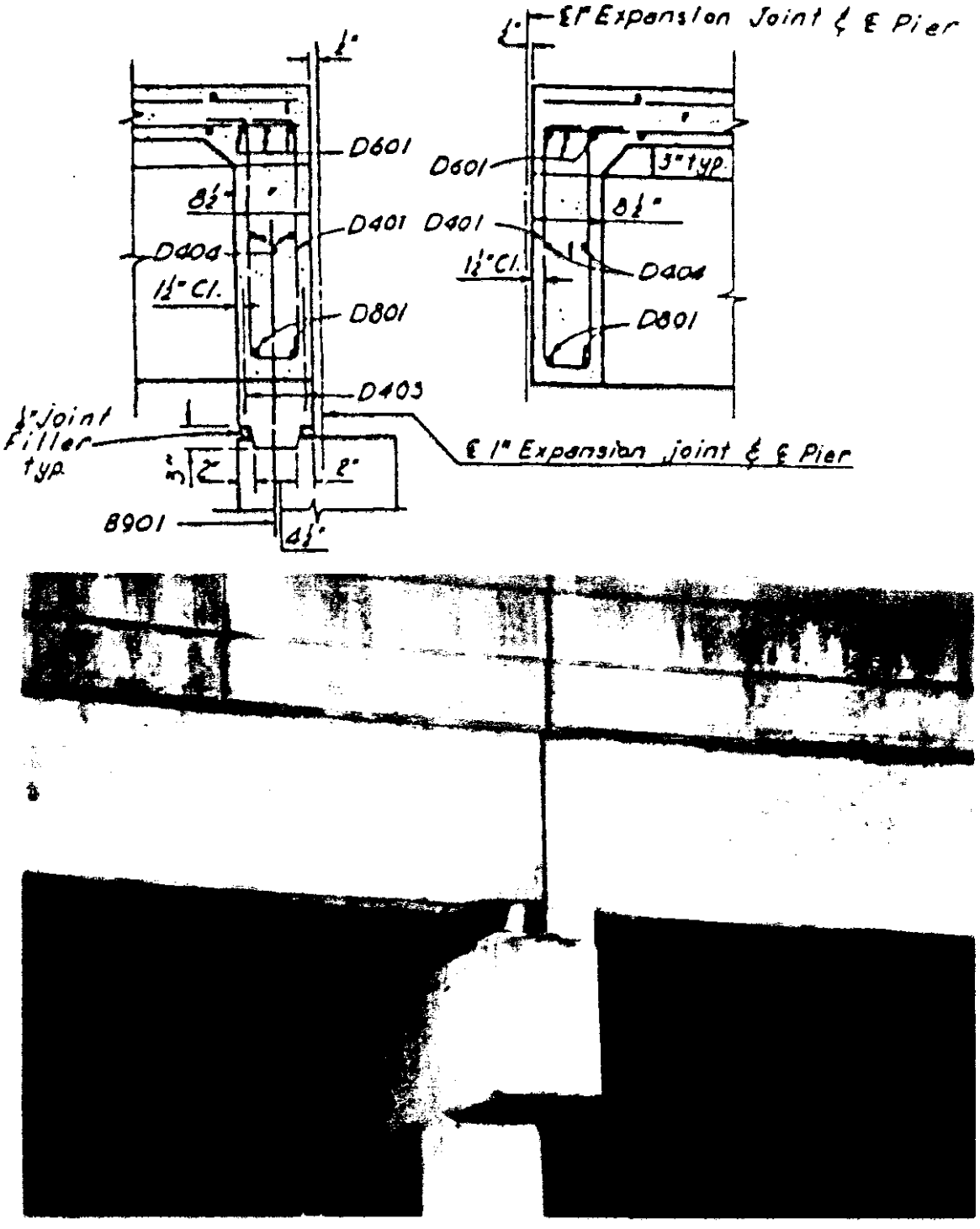

Figure 5. Bridge Expansion Joints

translation before a span may fall to approximately three inches.

Bents

A typical bent consists of five columns, each on a separate foundation. The columns are evenly spaced across the width of the bridge. The columns are monolithic with the bridge superstructure, tying directly into a transverse diaphragm in the T-girder system. The bents at the expansion joints are different in that the columns tie into a bent cap beam. The bents at the wider sections of the bridge are similar, except that they have more columns. The taller bents toward the ends of the bridge have a transverse beam at approximately mid-height of the columns. These mid-height beams were not modelled in the structural analyses.

Columns

The typical columns in the westbound bridge are square, 20 inches on a side, and contain eight No. 7 bars evenly spaced around the perimeter. The columns frame rigidly into both the foundation and the superstructure. The columns constructed for the widening of the westbound bridge contained No. 4 stirrups spaced at 12 inches on center. No details were obtained for the columns of the original bridge structure; however, typical detailing of columns at that time called for less transverse reinforcement. None of the columns in the westbound bridge have sufficient transverse reinforcement to allow for the formation of a ductile plastic hinge. If the moment capacity of the columns is exceeded, the column strength will degrade rapidly, and energy dissipation will be minimal. Figure 6 shows a cross-section and elevation of a typical column.

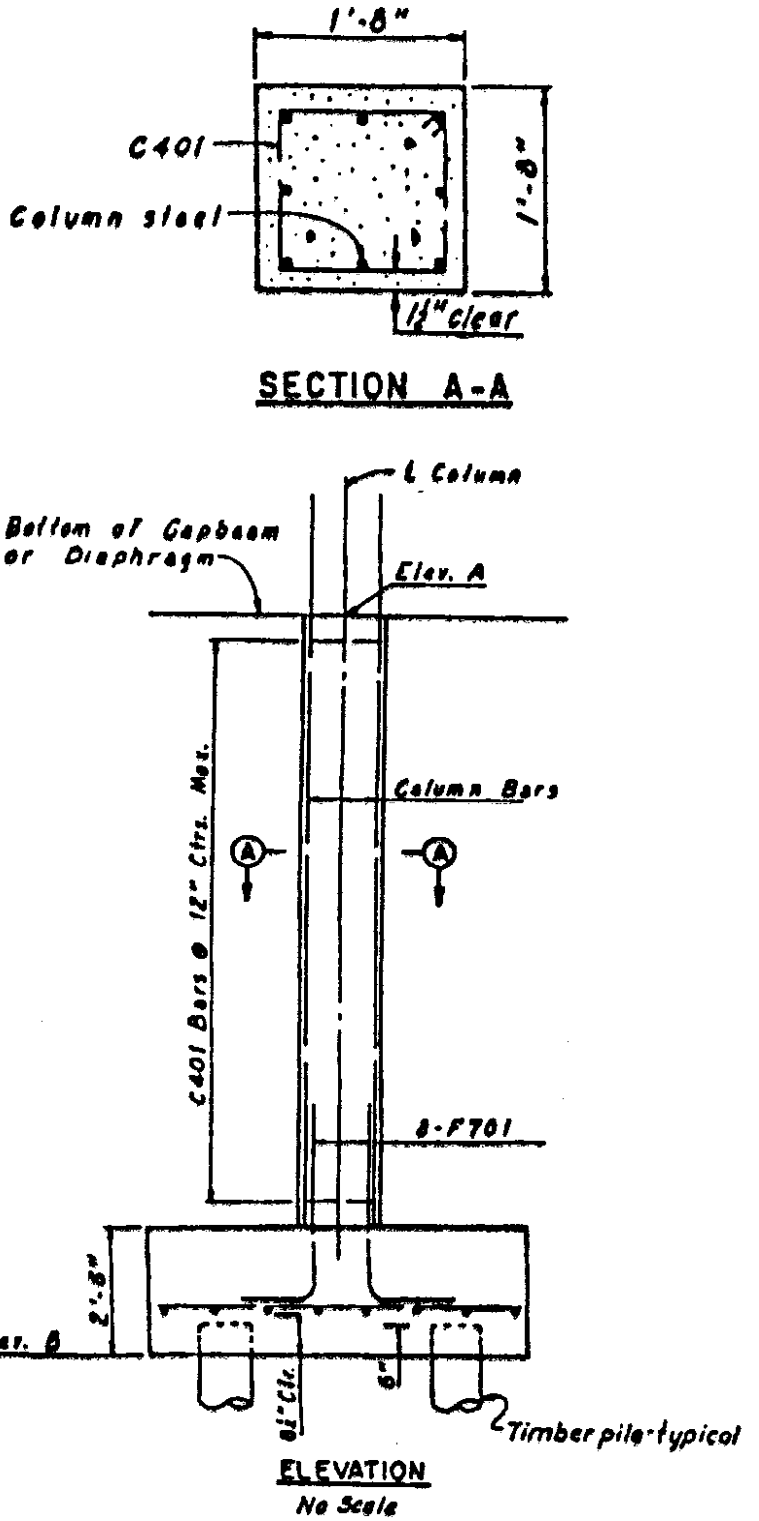

Figure 6. Typical Column Cross-section and Elevation

The column longitudinal reinforcement continues into the cap beam or diaphragm. At the bottom of the columns, the longitudinal reinforcement is lap spliced with reinforcement from the pile cap. Based on previous research (4), it is likely that the short splice length and lack of adequate confinement from transverse reinforcement will result in rapid strength degradation once the nominal moment strength of the columns is reached.

Figure 7 shows the nominal strength interaction curve for the typical column. The interaction curve is based upon expected in-situ material strengths of f 'c = 4500 psi and fy = 45,000 psi. No strength reduction factors were applied when developing the interaction curve. The average axial load due to gravity for a column in the westbound bridge is approximately 60 kips. While this value will change somewhat under seismic loading, it is unlikely that the columns would have a moment capacity exceeding 200 foot-kips.

Foundations

The columns of the westbound bridge are supported on concrete pile caps, which in turn are typically supported on four timber piles. Typical of the practice at the time of construction of this bridge, no mechanical connection is provided between the piles and the cap. Figure 8 shows a typical foundation layout. Reinforcement consists of eight No. 8 bars in each direction.

The pile stiffnesses used in the structural analyses were based on the lateral load tests on test piles at the Mercer Slough site performed by Kramer (2). The test

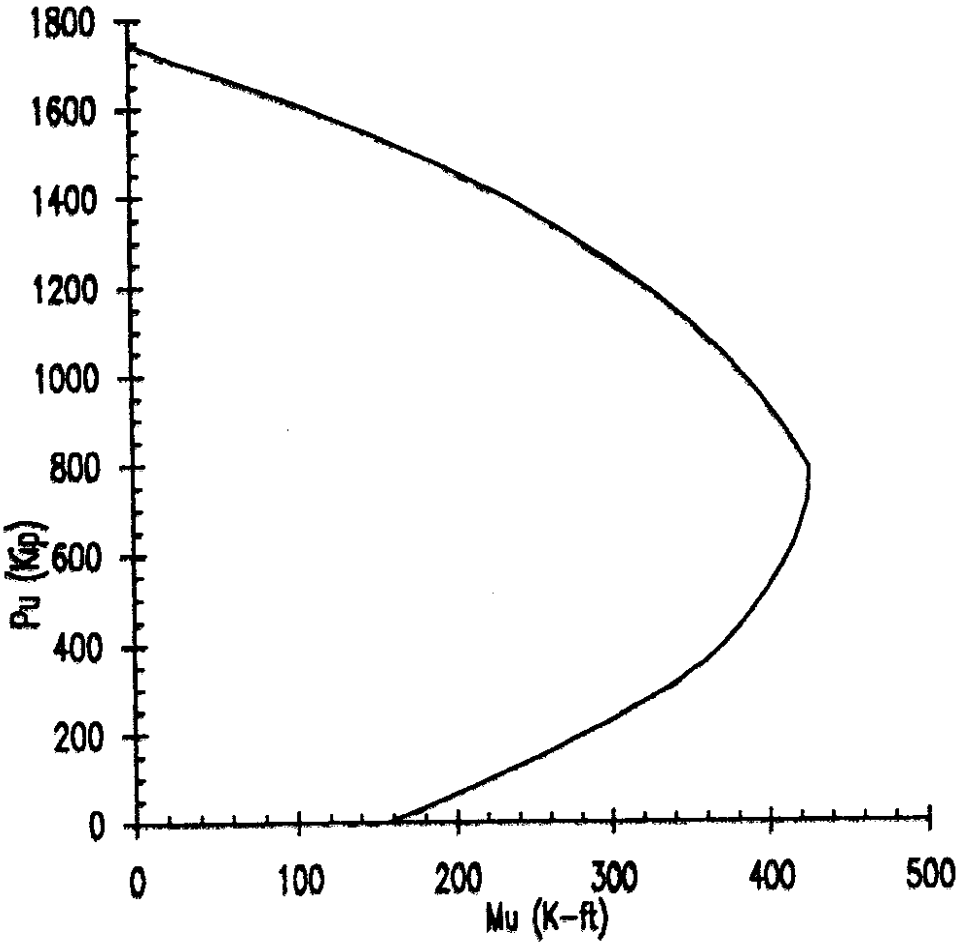

Figure 7. Typical Column Strength Interaction Curve

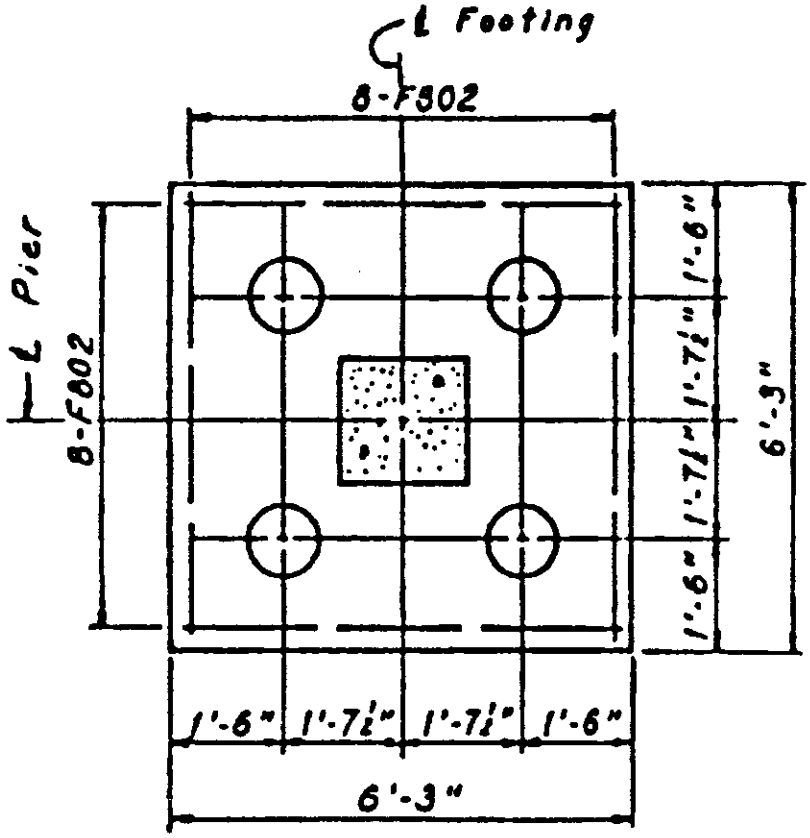

Figure 8. Typical Footing Plan

piles were eight-inch diameter steel pipe piles driven to a depth of approximately 40 feet. The test piles were loaded both statically and dynamically. Results from the static tests indicated a nonlinear load-deflection relationship. The dynamic tests (reported in reference 3) resulted in stiffnesses which varied with both load magnitude and frequency. The results of the dynamic pile tests were not incorporated into the structural analyses.

The pile stiffnesses used in the structural analyses were based on the results of the static pile tests. Load-deflection data from the static load tests of two test piles are shown in Figure 9. Based on the work of Scott (5), and in consultation with C.B. Crouse of Dames and Moore Inc., a lateral soil stiffness was developed. The lateral pile head stiffnesses were then determined based on the calculated lateral soil stiffness and the material properties and geometry of the piles supporting the westbound bridge. An average pile stiffness value of 24.6 kips/foot was calculated after consideration of different pile lengths and pile head fixities. In recognition of the inexactness used to determine this pile stiffness value, a lower stiffness value of 2/3 the average value and a higher stiffness value of 4/3 the average value were also considered in the structural analyses. These various pile stiffnesses are henceforth referred to as soft, intermediate and stiff piles. A vertical pile stiffness value was determined based on the elastic properties of the pile assuming end bearing only. No pile group effects were considered as the piles are spaced at more than three pile diameters center-to-center (Lam and Martin (6)).

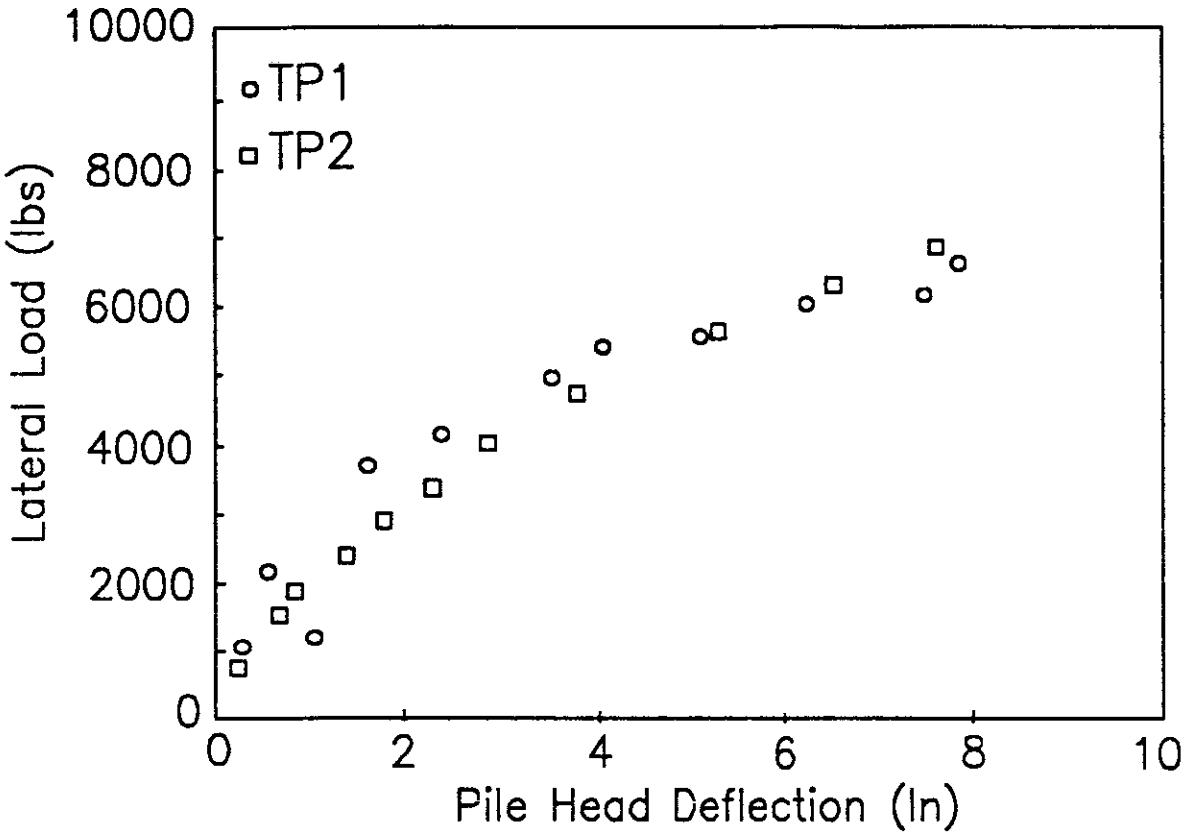

Figure 9. Static Loading Results of Test Piles

FINDINGS AND INTERPRETATION

LINEAR ANALYSES

Introduction

Linear dynamic structural analyses were performed on the westbound lanes of the I-90 bridges crossing Mercer Slough. Modal, spectral and time history analyses were performed. The linear analyses were used to investigate the effects on bridge response of column stiffness, foundation stiffness, soil profile, and seismic input.

Modelling

The bridge analysis program SEISAB, provided by Imbsen and Associates Inc., was used to perform the linear analyses. SEISAB is designed to facilitate the required input for the dynamic analysis of bridge structures. Bridges are modelled as stick figures using only beam-column elements, and mass is lumped at the nodes of the model. Several methods are provided for modelling piles, abutments and joints.

Piles

The piles of the bridge were modelled as a set of discrete springs, as shown in Figure 10. The axial stiffness was based on length, cross-sectional area, and modulus of elasticity assumed for the timber piles. Rotational stiffness for the pile head was calculated based on the rotational stiffness of piles treated as beam elements with the bottom ends fixed. The lateral stiffnesses were based on the experimental work of Kramer (2). Three values of stiffnesses were used: a most

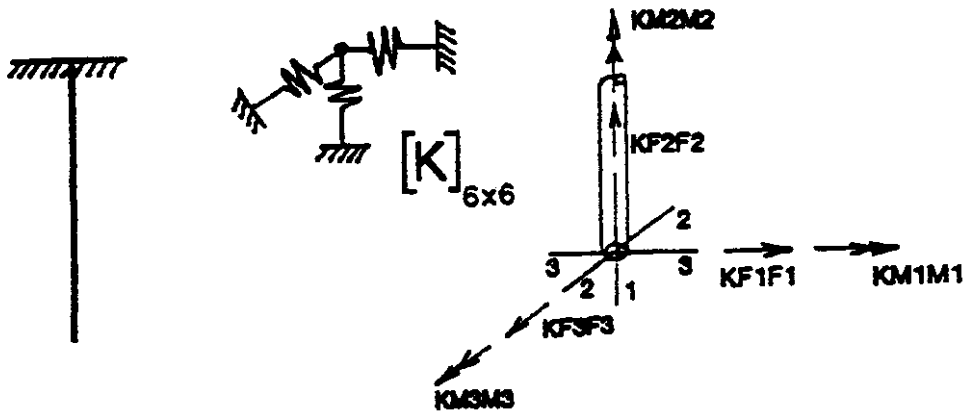

Seisab Pile Model

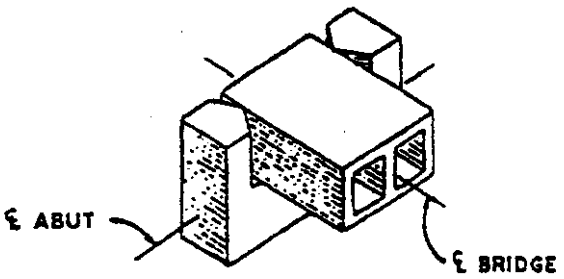

Seisab Abutment Model

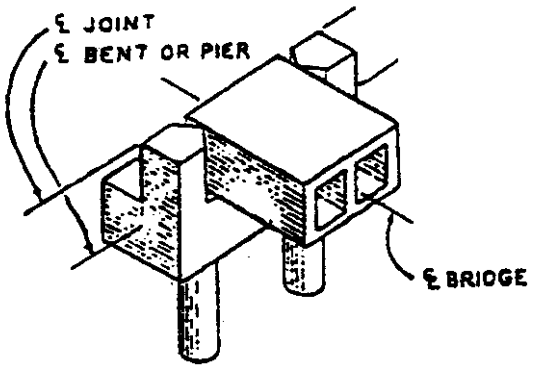

Seisab Joint Model

Figure 10. SEISAB Pile Model, Abutment Model and Joint Model Adapted from SEISAB User's Manual (7)

likely value of 24.6 kips/ft, and values which were one third higher and lower. There was, therefore, a factor of two difference between the lowest and highest stiffnesses. The piles were modelled as completely embedded, so there was no beam action above the soil surface.

Abutments

The abutments of the westbound bridge are designed to allow the bridge to move longitudinally, but to restrict transverse motion. Rotational motion is also allowed. Figure 10 depicts the idealization of the span-to-abutment connection used in SEISAB. With this model, the only restraint provided by the abutment is in the transverse direction.

Joints

The westbound bridge is typically divided into units of four continuous spans, with a rocker-type joint between each unit. The gap between adjacent sections at this joint is approximately one inch. Thus, there is some freedom of relative longitudinal motion at the joints. The rocker configuration allows some relative rotational motion about both the vertical and transverse axes of the joints. The only restraint is provided in the transverse direction. Figure 10 shows the computer idealization of the joints. The model does not incorporate the effects of closing of the joints, and subsequent contact of adjoining sections, that is likely in an earthquake. This change in joint status is a nonlinear effect and cannot be considered in SEISAB. Closing of the joints was considered in the nonlinear analyses that are discussed later.

Columns

The stiffness of the columns will vary as the sections crack, resulting in changes in the natural frequencies of the bridge. Analyses were carried out based on both uncracked and cracked section moduli for the columns. These values were based on the work of Priestley (8), who suggests that the cracked values are more relevant as they represent the stiffness as the member approaches its yield strength.

Bridge Model

The structural model used in the SEISAB runs consisted of a twenty-span section of the bridge (five four-span sections), as shown in Figure 11. These sections are typical of the geometry in the center region of the bridge. Joints were incorporated at the two ends (at the abutments) and between each four-span section. Each bent consisted of a cross-member supported on five columns. Each column was rigidly attached to a pile cap, which was supported on four pile elements. All mass in the model was concentrated at the nodes.

Preliminary runs were performed using bridge models of 8, 12, 16, 20, 24, 28, 32 and 36 spans. The displacements and member forces of the models of various lengths were compared. The response in the middle spans of models of sixteen spans and longer is largely controlled by the stiffness of the columns and the foundations, and it is not significantly affected by the stiffness of the abutments. As the actual bridge is over 80 spans, it is likely that abutment effects will be significant only in a few spans near each end. A model of twenty spans was used for the SEISAB runs so that the results were not dependent on the modelling of the abutments.

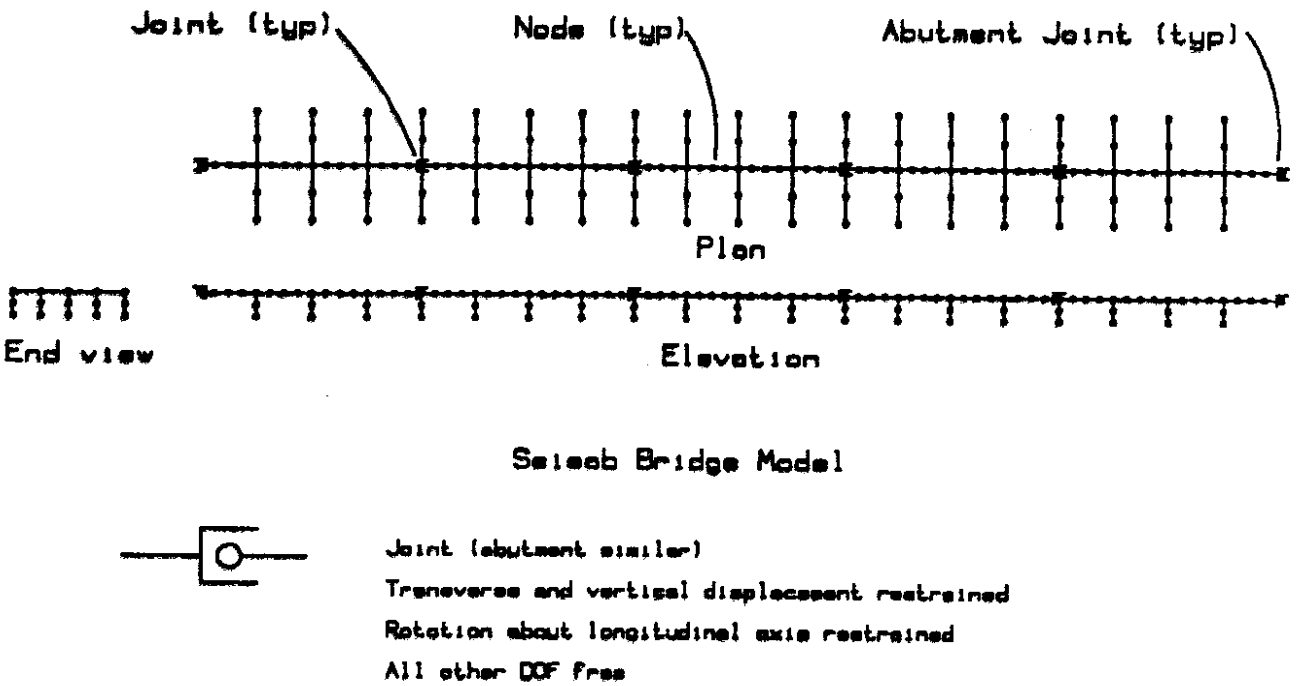

Figure 11. SEISAB Bridge Model

Spectral Analyses

SEISAB was used to perform response spectra analysis of the westbound bridge. Spectral analysis involves determining the fundamental periods of the structure being modelled, the mode shapes which correspond to those periods, and the participation factors for each mode shape. The response of the structure is determined by combining the response of the individual modes to the input acceleration spectrum. The response to each mode is combined with those of the other modes based on the participation factors to obtain the total response. Therefore, the recombination of the modal response may not necessarily yield the actual maximum response to the earthquake ground motion.

Modal analyses were performed for each of the six structural models (two column stiffnesses, three pile stiffnesses) in order to determine the fundamental frequencies of the structures. Results of these runs are presented in Figure 12. Only the two lowest fundamental periods are shown in the figure. The first mode shape (corresponding to the longest period) is a longitudinal translation of the entire structure. The second mode shape is a transverse bowing of the bridge in single curvature. All of the fundamental periods are in the 0.82 to 1.33 second range.

Two spectral analyses were performed for each of the six structural models. One set of analyses used the ATC-6 acceleration spectra, and the other used the acceleration spectra developed by Tsiatas, et al (9), which have been proposed as the design response spectra for the Washington State Department of Transportation.

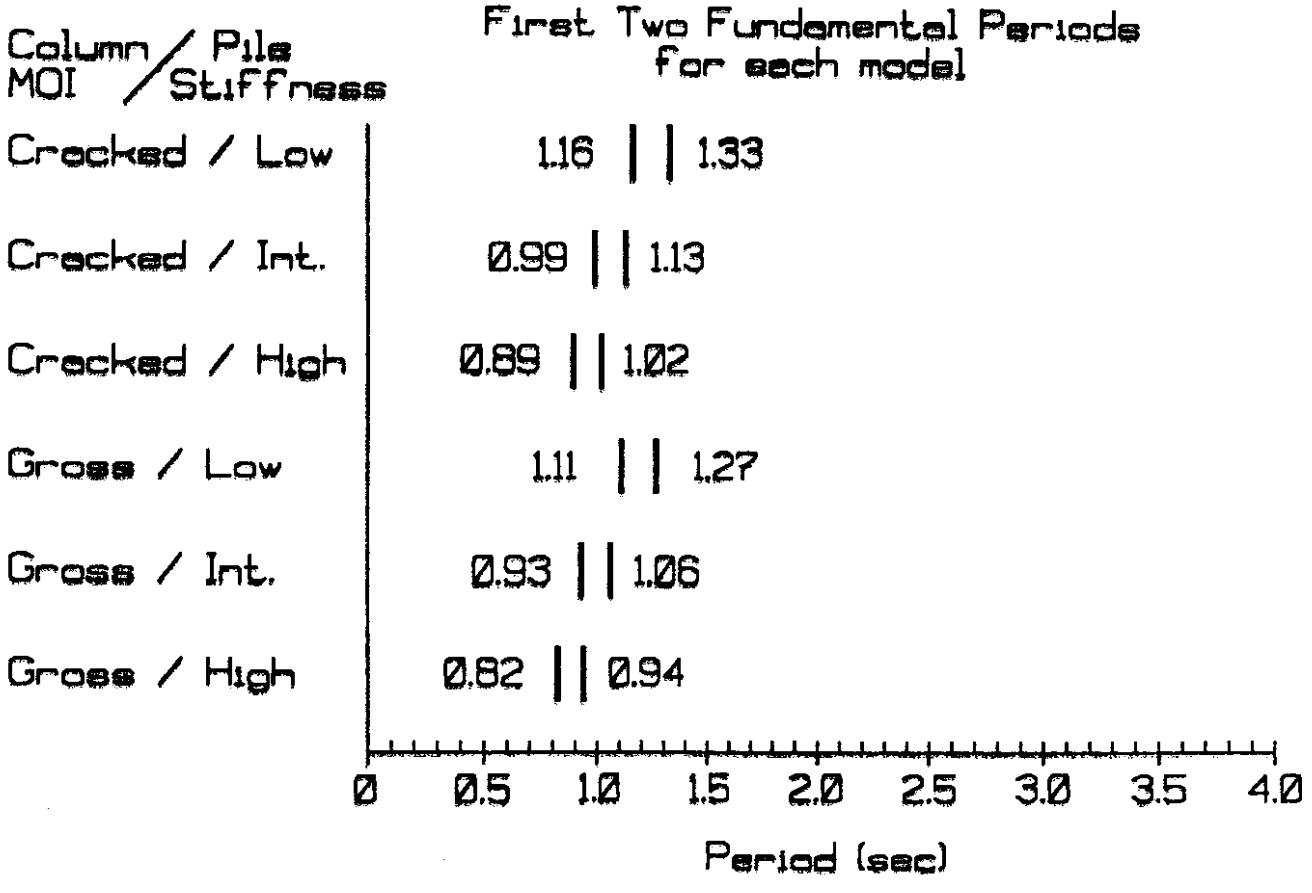

Figure 12. Bridge Fundamental Periods

The AASHTO Specifications (10) for bridge spectral analysis are based on the ATC-6 response spectra. These spectra are chosen based on the expected level of ground acceleration and the type of soil at the site of the bridge. As discussed previously, a peak bedrock acceleration level of 0.25g was selected for this study. SEISAB does not offer the ATC spectrum based on 0.25g, so the spectrum based on 0.3g was used. Figure 13 shows the ATC-6 spectrum for a soft soil site based on 0.3g bedrock acceleration.

The results of the ATC-6 spectral analyses are presented in Figures 14. The maximum transverse displacements of the six structural models are shown in the figure. Because the four-span sections are free to move longitudinally relative to each other and because the longitudinal column and foundation stiffnesses are similar to their respective transverse stiffnesses, the longitudinal displacements are very similar to the transverse displacements. Therefore, only the transverse displacements are presented. The structural models had maximum transverse displacements at the center spans ranging from 0.36 to 0.58 feet.

The maximum column moments of the six structural models are also shown in Figure 14. The maximum column moments were at the center spans and ranged from 230 to 340 foot-kips, which all exceed the likely capacity of the columns of 200 foot-kips. However, it is important to note the input spectrum was based on 0.3g rather than the targeted 0.25g acceleration.

The second set of spectral analyses were based on spectra developed by Tsiatas, et al (9). These spectra were developed to model the response resulting

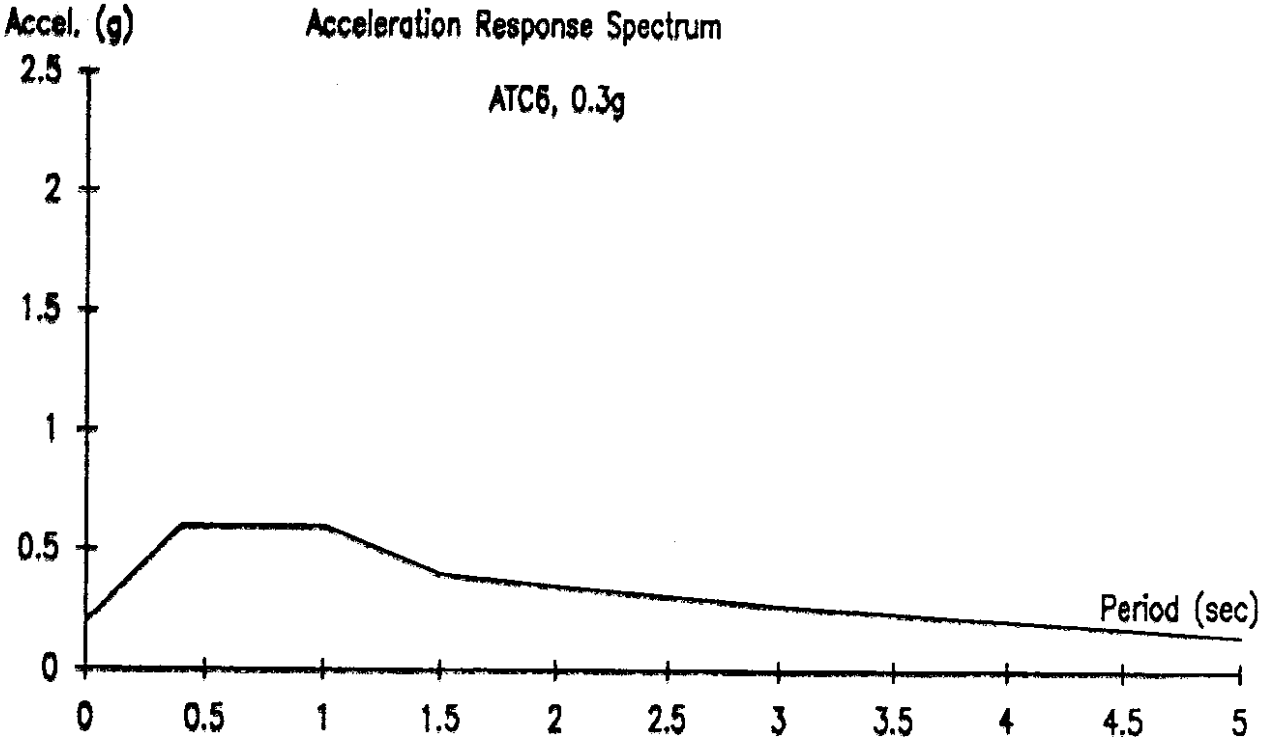

Figure 13. ATC-6 Acceleration Response Spectrum

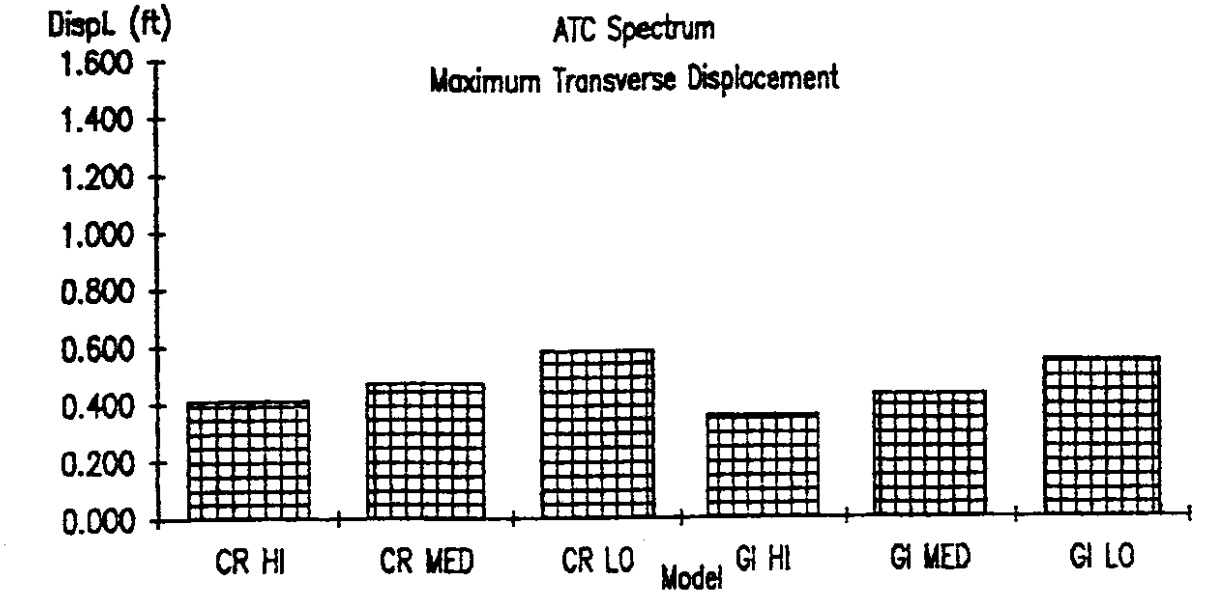

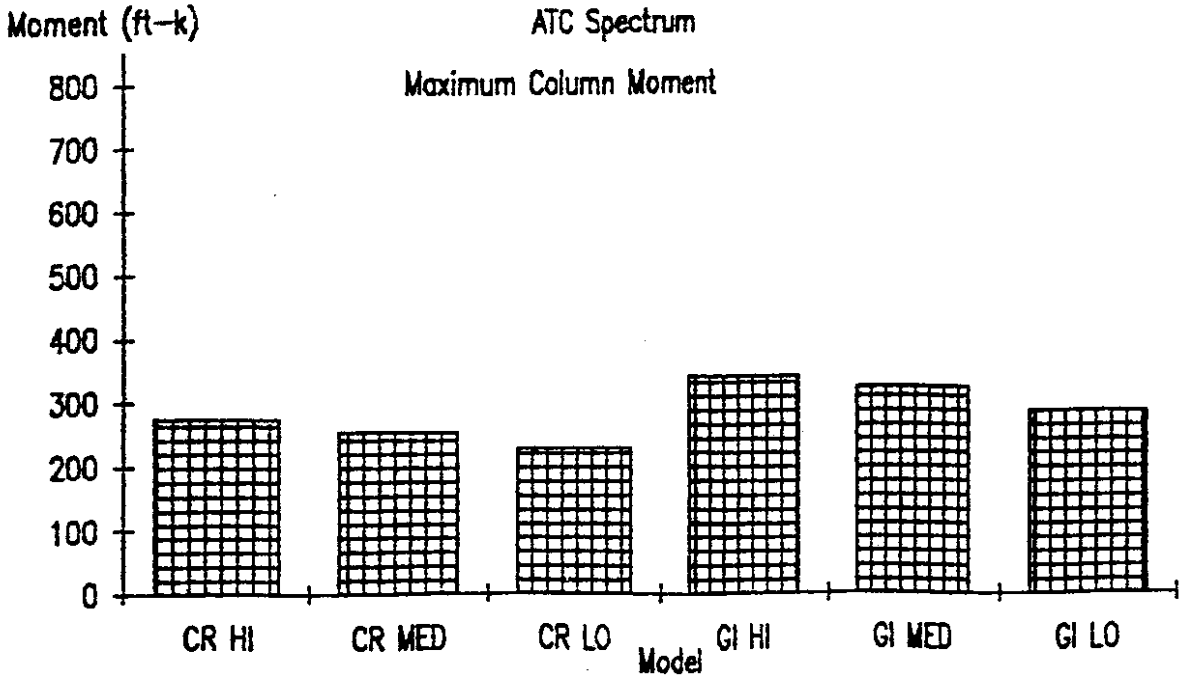

Figure 14. ATC-6 Spectral Analysis Maximum Transverse Displacements and Maximum Column Moments

from earthquakes in Washington state more accurately than the ATC-6 spectrum. The spectra are based on subduction earthquakes and include adjustments which attempt to account for nine different soil profiles representative of sites around Washington state. The spectrum used for the spectral analyses of this study was the average of the 0.2g and 0.3g spectra obtained for cohesionless soils of 50 to 100 feet depth and blow counts of 100 or greater. Figure 15 shows the acceleration response spectrum used for the second set of spectral analyses.

The maximum transverse displacements and maximum column moments resulting from these spectral analyses are given in Figure 16. The maximum transverse displacements occurred in the center spans and ranged from 0.33 to 0.43 feet. The maximum column moments ranged from 170 to 315 foot-kips. The most likely maximum column moment, for the cracked column and medium pile stiffness model, is 195 foot-kips, which is slightly less than the estimated capacity of the columns.

Time-History Analyses

SEISAB was used to perform time-history analyses based on input ground motion acceleration time-histories. The input acceleration time-histories were provided by Kramer (3) and represent the expected acceleration of the soil at the surface when the underlaying bedrock is subjected to a particular input acceleration. Five different profiles from the Mercer Slough were analyzed by Kramer for three bedrock seismic inputs (Castaic, El Centro and Lake Hughes). The resulting acceleration time-histories were used as input in the analyses and are given in

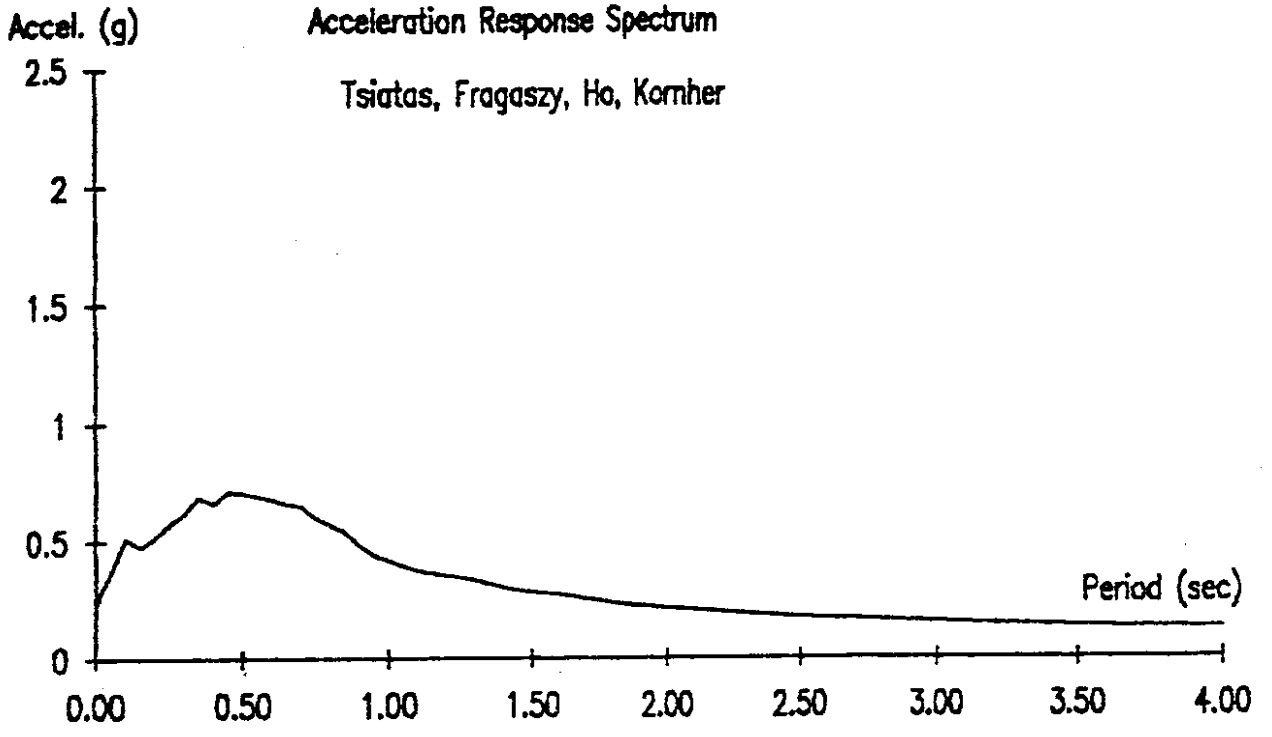

Figure 15. Proposed Washington State Acceleration Response Spectrum for Soil Group 5 (9)

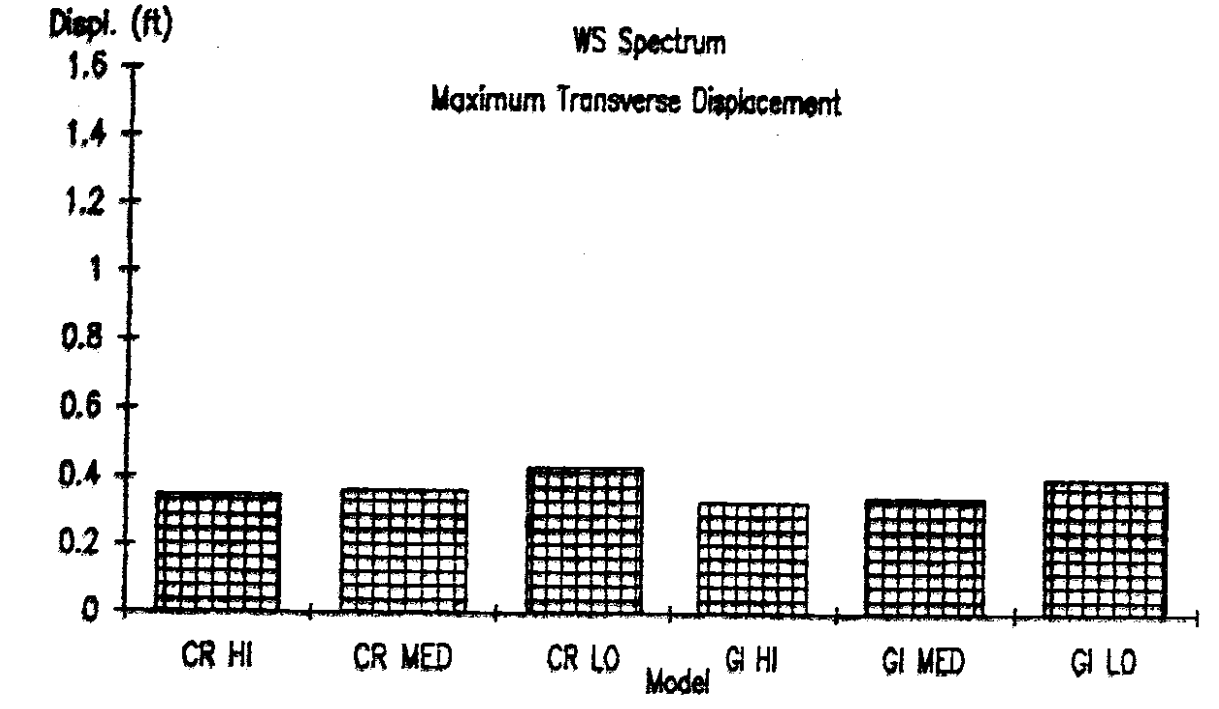

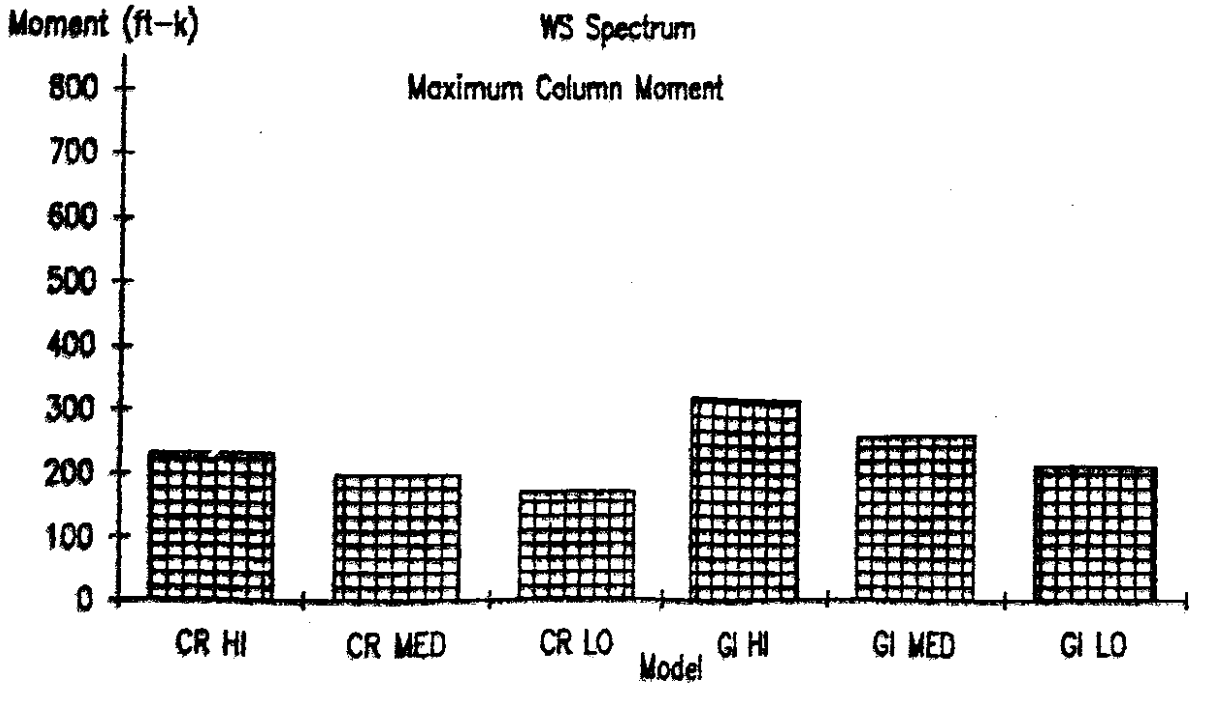

Figure 16. Spectral Analysis Using Proposed Washington State Spectrum Maximum Transverse Displacements and Maximum Column Moments

Appendix A. Each of the six structural models (two column and three pile stiffnesses) was analyzed using ground acceleration time-histories for the five soil profiles and three earthquakes.

SEISAB performs time-history analysis by solving the equations of motion in a stepwise manner, based on the input ground accelerations. The SEISAB analysis is linear as the geometry and stiffness of the structure are not updated from time step to time step. Therefore, there is no capacity to model plastic hinging, joint contact/noncontact, or degrading foundation stiffness. Also, SEISAB does not allow the simultaneous input of different time-histories to different sections of a bridge, as is likely to be the case for the Mercer Slough bridges in an earthquake. The joint contact/noncontact and differential ground motion input problems are addressed in the nonlinear analyses section.

The same structural models were used for the time-history analyses as for the spectral analyses. The results of the time-history analyses are summarized in Figures 17 to 22. Each set of figures presents the maximum transverse displacement and maximum column moment measured in the center spans for each section of the slough (soil profile) and each earthquake input for a given structural model. The displacements are of the structure relative to the ground.

Results from the time-history analyses vary widely. The maximum transverse displacements range from 0.2 to 1.6 feet, and the maximum column moments range from 80 to 850 foot-kips. In general, the input based on the Castaic earthquake resulted in the smallest response and input from the Lake Hughes earthquake

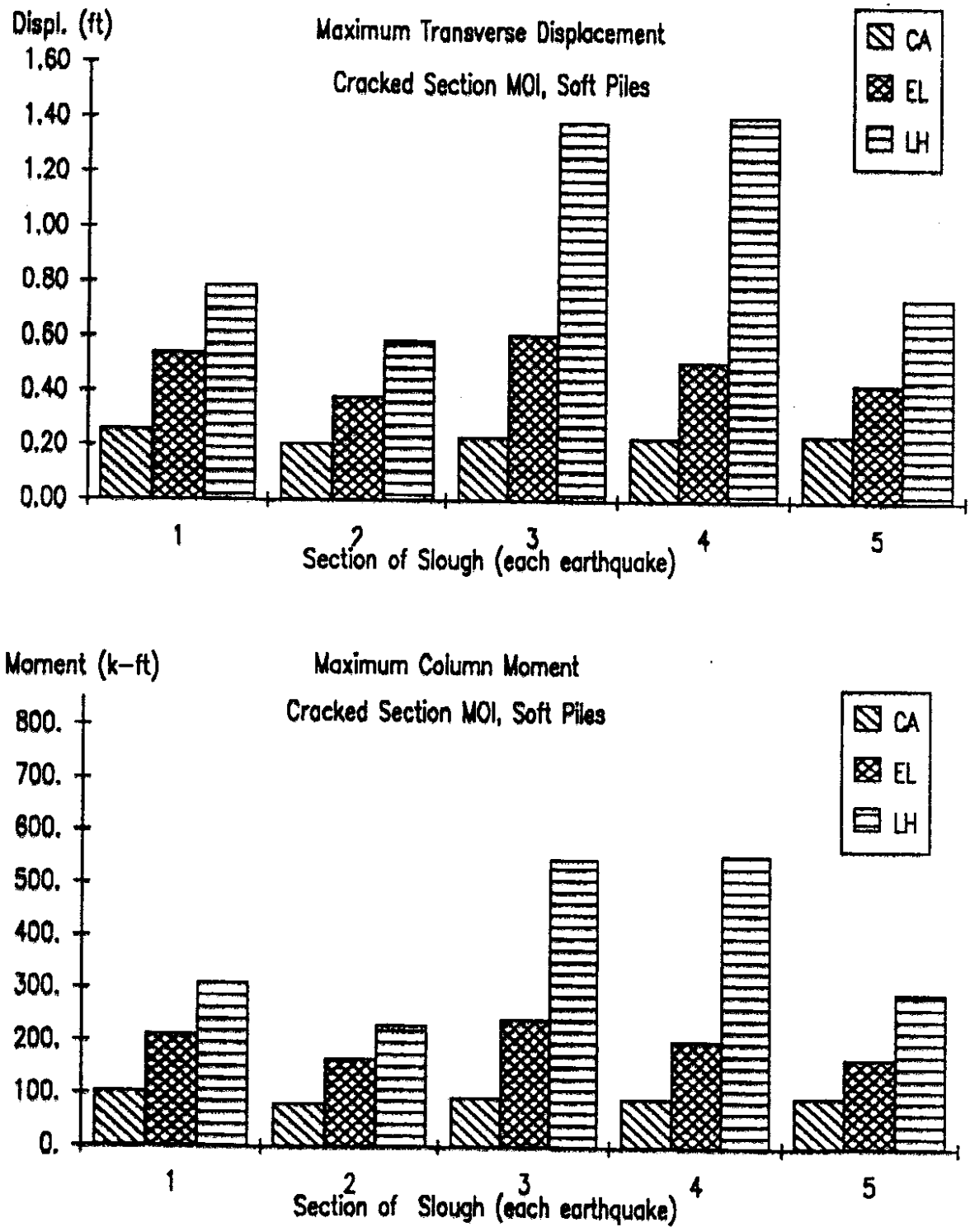

Figure 19. Cracked Column, Soft Pile Model Maximum Transverse Displacements and Maximum Column Moments

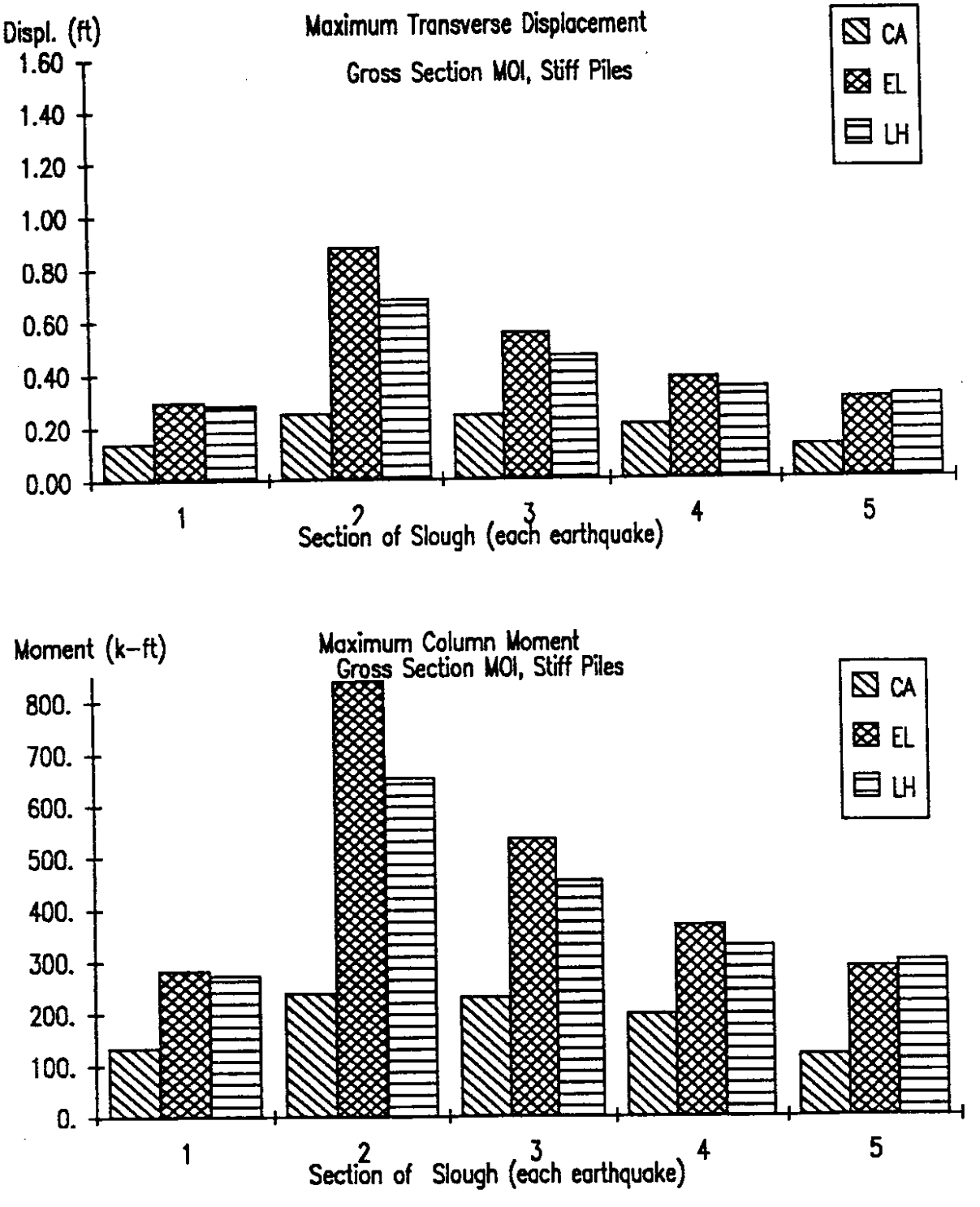

Figure 20. Uncracked Column, Stiff Pile Model Maximum Transverse Displacements and Maximum Column Moments

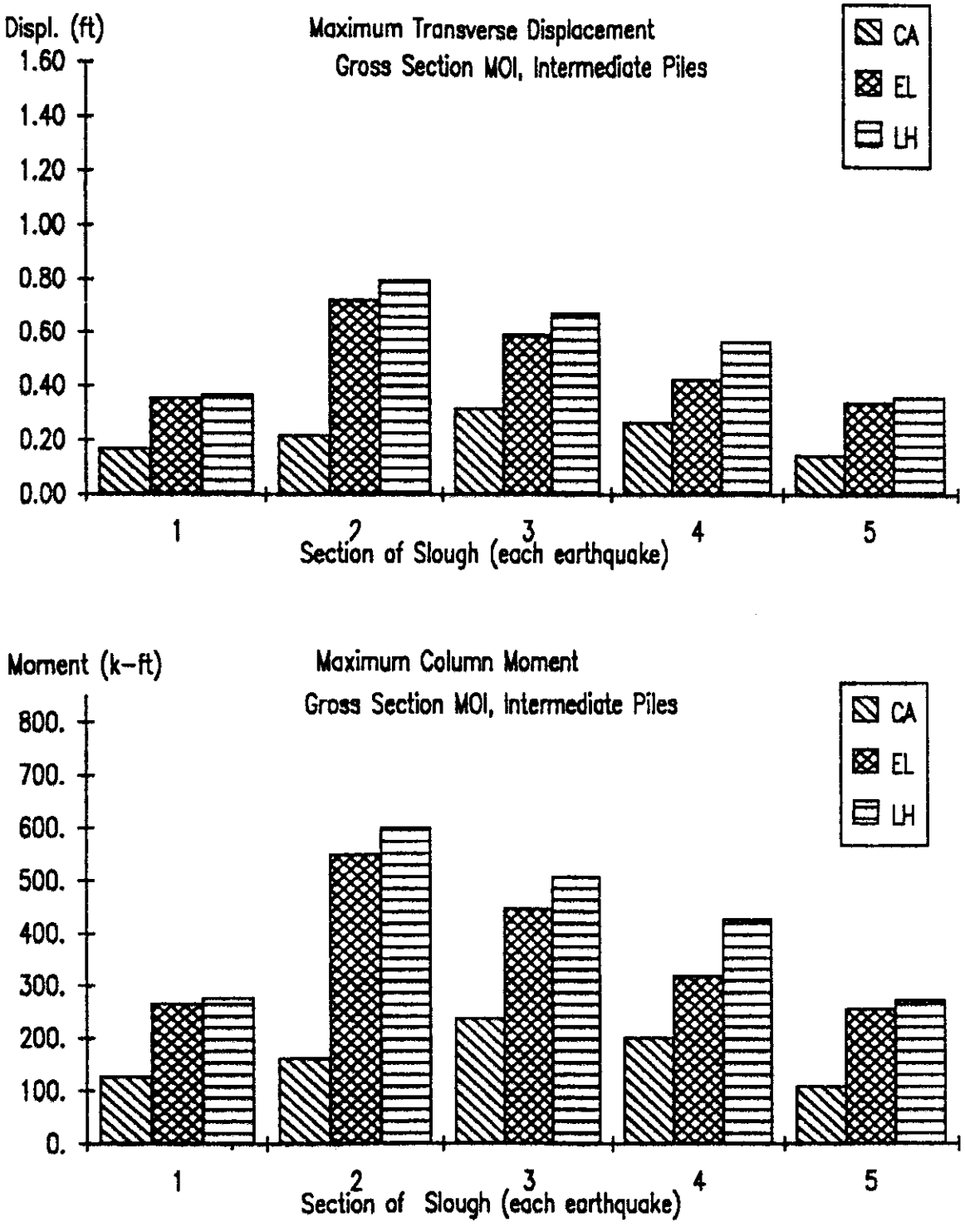

Figure 21. Uncracked Column, Intermediate Pile Model Maximum Transverse Displacements and Maximum Column Moments

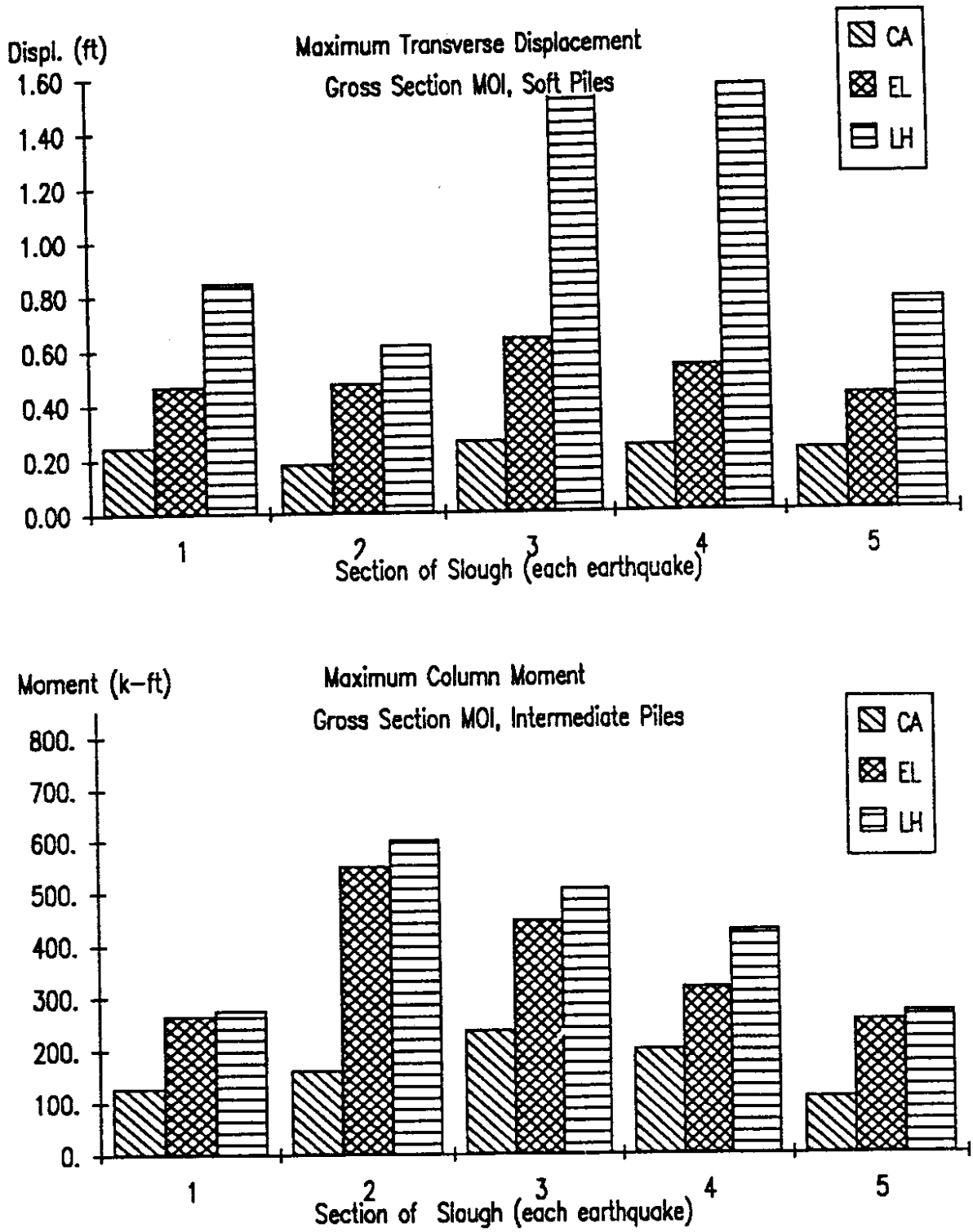

Figure 22. Uncracked Column, Soft Pile Model Maximum Transverse Displacements and Maximum Column Moments

resulted in thelargest response. The results show fairly low sensitivity to the stiffnesses of the columns. However, the results are very sensitive to the stiffnesses of the foundations and the different soil profiles.

As the analyses assume that all members behave elastically, the column moments are proportional to the displacements. Because the actual columns will not continue to behave elastically once their moment capacity is exceeded, values of column moments that are much in excess of the likely column capacity of 200 foot-kips are not realistic. However, the amount by which the elastic moments exceed capacity is an indicator of the likelihood that the columns will be overstressed. Column moments in excess of capacity also indicate that displacements will be larger than those predicted by the elastic analysis.

Figure 23 presents the maximum transverse displacements, end forces and moments for a column resulting from the analysis incorporating cracked column and medium pile stiffnesses for section 3 soil profile with Lake Hughes input. Much of the lateral displacement occurs in the foundation. The peak column moment occurs at the top of the column as the bent beams are typically monolithic with the superstructure and hence are stiffer with regard to rotation than are the pile caps. The column shear strength is estimated to be between 60 and 87 kips, depending on the axial load level in the column. Therefore, the column will probably be adequate in shear. The shear in the column is distributed to the four piles by the pile cap, resulting in an end shear of approximately 15 kips per pile.

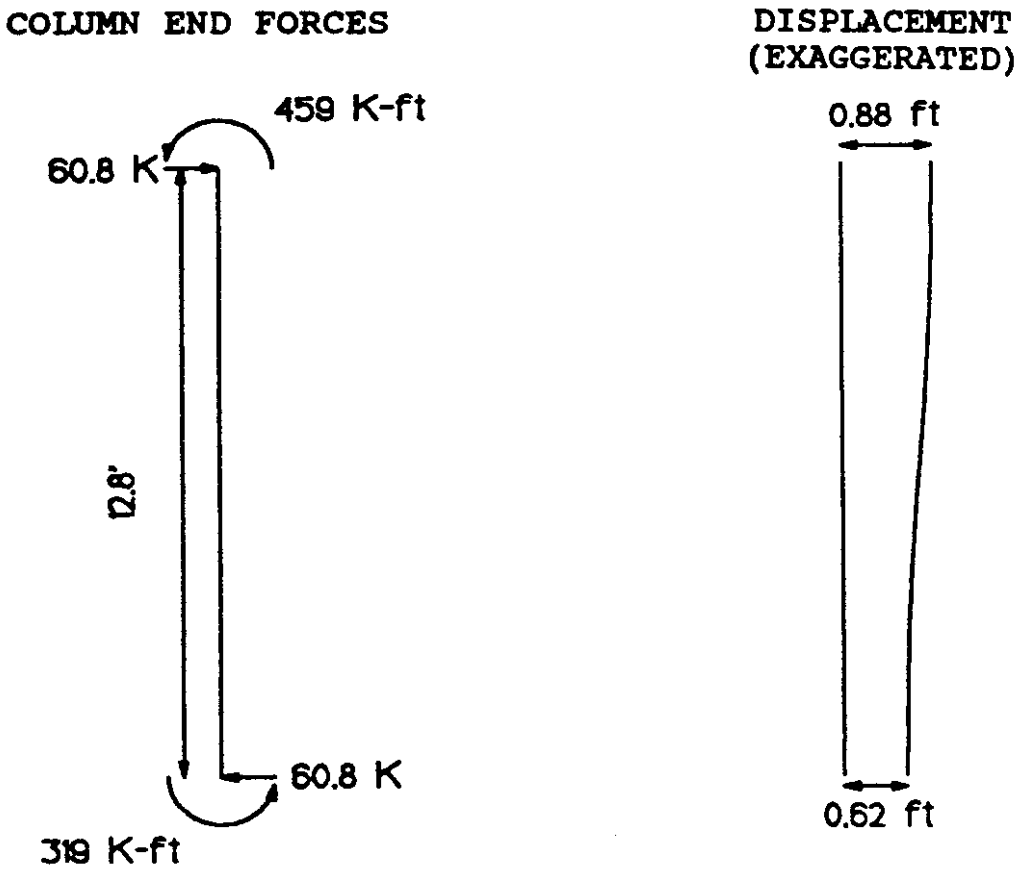

Figure 23. Maximum Column End Forces, Moments and Displacements Cracked Column, Intermediate Pile Model, Lake Hughes Section 3 Input

Discussion of Results

The linear analyses show wide variations in results. The spectral analyses, using the ATC-6 spectrum and the proposed Washington state spectrum, resulted in transverse bridge displacements ranging from 0.3 to 0.6 feet and column moments ranging from 170 to 340 foot-kips. In general, the time-history analyses resulted in larger responses than those from the spectral analyses, with displacements ranging from 0.2 to 1.6 feet and column moments ranging from 80 to 850 foot-kips.

Results from the ATC-6 spectrum are likely to be higher than the expected displacements and columns for the site because of the use of 0.3g bedrock acceleration rather than 0.25g acceleration in the spectrum. This observation is reflected in the results from the proposed Washington state spectrum, which was developed to more accurately represent the expected earthquake response for sites in Washington state, being lower than those from the ATC-6 spectrum. However, the results from the time history analyses, with input developed by Kramer (3) to reflect the expected ground response at the Mercer Slough site, were generally substantially higher than those obtained from either of the spectral analyses. Subsequent to the running of the time-history analyses, further research by Kramer into the dynamic properties of the peaty soil has indicated that ground motions may be considerably less than that used for the input for the time-history analyses. Therefore, the conclusion may be reached that results from the spectral analyses using the proposed Washington state spectrum may be the most reasonable. These results indicate that the columns are at or near their moment capacity. The columns

are likely to be adequate for shear. These analyses also indicate that the large displacements occurring in the bridge may result in some spans dropping from their supports during an earthquake.

NONLINEAR ANALYSES

Introduction

Nonlinear dynamic structural analyses were performed on the westbound lanes of the I-90 bridges crossing Mercer Slough. The nonlinear analyses were used to investigate the effects on bridge response of different simultaneous seismic input and opening and closing of the expansion joints. The effects of incorporating large displacement theory were also evaluated in the nonlinear analyses.

Modelling

The structural analyses program ANSYS was used to performed the nonlinear analyses. A simplified version of the structural model used in the SEISAB runs was employed in the ANSYS runs. Where the SEISAB models used beams and springs to model the bents and foundations, the ANSYS models used a set of equivalent springs for the entire bent-foundation system. The SEISAB models were three dimensional; the ANSYS models were two dimensional. The SEISAB models used intermediate nodes to smooth the mass lumping over the structure; the ANSYS models have no intermediate nodes. These simplifications result in models with significantly fewer degrees of freedom, about 120 for a twenty-span ANSYS model versus about 4300 for the analogous SEISAB model. These simplifications allow the

modelling of larger structures and the inclusion of nonlinearities which would have produced prohibitive computational cost otherwise.

The bent-foundation system was modelled using an equivalent spring for each of three degrees of freedom. The spring stiffnesses were evaluated by modelling the bent using finite elements and applying unit loads to the center of the bent. The finite element model was based on the same section properties for the columns and bent beams that were used for the cracked column structural model in the SEISAB runs. For the finite element model, the pile members were based on the intermediate pile stiffness value. Figure 24 shows the finite element model used to develop the equivalent spring stiffnesses for the bent-foundation system.

Figure 25 shows a twenty-span model used in several of the nonlinear analyses. The idealization of the bent-foundation system is also shown in the figure. The equivalent springs only resist load in the orthogonal directions. The input ground motions were applied at the ground node under each node of the superstructure. These motions were input to the model as transverse displacement time-histories, which were obtained by twice integrating the acceleration time-histories developed by Kramer (3) and presented in Appendix A.

Twenty-Span Model

A twenty-span model representing the same structure as that used in the SEISAB runs was subjected to five seismic inputs that were also used in the SEISAB runs. The purpose of these analyses on the twenty-span model was to verify the ANSYS modelling and to provide a baseline to which the nonlinear runs could be

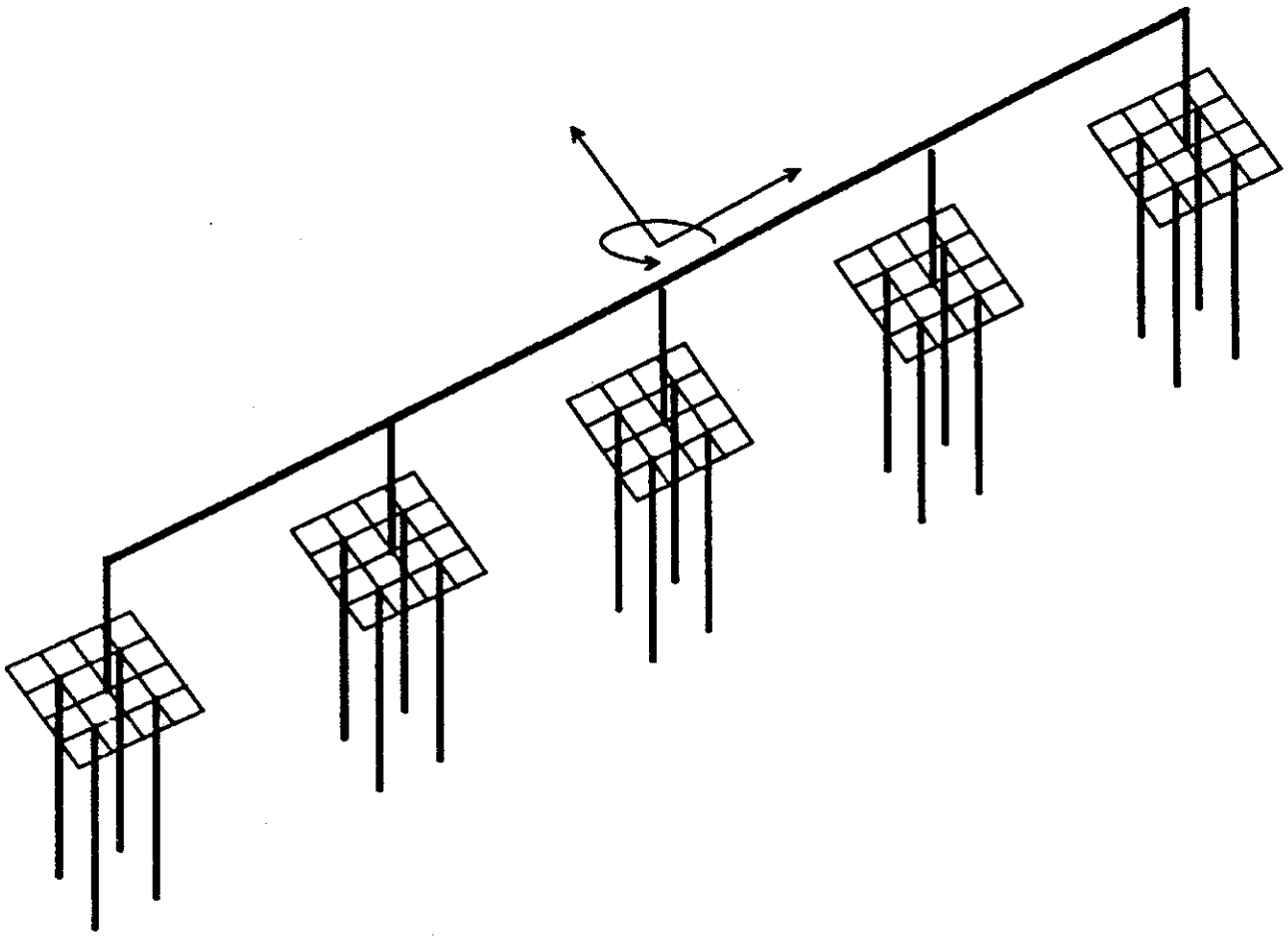

Figure 24. Finite Element Model of Bridge Bent

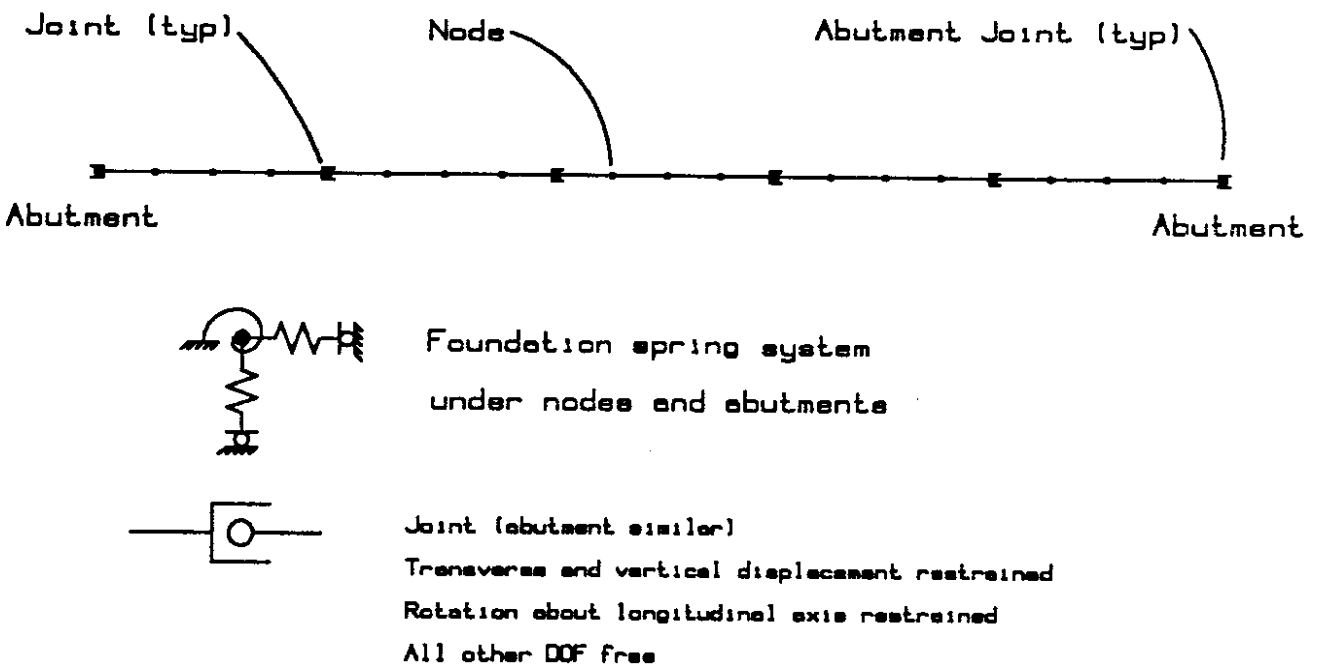

Figure 25. Twenty-Span Simplified Model

compared. The five runs which were performed on the twenty-span model incorporated cracked column stiffnesses, intermediate pile stiffness, and the Lake Hughes ground input. The structural model was chosen as it provides the best estimate of the actual structure and foundation conditions. The Lake Hughes input was chosen as it resulted in the largest displacements and column moments in the SEISAB runs. The bridge response using this input is more likely to be influenced by the joint effects and differential motion than is that of the other inputs which resulted in smaller responses.

Results of the ANSYS runs on the twenty-span model with Lake Hughes input are summarized in Appendix B. Two graphs are shown for each of the five soil profiles (sections). The first graph of each pair shows the displacement trace of a point on the superstructure near the center of the spans (the same point monitored in the SEISAB runs) and the ground motion input to the foundation node connected to that point. The period of the relative displacement plots generated in the ANSYS runs is approximately 1 second, corresponding closely to the fundamental transverse period determined in the SEISAB runs.

Figure 26 compares the maximum relative displacements obtained using the simplified model with the maximum transverse displacements resulting from the corresponding SEISAB runs. At sections 1, 3, 4, and 5 the results compare well. Only at section 2 is there a significant difference. However, all of the runs exhibit displacements of similar magnitude, which indicates that the simplified, two-dimensional ANSYS model is a reasonable analog of the more complicated, three-

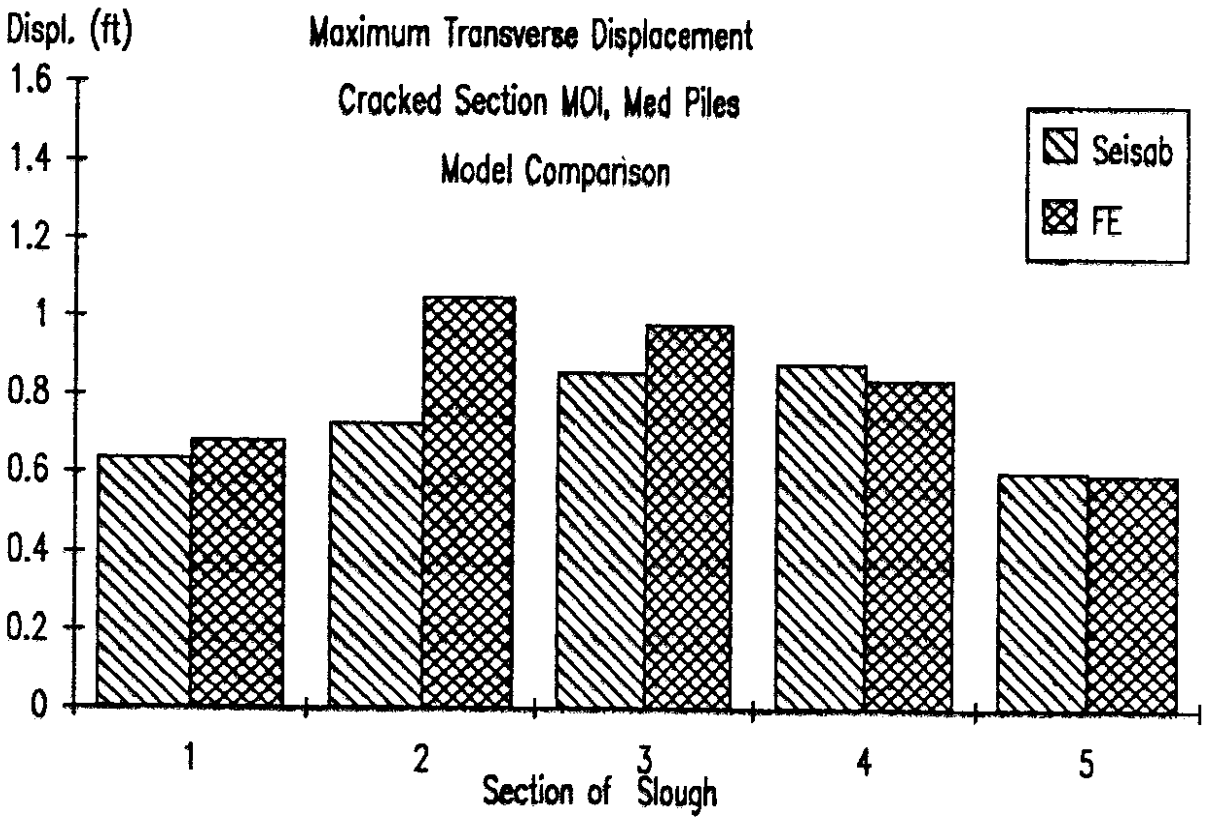

Figure 26. Comparison of Simplified ANSYS Model and SEISAB Runs

dimensional SEISAB model. The simplified model was judged to be adequate to evaluate the effects on bridge response of more spans, different ground motion inputs and nonlinear joints.

Sixty-Four-Span Model

A sixty-four-span model of the bridge was analyzed to investigate the effects of different ground motions acting on the bridge at the same time. The sixty-four-span model was divided into eight sections of eight spans each. Different sections of the bridge were subjected to different ground motions so as to approximate the effect of different soil profiles along the length of the bridge. The first eight spans were subjected to the section 1 ground motion. The second eight spans were subjected to the section 2 ground motion. The next 32 spans were subjected to the section 3 ground motion. The next eight spans were subjected to the section 4 input, and the final eight spans were subjected to the section 5 input.

Results of the runs on the sixty-four-span model with different ground motions are summarized in Appendix C. Two graphs are shown for each of the five regions of different ground motion input. The first graph shows a time-history plot of the displacement of a point on the bridge and of the corresponding point on the ground surface below. The second is a plot of the relative displacement of the two nodes.

Figure 27 shows the maximum relative displacements at the center of the twenty-span model for each of the five ground motions and maximum relative displacements at the center of the corresponding sections of the sixty-four-span model. The maximum displacements from the twenty-span model with one seismic

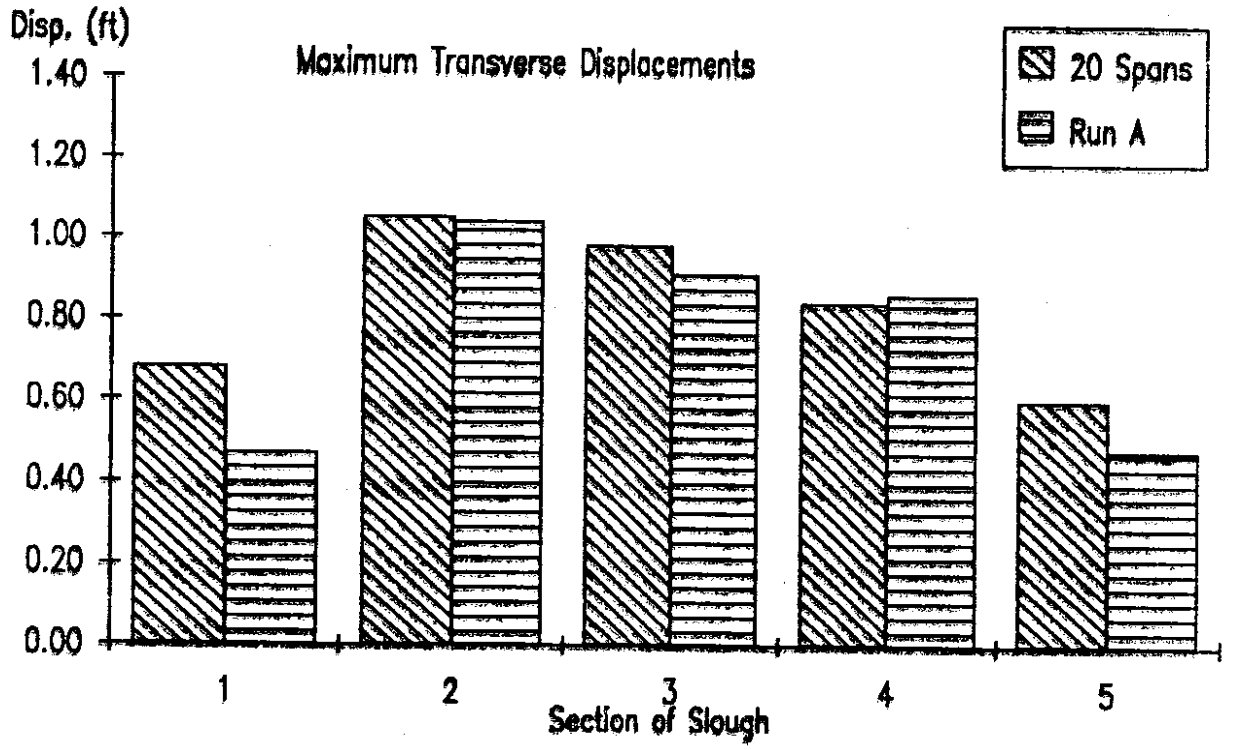

Figure 27. Comparison of Twenty-Span Model Results and Sixty-Four-Span Model Results (Run A)

input are generally comparable to those from the sixty-four-span model with five simultaneous seismic inputs. The displacements at the end sections from the sixty-four-span models are smaller than those from the twenty-span model. This is because the end section displacements were measured only four spans away from the abutments, as opposed to ten spans away from the abutments in the twenty-span models. Therefore, the end section displacements in the sixty-four-span model are reduced because of restraining effects from the abutments.

Time-Delayed Input Model

The sixty-four-span model was subjected to time-delayed input to examine the effects of the bedrock motion not being input into the soil strata simultaneously. Different sections of the bridge were subjected to input ground motions from different sections of the Lake Hughes ground motions delayed to represent the seismic event passing through the site. The bridge was again divided into eight sections of eight spans each. The sections were subjected to the same ground motions as before, except that the input was delayed by approximately 0.1 seconds from one section to the next. This delay represents the smallest time necessary for a seismic compression wave to pass through the bridge site along the length of the bridge (based on reference 11). This delay is probably longer than that which would be experienced at the site, but as such it will exaggerate the effects of out-of-phase ground motion. No attempt was made to model the possible reflections and interference of the ground motion waves as they interact in the slough.

The results of the sixty-four-span time-delayed analyses are summarized in

Appendix D. For each of the five sections, a time-history is presented showing the displacement of the reference point on the bridge and the corresponding point on the ground surface. This is followed by a trace of the relative displacement between the two nodes. Figure 28 compares the maximum relative displacement at the center of the twenty-span model with the maximum relative transverse displacement at the center of the corresponding sections of the sixty-four-span model (Run A) and the sixty-four-span model with time-delayed input (Run B). The maximum displacements are generally comparable for all of the runs. The time-delayed input resulted in only a slight difference in displacements.

Large Displacement Theory Model

The sixty-four-span model was analyzed using large displacement theory and the results compared to the sixty-four-span model analyzed previously (Run A). With large displacement theory, the stiffness matrix of the model is updated at each iteration to account for changes in structure geometry resulting from displacements occurring during the previous time step. Differences in results would only occur if the geometry of the deformed structure is significantly different from that of the undeformed structure. The ability to solve large displacement problems comes at the cost of increased computational effort.

Figure 29 compares the maximum relative displacements at the center of the twenty-span model with the maximum relative displacements at the center of the corresponding sections of the sixty-four-span model (Run A), the sixty-four-span model with time-delayed input (Run B), and the sixty-four-span model with large

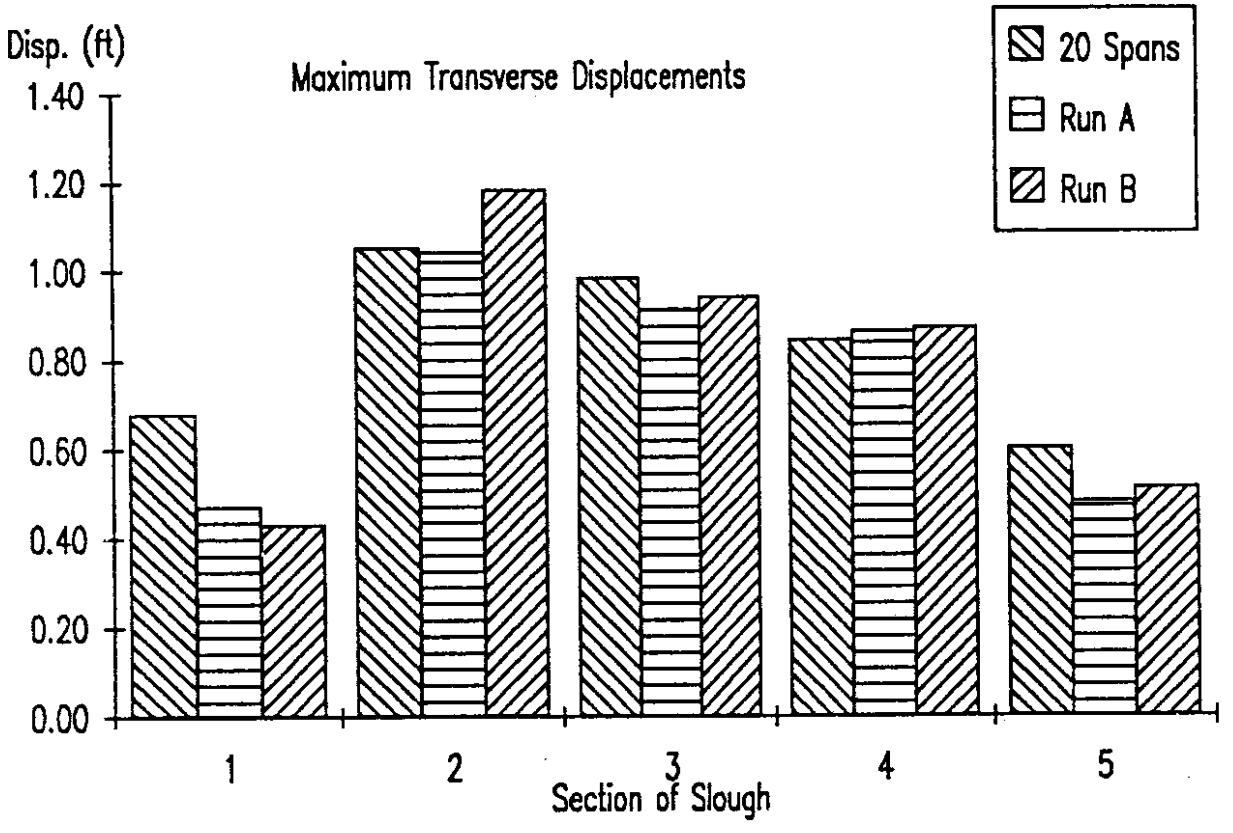

Figure 28. Comparison of Results for Twenty-Span Model, Sixty-Four-Span Model (Run A) and Sixty-Four-Span Model with Time-Delayed Input (Run B)

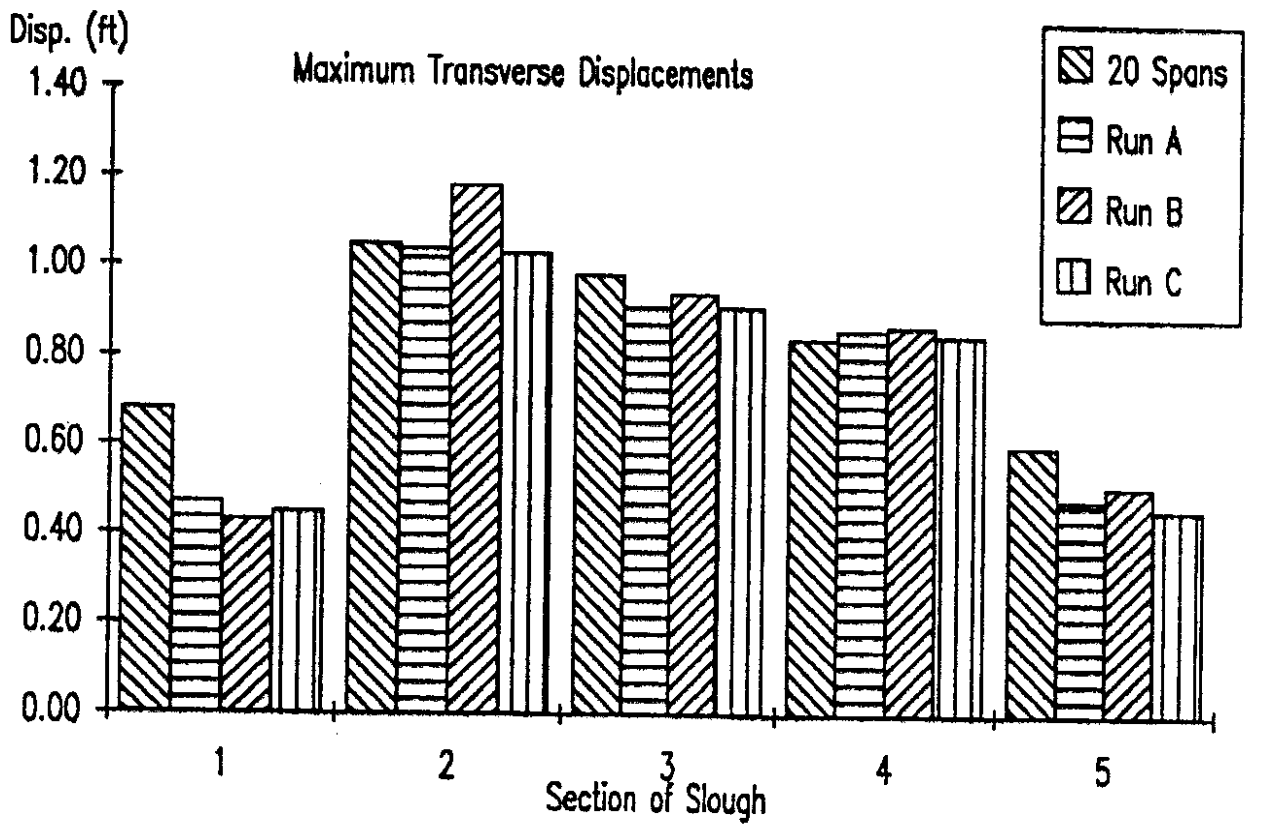

Figure 29. Comparison of Results for Twenty-Span Model, Sixty-Four-Span Model (Run A), Sixty-Four-Span Model with Time-Delayed Input (Run B), and Sixty-Four-Span Model with Large Displacement Theory (Run C)

displacement theory (Run C). The results obtained using large displacement theory (Run C) and small displacement theory (Run A) are nearly identical.

Nonlinear Joint Model

The sixty-four-span model with large displacement theory was expanded to include the effects of the bridge expansion joints closing and opening. Closing of the joints would act to restrict longitudinal translation and rotation and to transfer forces from one section to the next. Figure 30 shows details of the nonlinear joint incorporated into the analysis model. The cross-members are the width of the actual bridge, and the initial joint gap is 0.1 feet which approximates the specified spacing of the expansion joint. The cross-members have very low mass so that the dynamic properties of the bridge are not affected by the additional members. The nodes on each side of the gap at the ends of the spans are constrained to move together laterally, but not longitudinally or in rotation.

Results of the runs on the sixty-four-span model incorporating the nonlinear joints are summarized in Appendix E. The results are presented with a time-history showing the displacement of a reference point on the bridge and of the corresponding point on the ground surface below, followed by a trace of the relative displacement of the two nodes. Figure 31 shows a comparison of the maximum relative displacement at the center of each section of the sixty-four-span nonlinear joint model (Run D) with the maximum relative displacements at the center of the corresponding sections of the previous runs. The results from Run D indicate that

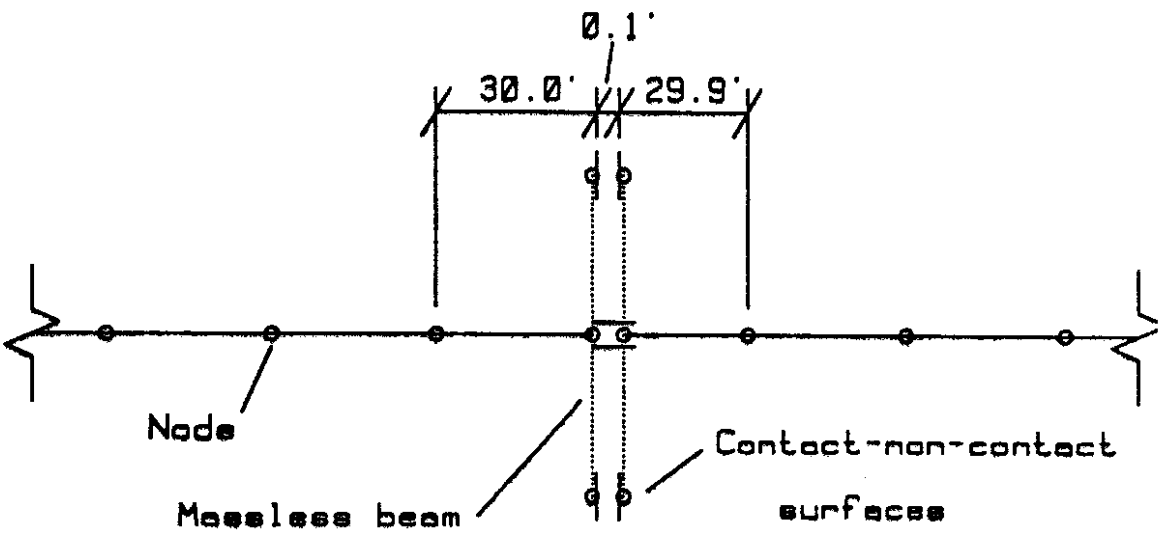

Figure 30. Nonlinear Joint Model

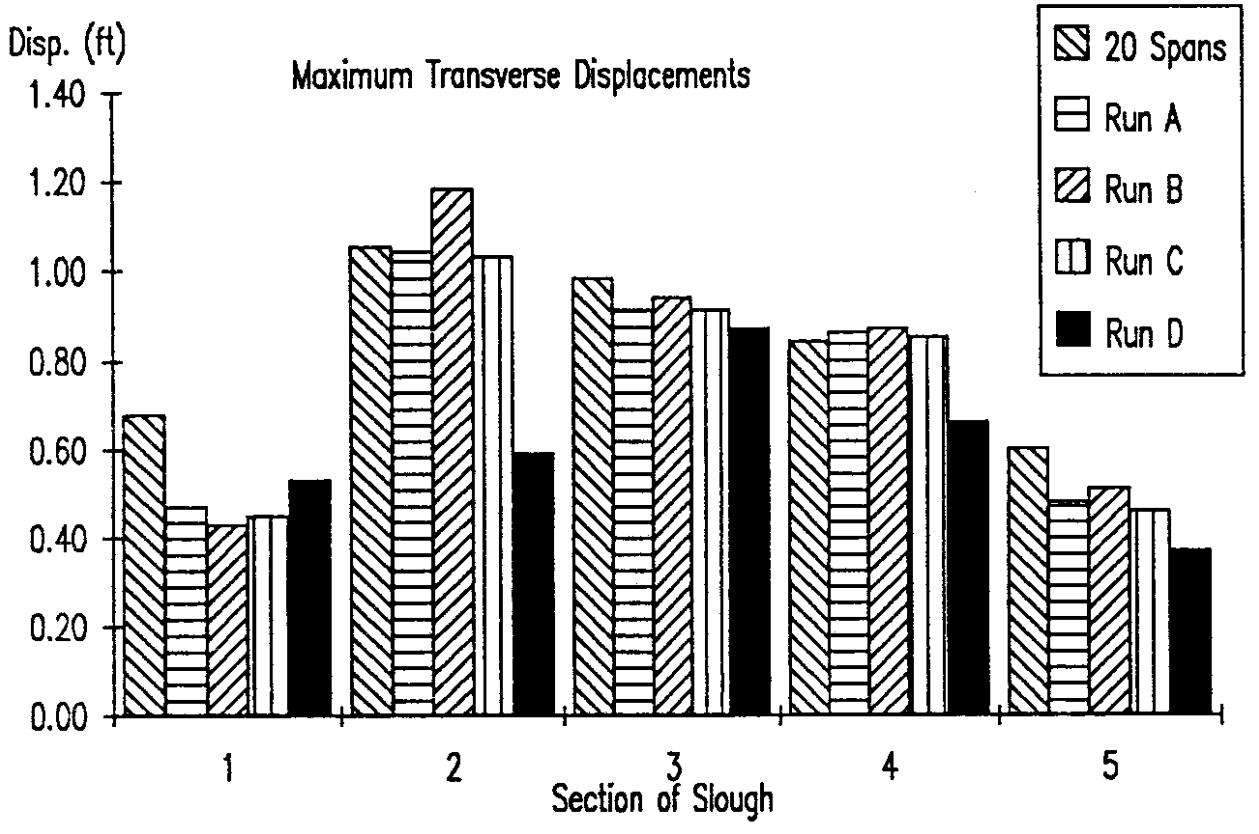

Figure 31. Comparison of Results for Twenty-Span Model, Sixty-Four-Span Model (Run A), Sixty-Four-Span Model with Time-Delayed Input (Run B), Sixty-Four-Span Model with Large Displacement Theory (Run C), and Sixty-Four-Span Model with Nonlinear Joints (Run D)

nonlinear joint behavior does affect bridge response. Overall, the effect of the nonlinear joints is to lessen the maximum displacements.

Displacements occurring at the expansion joints are given in the figures contained in Appendix F. These figures show the relative displacement in the longitudinal direction of the two points on either side of an expansion joint. For the nonlinear joint model results, this represents the opening and closing of the joints. Note that the joints are not closed until the relative displacement is -0.1 feet as there is an initial gap of 0.1 feet in the joint. With the simple joint model (i.e. the model without nonlinear joints), the joint displacements may exceed -0.1 feet as there is no restraint provided at the joint.

The nonlinear joint model displacements tended to be more averaged than those of the simple joint model. Displacements in sections of the bridge which experienced large motions were diminished as a result of restraint by sections of the bridge in which less motion took place. With the nonlinear joint model, the largest joint opening was 0.24 feet. The joints which had the largest displacements were those between the sections of the bridge subjected to different ground motion input. In a real seismic event, the input would vary continuously, not suddenly, probably resulting in smaller joint displacements than those shown in the figures.

With reference to Figure F.3, it can be seen that the gap near the center of the simple joint model experienced very little opening and closing. The spans on either side of the joint were subject to the same input ground motion and the simple joints did not transmit or cause additional disturbances in the motion of the model.

In the nonlinear joint model, however, there was significant relative motion, probably due to disturbances caused by the closing and opening of the joints.

Discussion of Results

The overall results of the nonlinear ANSYS analyses indicate that the linear SEISAB runs probably provide conservative results. The nonlinear analyses performed using the simplified bridge model indicated that the effects on bridge response of different ground motions along the length of the bridge and a staggering of the input motions was very small. Modeling the opening and closing of the expansion joints resulted in a general reduction in maximum bridge displacements when compared to those from simple joint models. The transmission of forces across the joints caused the areas of higher relative motion between spans to be damped and the areas of lower motion between spans to be accentuated.

CONCLUSIONS AND RECOMMENDATIONS

This research project investigated the seismic response of the westbound lanes of I-90 crossing Mercer Slough. Both linear and nonlinear dynamic analyses were performed. The applicability of various analysis procedures and the impact of different modelling assumptions were evaluated. Based on these analyses, an evaluation of the likely performance of the bridge in an earthquake was made.

ANALYSIS PROCEDURES

Several different dynamic structural analysis procedures were used in this study. These procedures included spectral analysis, linear time-history analysis and nonlinear time-history analysis. The bridge structure consists of over twenty four-span sections. The sections are connected by an expansion joint which provides vertical and lateral support to both of the sections. Relative longitudinal movement between the sections may take place until the expansion joint closes. The structure is wide, relative to its height, and it is supported on broad, low, multi-column bents. The pile foundations and the soil at the site of the bridge are potentially highly nonlinear in their response to seismic excitation. The site is large enough that different parts of the bridge may be subject to different seismic input. All of these factors pose significant challenges when performing a structural analysis.

Preliminary analyses were performed to determine how large a model would be required to capture the response of the overall bridge. A model of twenty spans, less than one quarter of the entire bridge length, was found to yield results consistent

with larger models. Results were found to be influenced by the abutment stiffness in spans near the abutments, but this influence diminished in spans away from the abutments.

Response spectra analyses were performed to provide a baseline for comparison with the time-history analyses. The response spectra runs were based on both generalized earthquake and soil conditions (ATC-6 spectrum) and specific earthquake and soil conditions for Washington state (proposed Washington state spectrum). Neither spectrum can be expected to completely reflect the unusual conditions of the peaty soil at the Mercer Slough site.

A series of linear time-history runs were performed to evaluate the effects of varying the column stiffnesses, varying the foundation stiffnesses, and varying the seismic input. Acceleration time-histories developed specifically for the Mercer Slough site were used as the input for these analyses. Bridge response was found to be sensitive to changes in the foundation stiffness. The results of the time-history runs were strongly dependent on the particular ground motions used. An important conclusion is that analysis results can be no more reliable than the seismic input.

Nonlinear time-history analyses were performed to evaluate the effects of different seismic input at different locations of the structure and the effect of opening and closing of the expansion joints. These nonlinear runs used a two-dimensional model with a greatly reduced number of degrees of freedom from that of the linear runs. This simplified model yielded results with were consistent with the more complex three-dimensional model. The effects of different simultaneous seismic

inputs and nonlinear joint behavior were found to be of little significance. Both factors tended to decrease the response of the structure.

The analyses indicate that a long, loosely connected bridge can be adequately modelled using a fairly short section of the bridge. Additionally, in a structure as long and as loose as the westbound lanes of the I-90 Mercer Slough bridge, the seismic response away from the abutments is not dependent on the behavior of the abutments. It may be possible to get reasonable results by analysis of only one bent or a several bent section, although this was not done in this study. Further, analysis of a single bent section of the bridge would allow the consideration of the effects of plastic hinging in the columns, nonlinear foundation stiffness and damping, and a more detailed examination of the soil-structure interaction.

BRIDGE PERFORMANCE

The analysis results show a wide variation in predicted bridge response. However, all of the analyses indicate that elements in the bridge would probably be close to or exceed their capacity during an earthquake. Problem areas which were identified in the study include the inability of the expansion joints to sustain large relative displacements and the possible overloading of the columns in flexure. Deficient reinforcement detailing of transverse reinforcement and splices in the columns, typical of the practice at the time of construction of the bridge, would result in little ductility in the columns if overloaded. The shear capacity of the columns appeared to be adequate.

Two important areas regarding the performance of the foundations were not addressed in this initial evaluation. Due to the large ground motions likely at the Mercer Slough site, the ability of the piles to sustain shearing deformations over their length should be examined. An assessment should also be made of the connection between the piles and pile caps. This may require field inspection of several of the pile connections and possibly also some form of nondestructive testing to determine the integrity of the embedded wood piles.

Results from the study showed that the choice of a particular seismic input could result in a nearly an order of magnitude change in predicted bridge response. This study also showed the difficulty of establishing a reliable prediction of ground response at a particular site, especially for a relatively unknown and complex soil such as the peaty soils found at the Mercer Slough site. Research subsequent to completion of the structural analyses has indicated that the time-histories used for the seismic input in this study are larger than that which would realistically be expected at the Mercer Slough site. It is recommended that additional analyses be conducted incorporating these recent findings.

IMPLEMENTATION

The dynamic structural analyses of the westbound lanes of the I-90 bridges crossing Mercer Slough indicated that several elements of the bridge may be vulnerable in a seismic event. Most of the time-history analyses did indicate that the columns were overstressed in flexure. However, the time-history analyses were based on seismic input that were later determined to overestimate the expected ground motions at the Mercer Slough site. Spectral analyses based on the ATC-6 spectrum also generally indicated that the columns were overstressed in flexure. However, this was for 0.3g bedrock, which is higher than the 0.25g value selected for the site. Finally, the spectral analyses based on the proposed Washington state spectrum indicated column moments that were at or near capacity. Thus, it is difficult to conclusively determine if the columns of the bridge would or would not be overloaded in an earthquake. If it is determined by WSDOT that column flexure performance must be improved, steel jacketing at the base and at the top of the columns should be added as retrofit measures. Additional analyses with ground motions based on the improved understanding of the dynamic properties of the peaty soil would provide a more rational basis for this assessment.

All of the analyses indicated that movement at the expansion joints during an earthquake would likely result in a loss of support of some of the spans. There is a need for joint restrainers and increased support widths at the expansion joints. During the period of this study, both of these retrofit measures have been applied to the I-90 bridges crossing Mercer Slough, as shown in Figure 32.

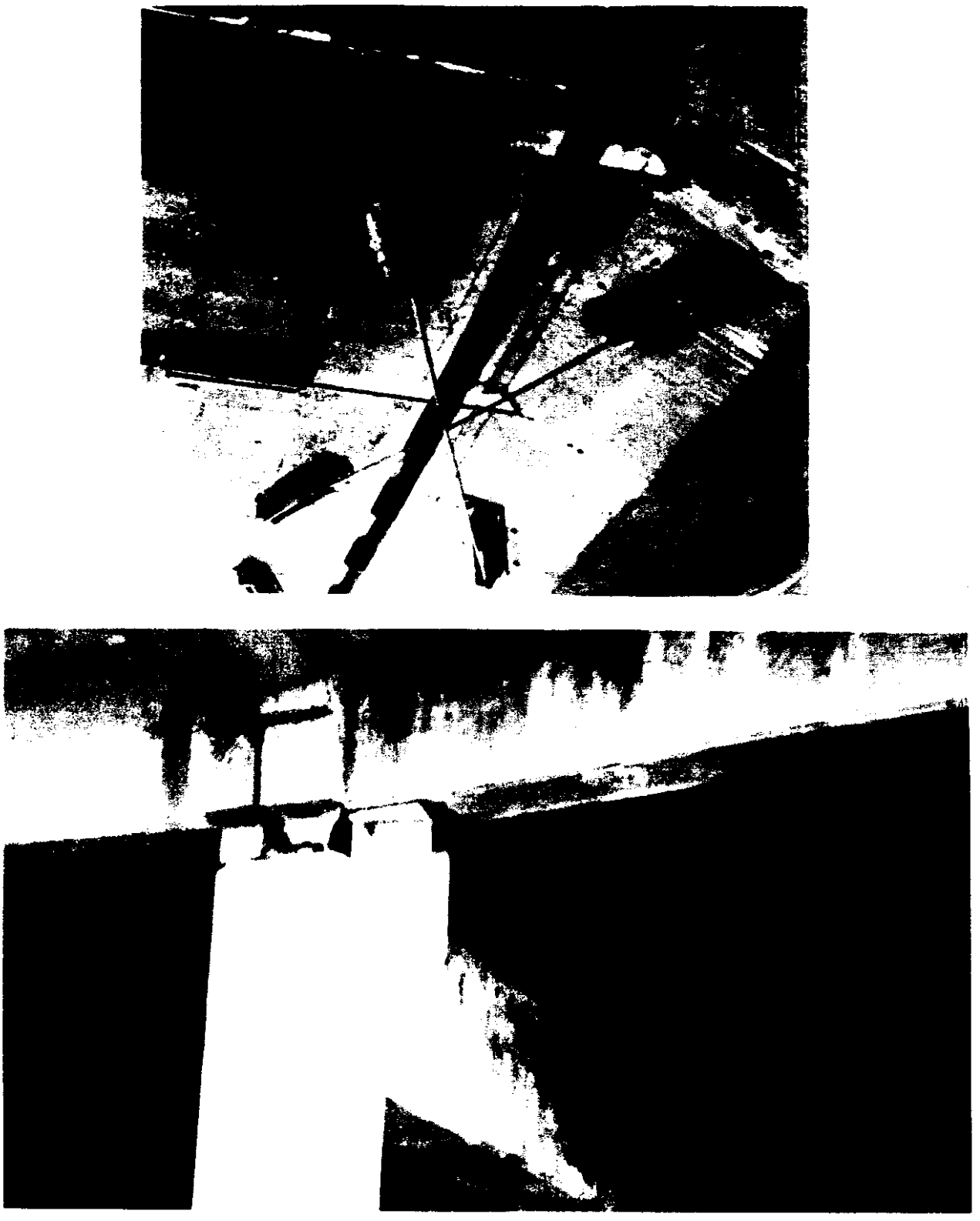

Figure 32. Retrofit Measures Applied to the I-90 Bridges Crossing Mercer Slough: Joint Restrainers and Increased Support Width

ACKNOWLEDGMENTS

The research described in this report was funded by the Washington State Department of Transportation. Valuable assistance was provided by Alan P. Kilian of the Materials Laboratory and Edward H. Henley, Jr. and Richard B. Stoddard of the Bridge and Structures Office. C.B. Crouse of Dames and Moore provided assistance in determining the stiffnesses of several of the foundation elements.

The research was performed at Washington State University. This research constituted part of Ian B.S. Cannon's Master's Degree program. Associate Professor David I. McLean was the principal investigator. The authors thank Professor William F. Cofer for his valuable input on the analytical modelling problems encountered during the research project.

Professor Steven L. Kramer of the University of Washington, principal investigator of a parallel project investigating the dynamic properties of the peaty soil and ground response at the Mercer Slough site, provided the time-histories used for seismic input in the analyses and also provided insight into the modelling of the foundations.

REFERENCES

1. Board of Inquiry (1990). "Competing Against Time," C.C. Thiel, ed., Office of Planning and Research, State of California, May, 264 pp.
2. Kramer, Steven L. (1991). "Behavior of Piles in Full-Scale, Field Lateral Loading Tests," Washington State Transportation Center, Seattle, Washington, October, 79 pp.
3. Kramer, Steven L. (1992). "Seismic Response - Foundations in Soft Soils," Draft Report for Washington State Transportation Center, Seattle, Washington, July, 185 pp.
4. Chai, Y.H., Priestley, M.J.N. and Seible, F. (1991). "Retrofit of Bridge Columns for Enhanced Seismic Performance," Seismic Assessment and Retrofit of Bridges, SSRP 91/03, pp. 177-196.
5. Scott, R.F. (1989). "Assessment of Existing Bridges - Foundation Assessment," California Institute of Technology.
6. Lam, I.P. and Martin, G.R. (1984). "Seismic Design for Highway Bridge Foundations," Proceedings, Lifeline Earthquake Engineering, ASCE Convention, pp. 7-21.
7. SEISAB User's Manual, Imbsen and Associates, Inc., May 1990.
8. Priestley, M.J.N. (1991). "Seismic Assessment of Existing Concrete Bridges," Seismic Assessment and Retrofit of Bridges, SSRP 91/03, pp. 84-149.

9. Tsiatas, G., Fragaszy, R., Ho, C. and Kornher, K. (1989). "Design Response Spectra for Washington State Bridges," Department of Civil Engineering, Washington State University, May.

10. Bridge Design Specifications Manual (1989). AASHTO, Washington, D.C.

11. Engineering Geology (1961). Soil Conservation Service.

APPENDIX A

GROUND RESPONSE ACCELERATION TIME-HISTORIES AND ACCELERATION RESPONSE SPECTRA

The Duration Modelled bar on the acceleration time-histories indicates the portion of the total time history used as input in the structural analyses. Three values of damping were used in developing the corresponding response spectra: 2, 5 and 10 percent damping.

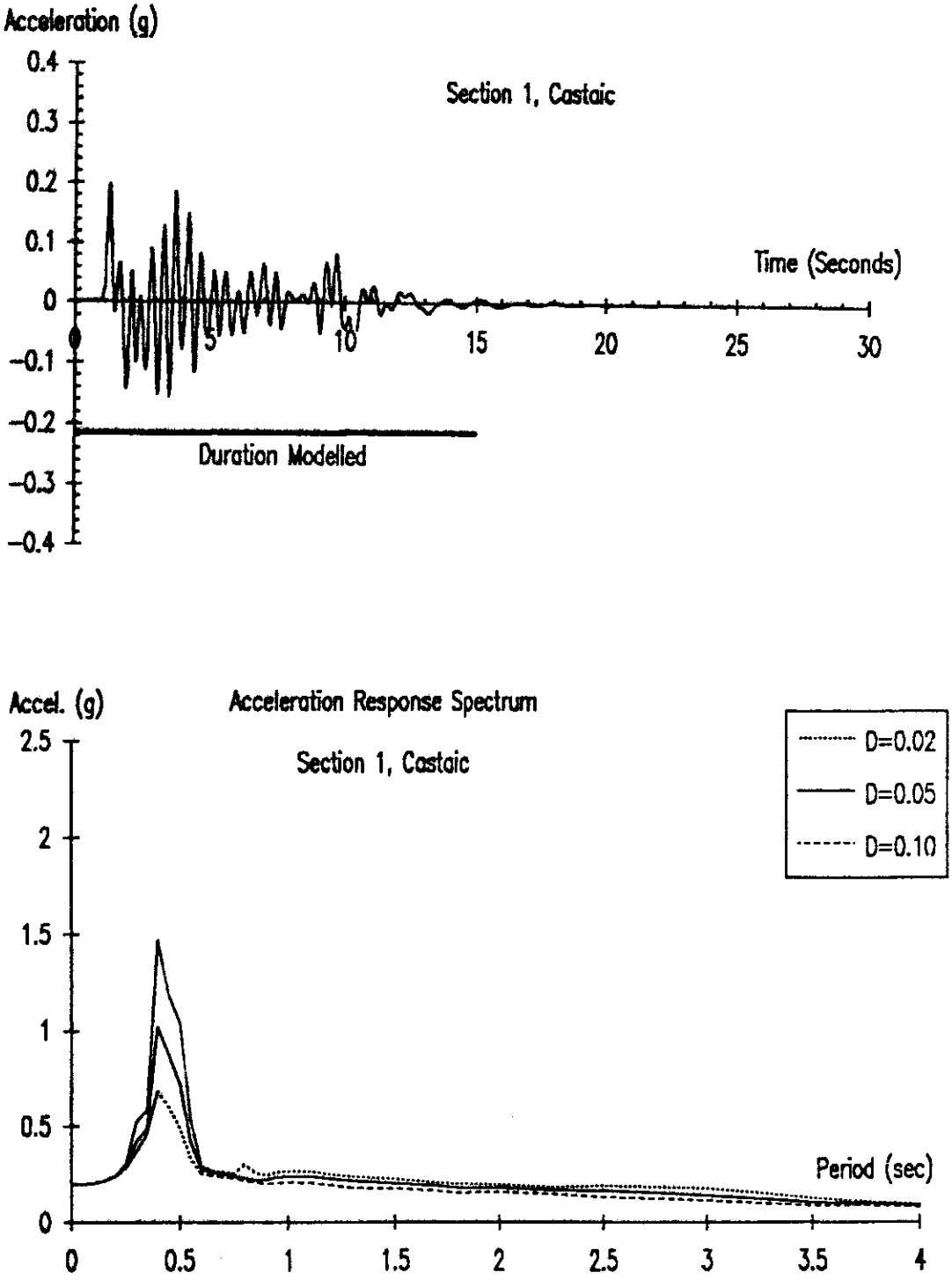

Figure A.1 Acceleration Time-History and Response Spectra for Castaic Earthquake, Section 1 Soil Profile

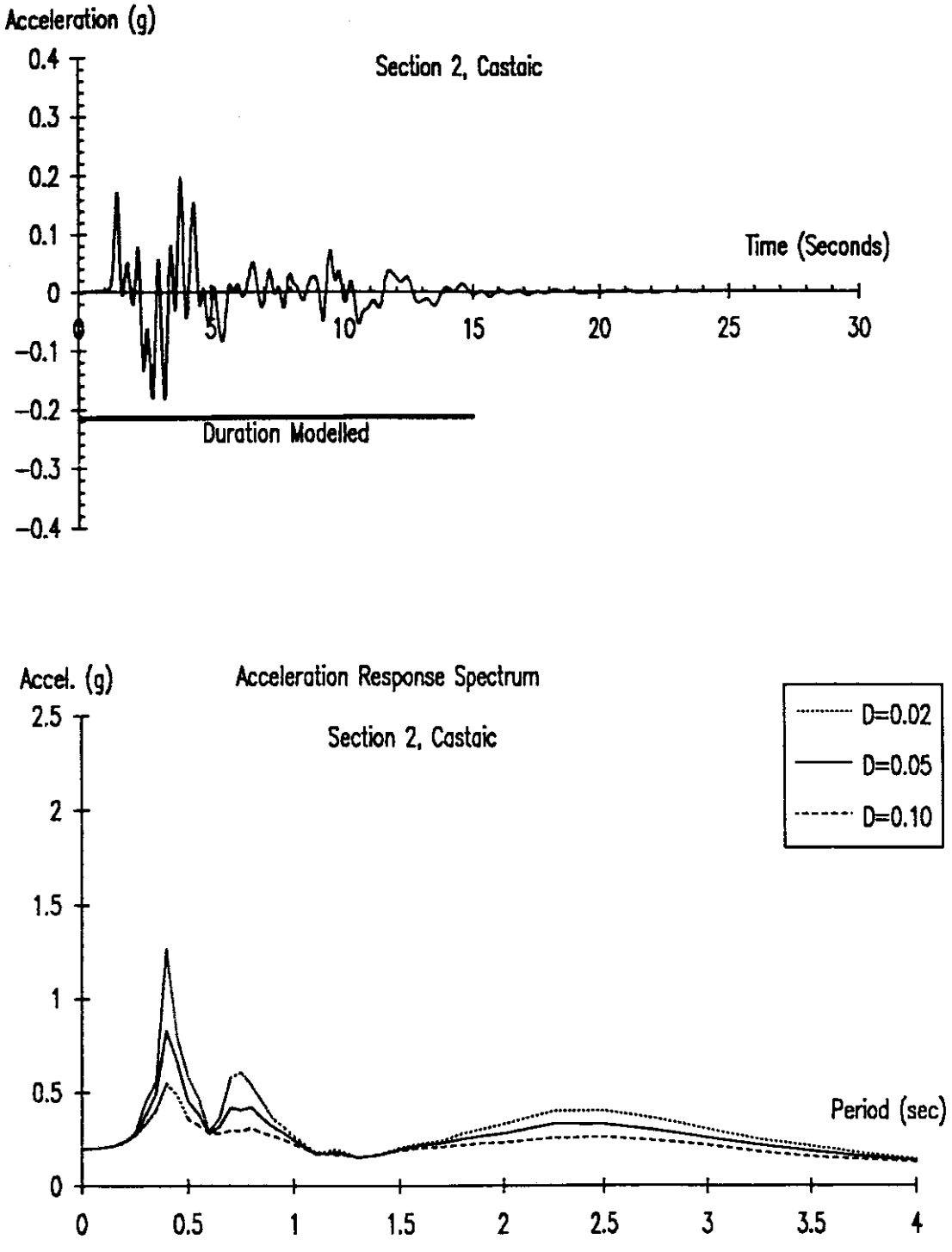

Figure A.2 Acceleration Time-History and Response Spectra for Castaic Earthquake, Section 2 Soil Profile

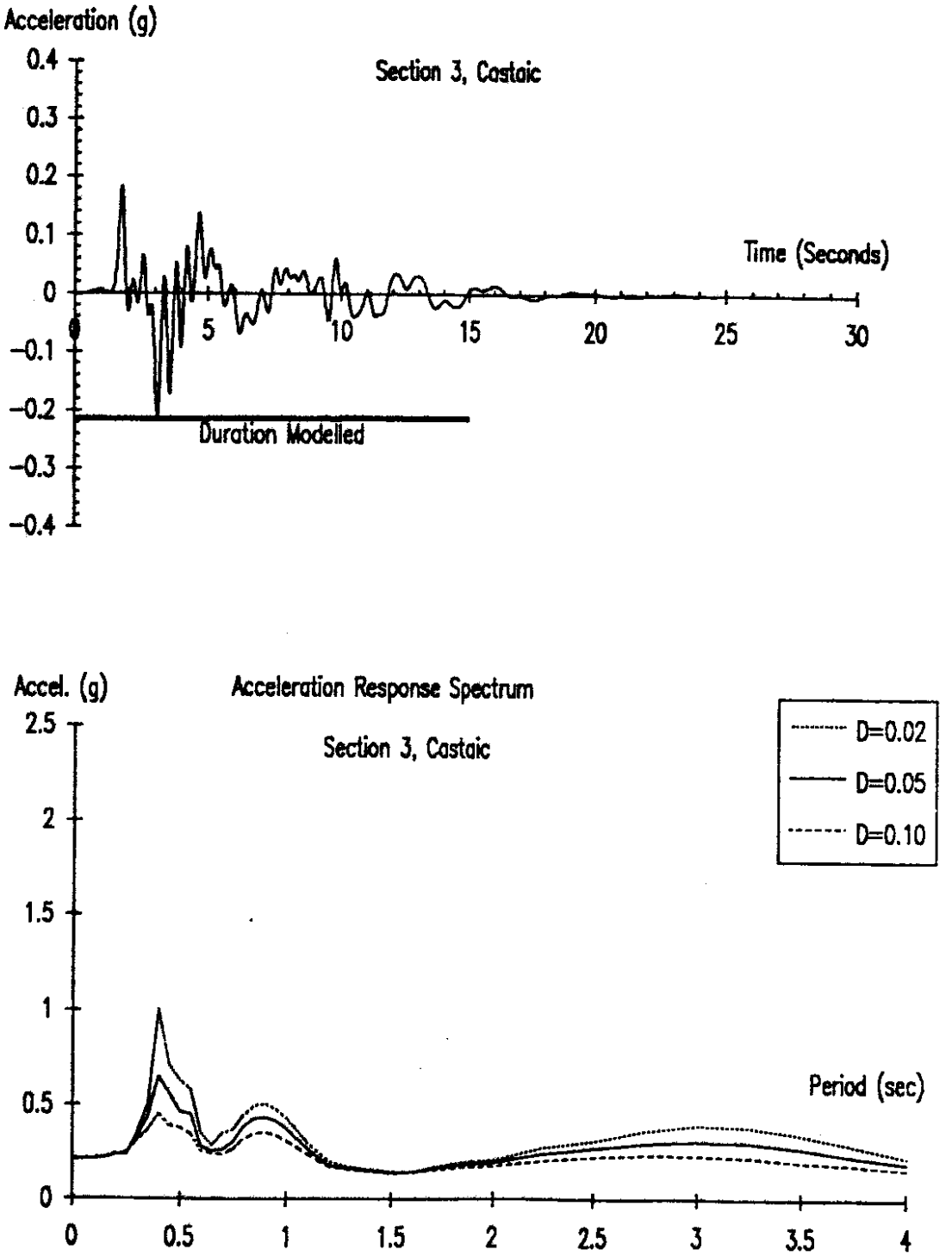

Figure A.3 Acceleration Time-History and Response Spectra for Castaic Earthquake, Section 3 Soil Profile

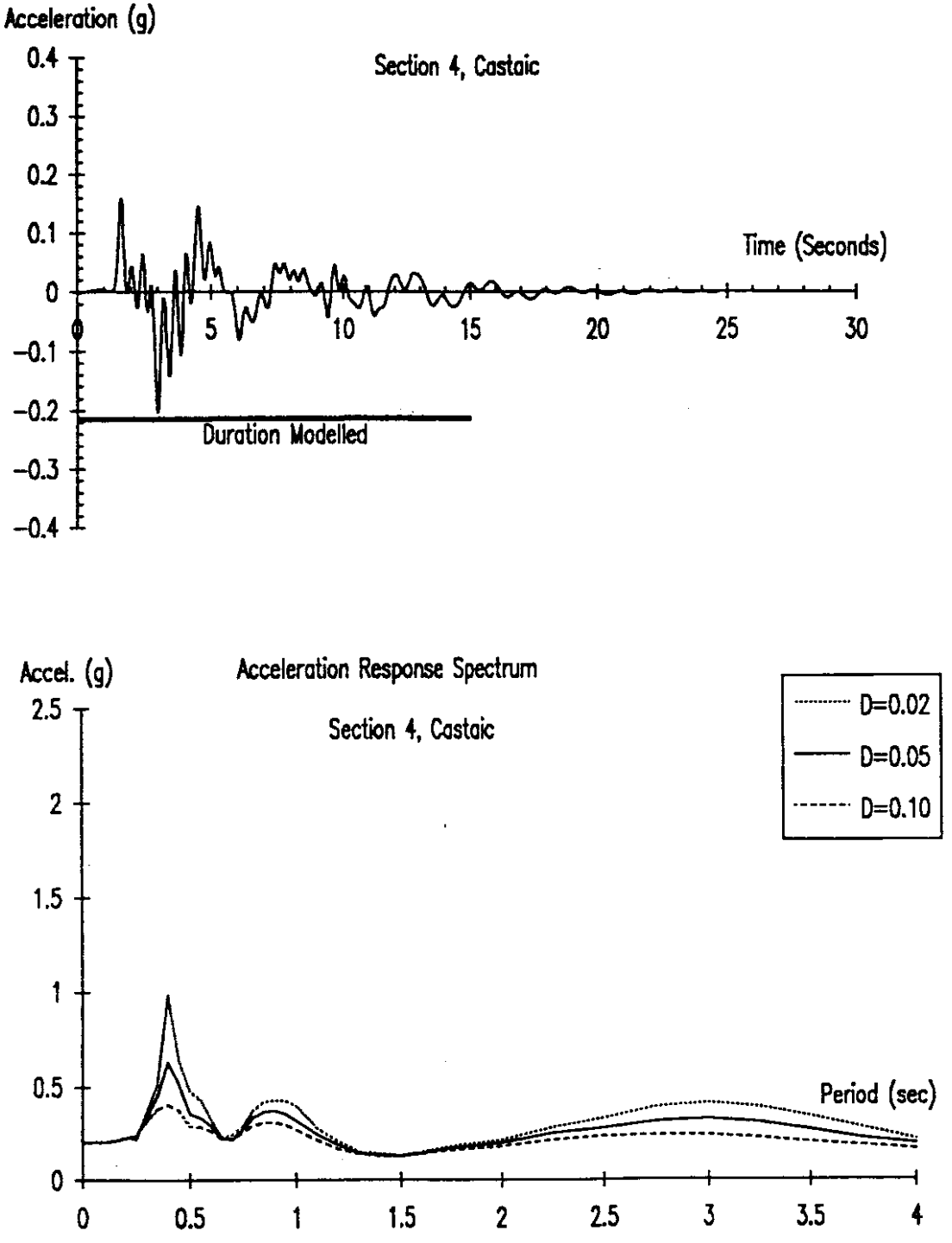

Figure A.4 Acceleration Time-History and Response Spectra for Castaic Earthquake, Section 4 Soil Profile

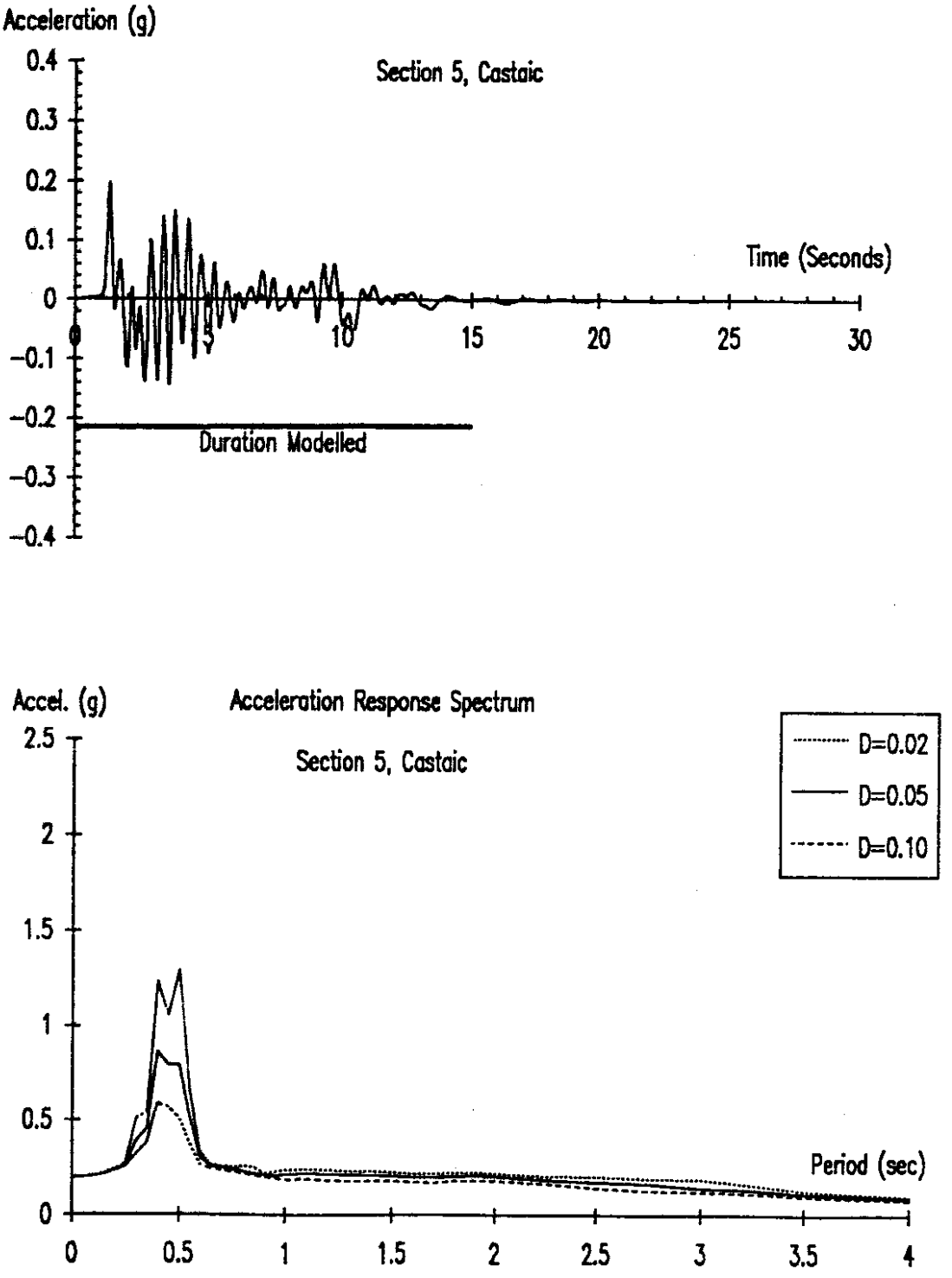

Figure A.5 Acceleration Time-History and Response Spectra for Castaic Earthquake, Section 5 Soil Profile

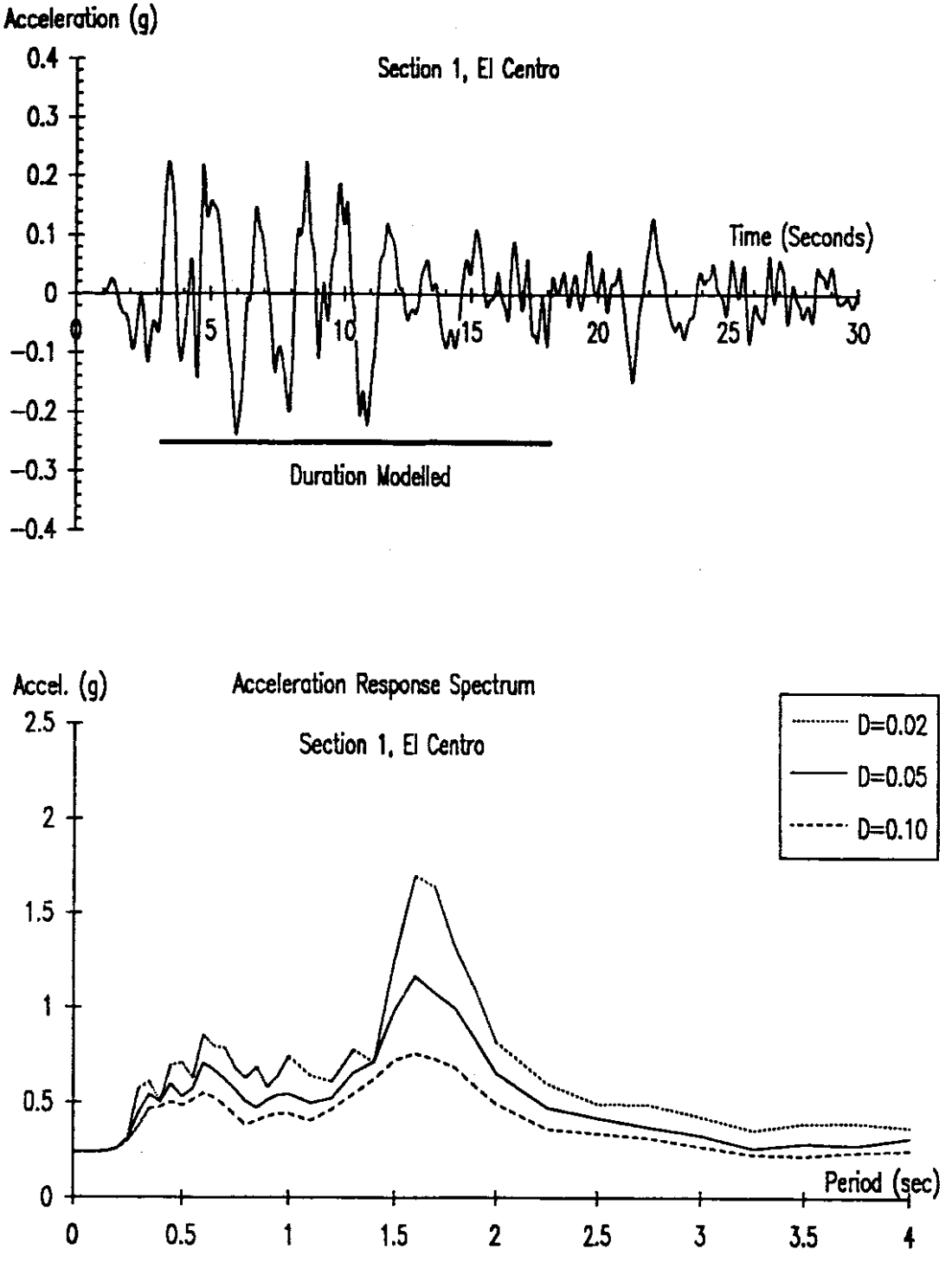

Figure A.6 Acceleration Time-History and Response Spectra for El Centro Earthquake, Section 1 Soil Profile

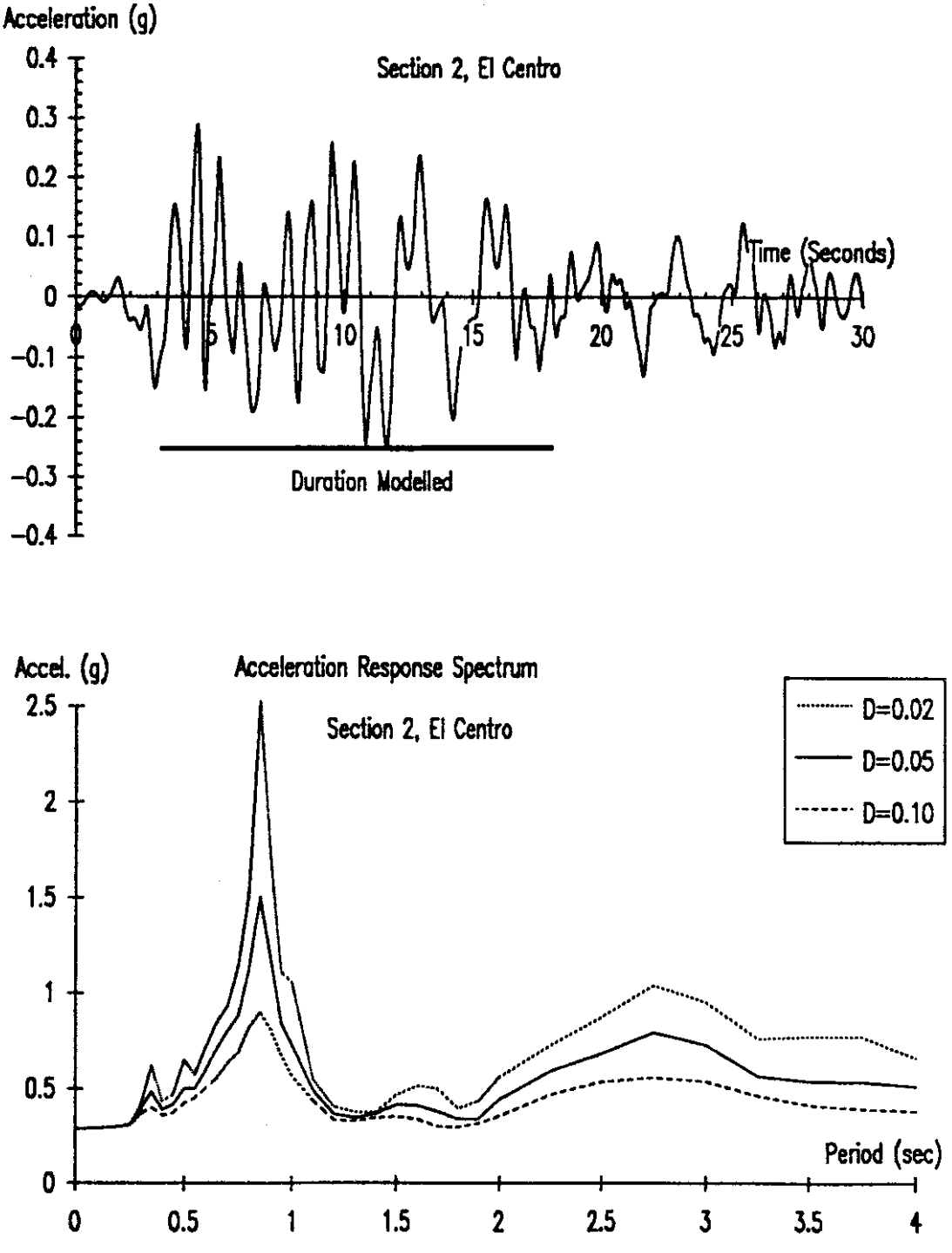

Figure A.7 Acceleration Time-History and Response Spectra for El Centro Earthquake, Section 2 Soil Profile

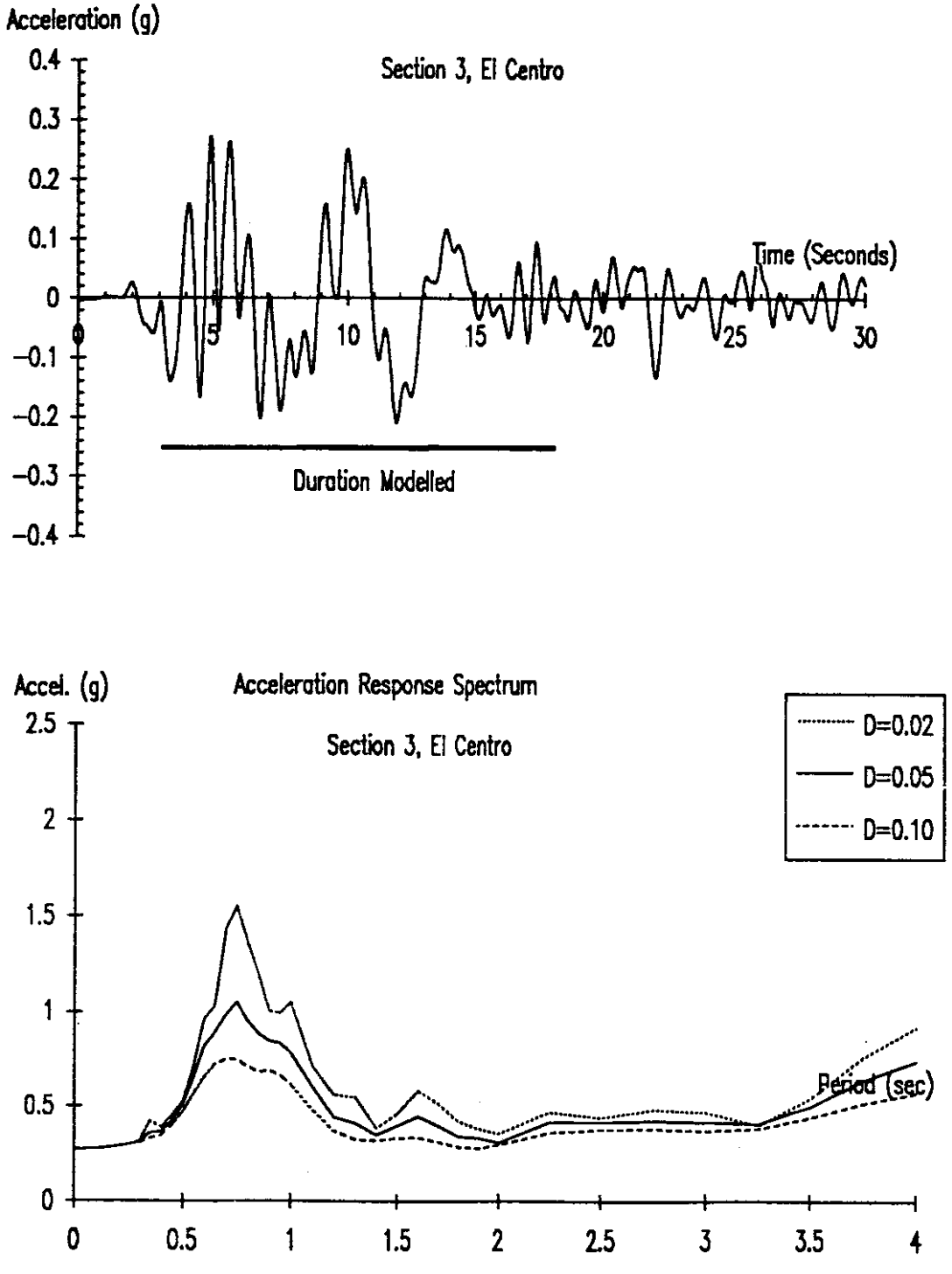

Figure A.8 Acceleration Time-History and Response Spectra for El Centro Earthquake, Section 3 Soil Profile

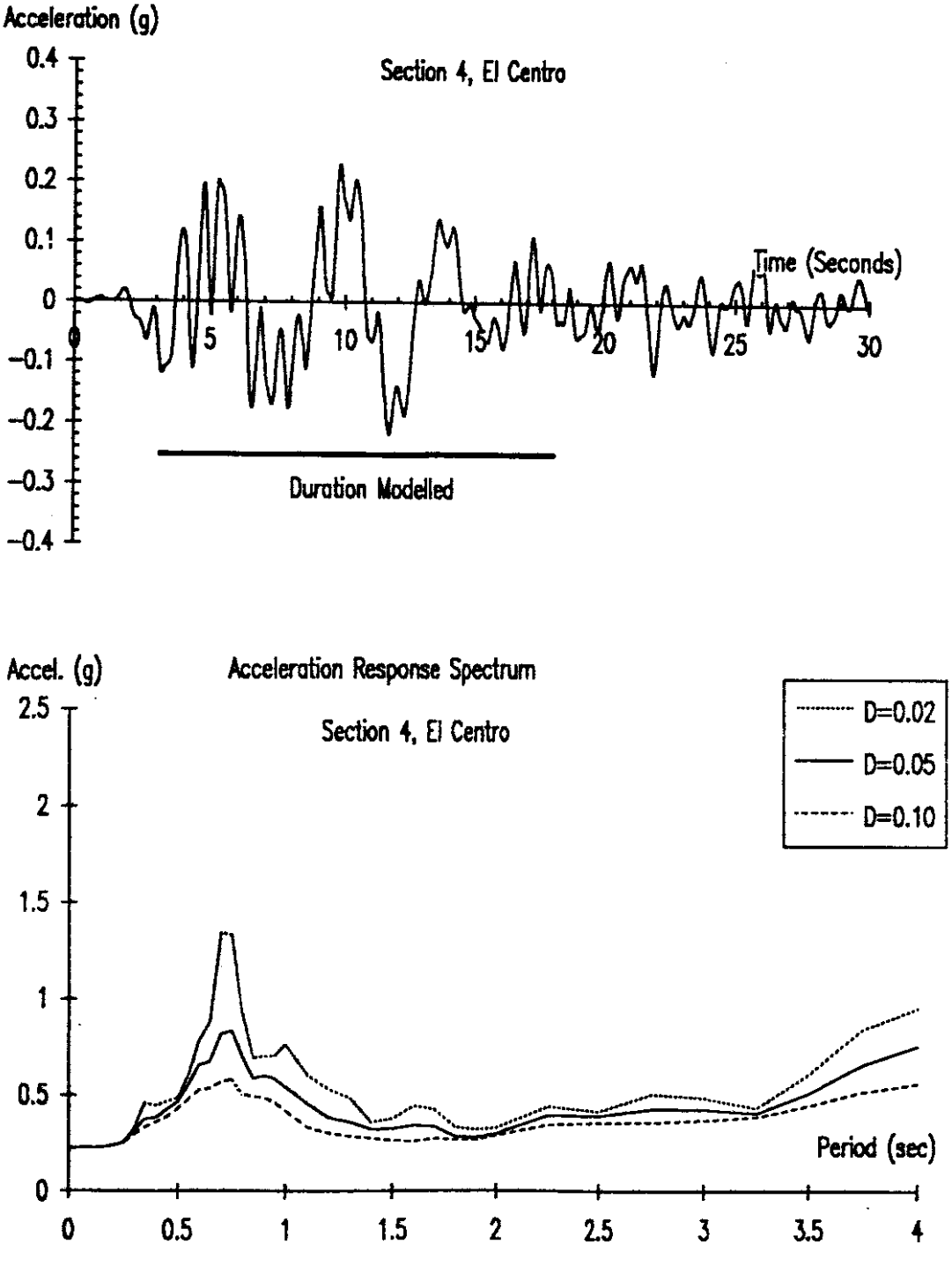

Figure A.9 Acceleration Time-History and Response Spectra for El Centro Earthquake, Section 4 Soil Profile

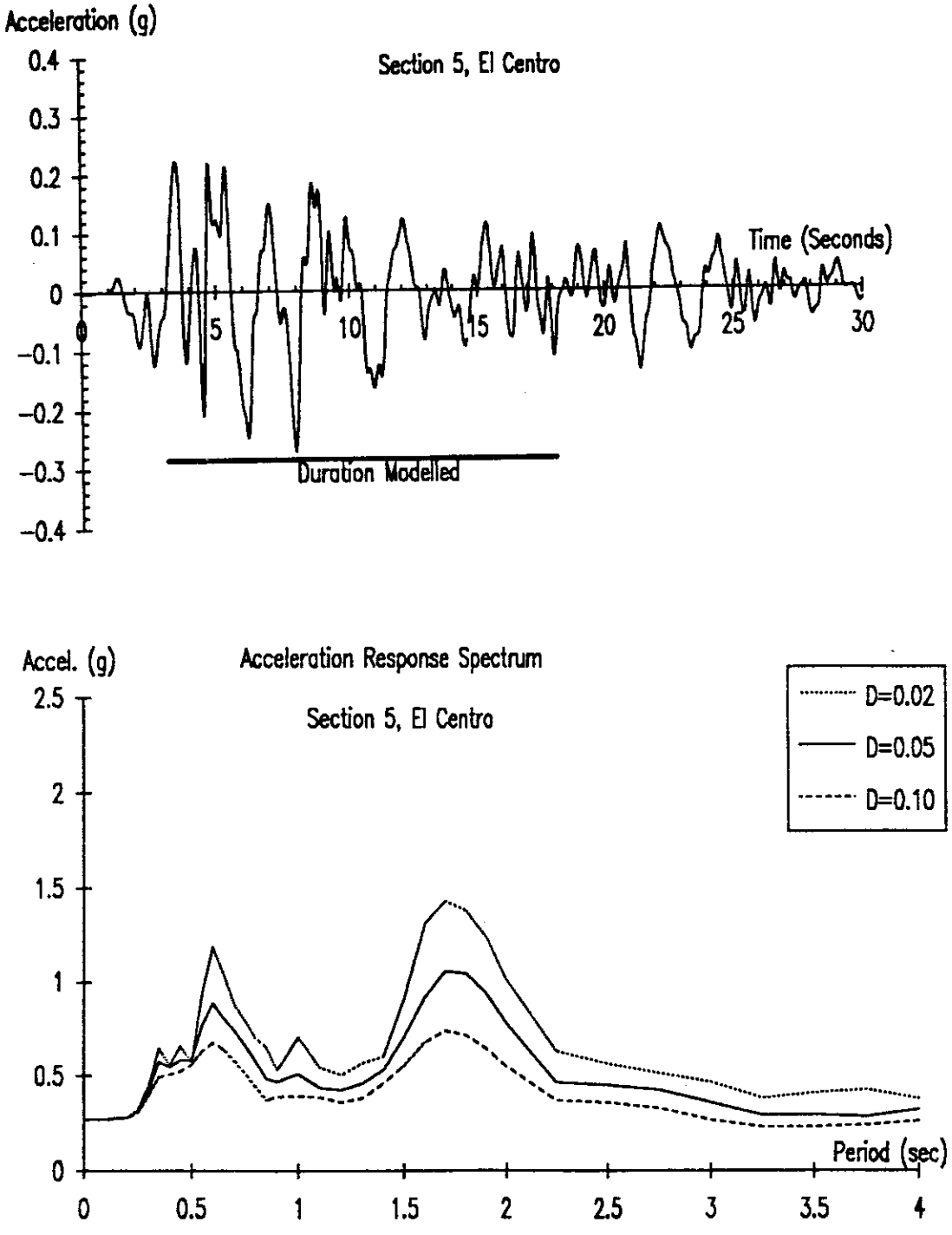

Figure A.10 Acceleration Time-History and Response Spectra for El Centro Earthquake, Section 5 Soil Profile

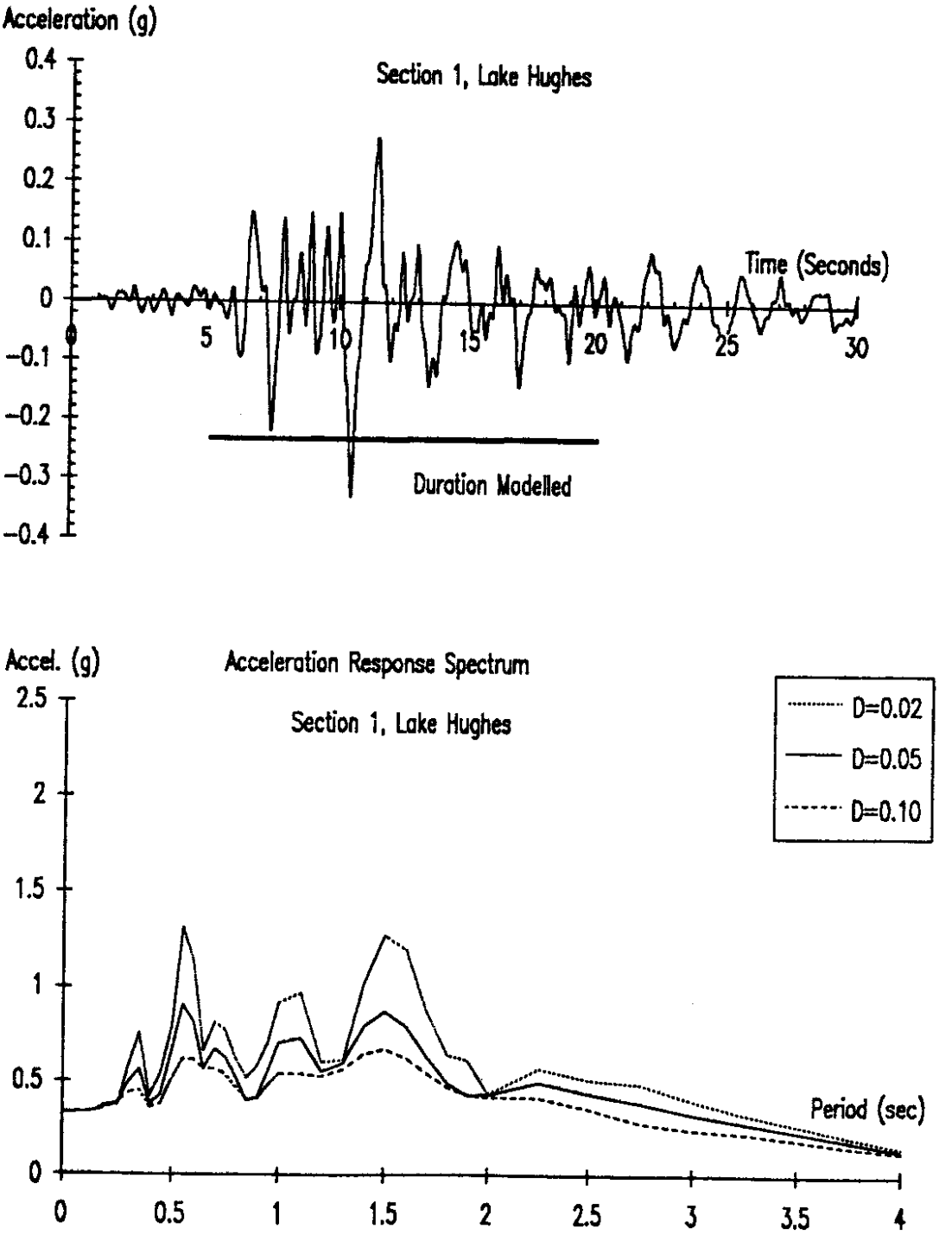

Figure A.11 Acceleration Time-History and Response Spectra for Lake Hughes Earthquake, Section 1 Soil Profile

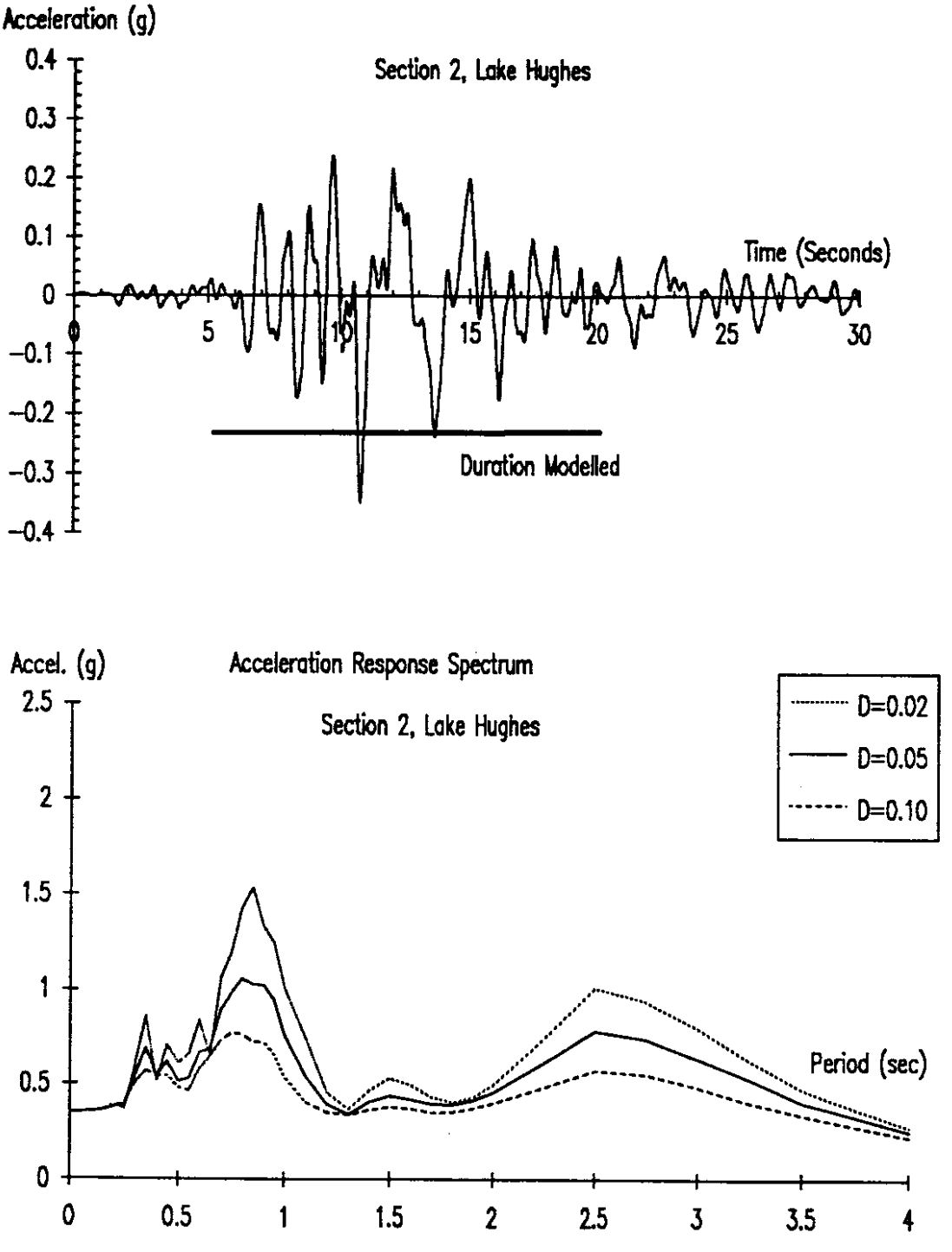

Figure A.12 Acceleration Time-History and Response Spectra for Lake Hughes Earthquake, Section 2 Soil Profile

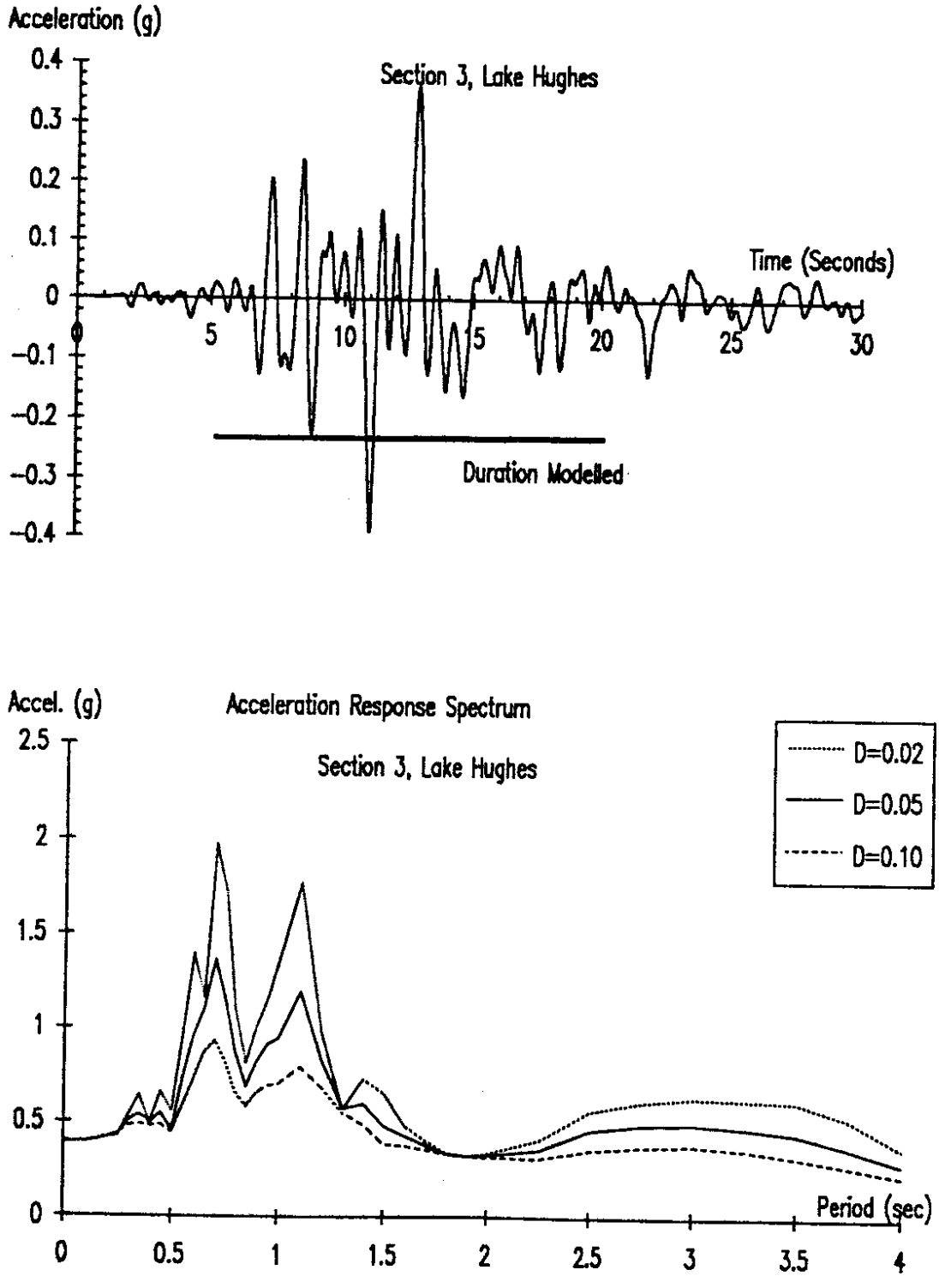

Figure A.13 Acceleration Time-History and Response Spectra for Lake Hughes Earthquake, Section 3 Soil Profile

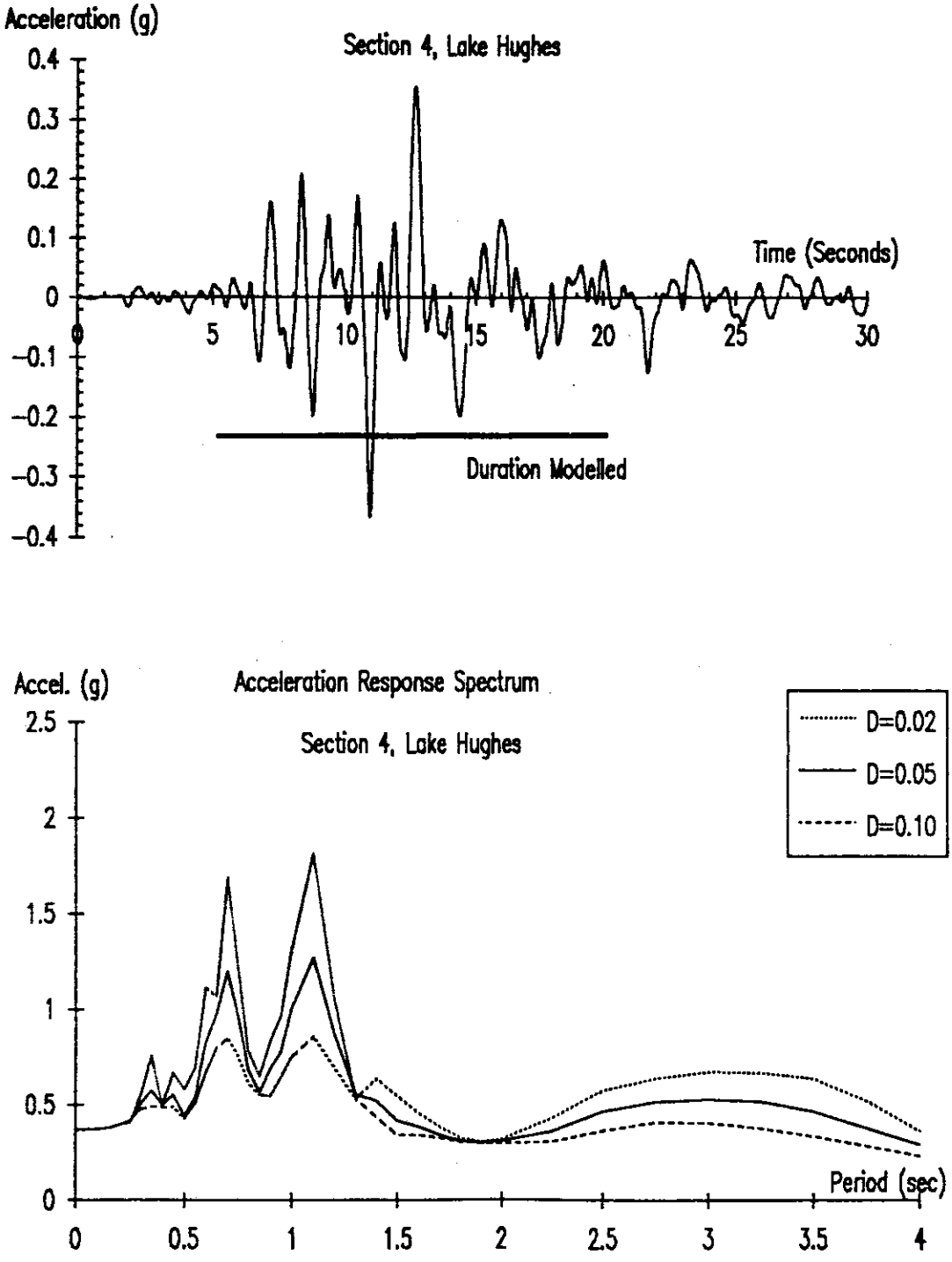

Figure A.14 Acceleration Time-History and Response Spectra for Lake Hughes Earthquake, Section 4 Soil Profile

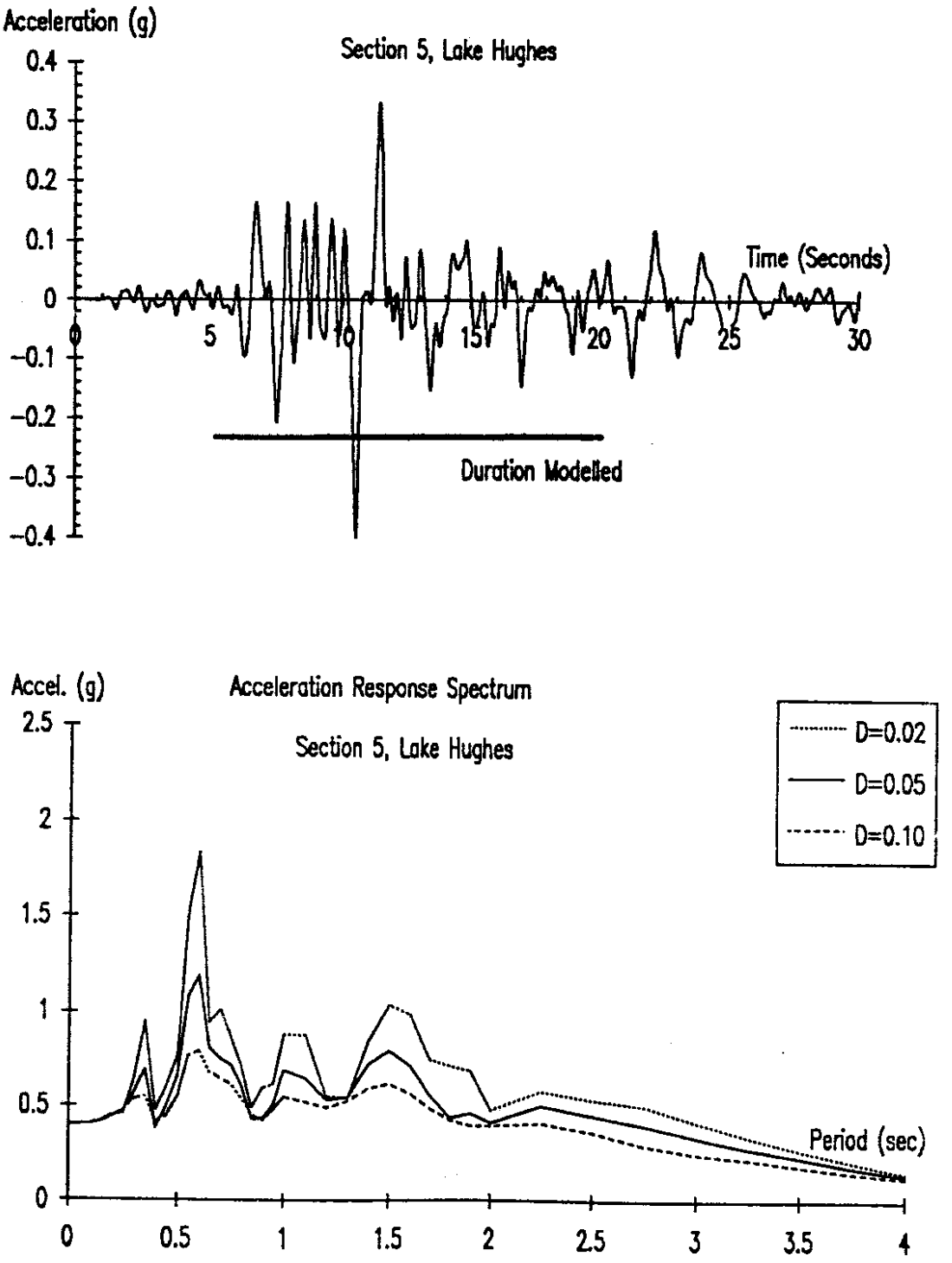

Figure A.15 Acceleration Time-History and Response Spectra for Lake Hughes Earthquake, Section 5 Soil Profile

APPENDIX B

RESULTS FROM TWENTY-SPAN ANALYSES

Two graphs are shown for each of the five soil profiles (sections). The first graph of each pair shows the displacement trace of a point on the superstructure near the center of the spans (the same point monitored in the SEISAB runs) and the ground motion input to the foundation node connected to that point. The bridge node is labelled 10 BRG; the ground node is labelled 110 GND. On the plots where it is difficult to identify the plot lines, the bridge in every case has a larger maximum displacement than the ground. The second plot for each run shows the relative displacement between the superstructure and the ground at the reference point.

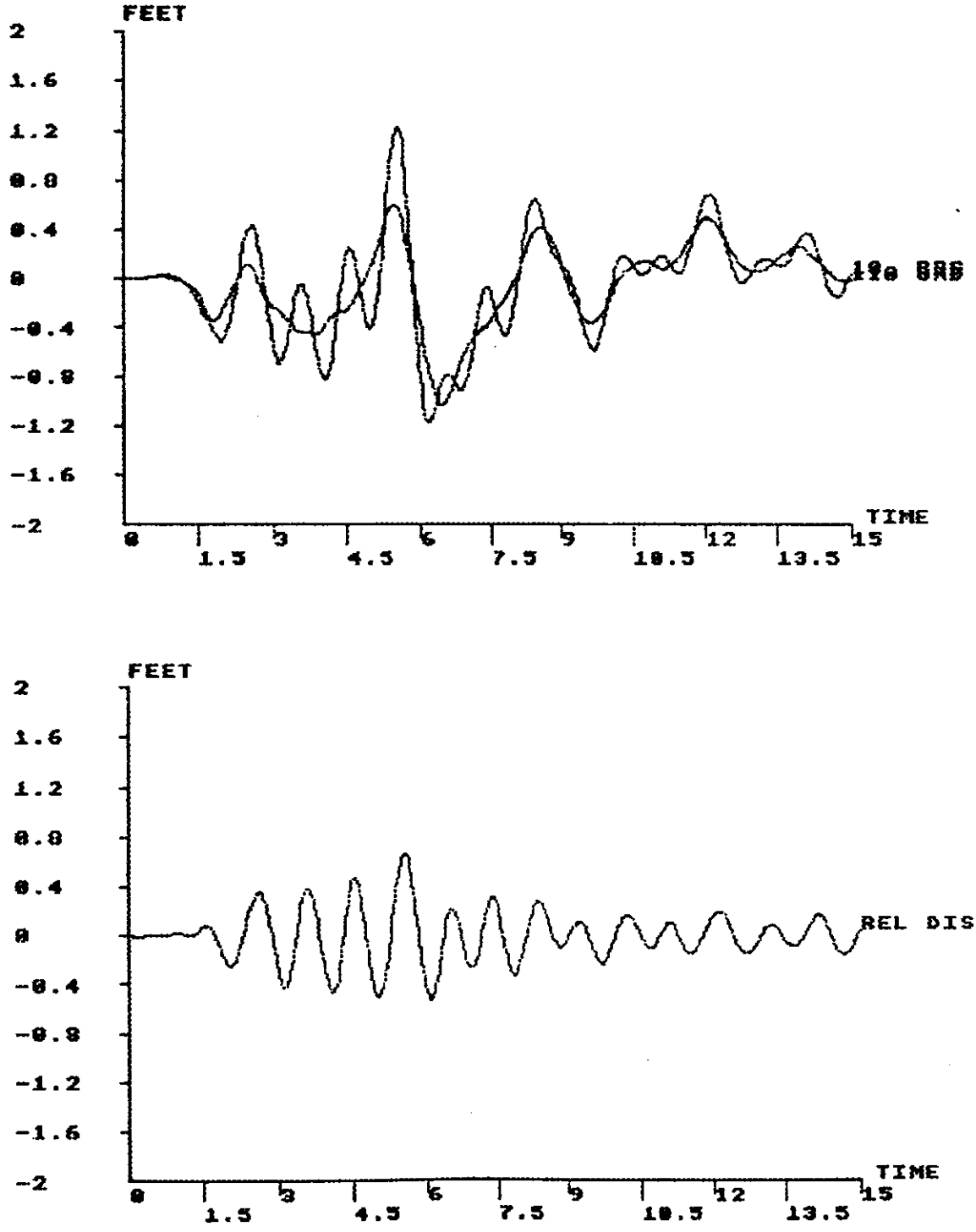

Figure B.1 Transverse Bridge and Ground Nodal Displacements and Relative Transverse Displacement, Lake Hughes Earthquake, Section 1 Soil Profile Twenty-Span Model

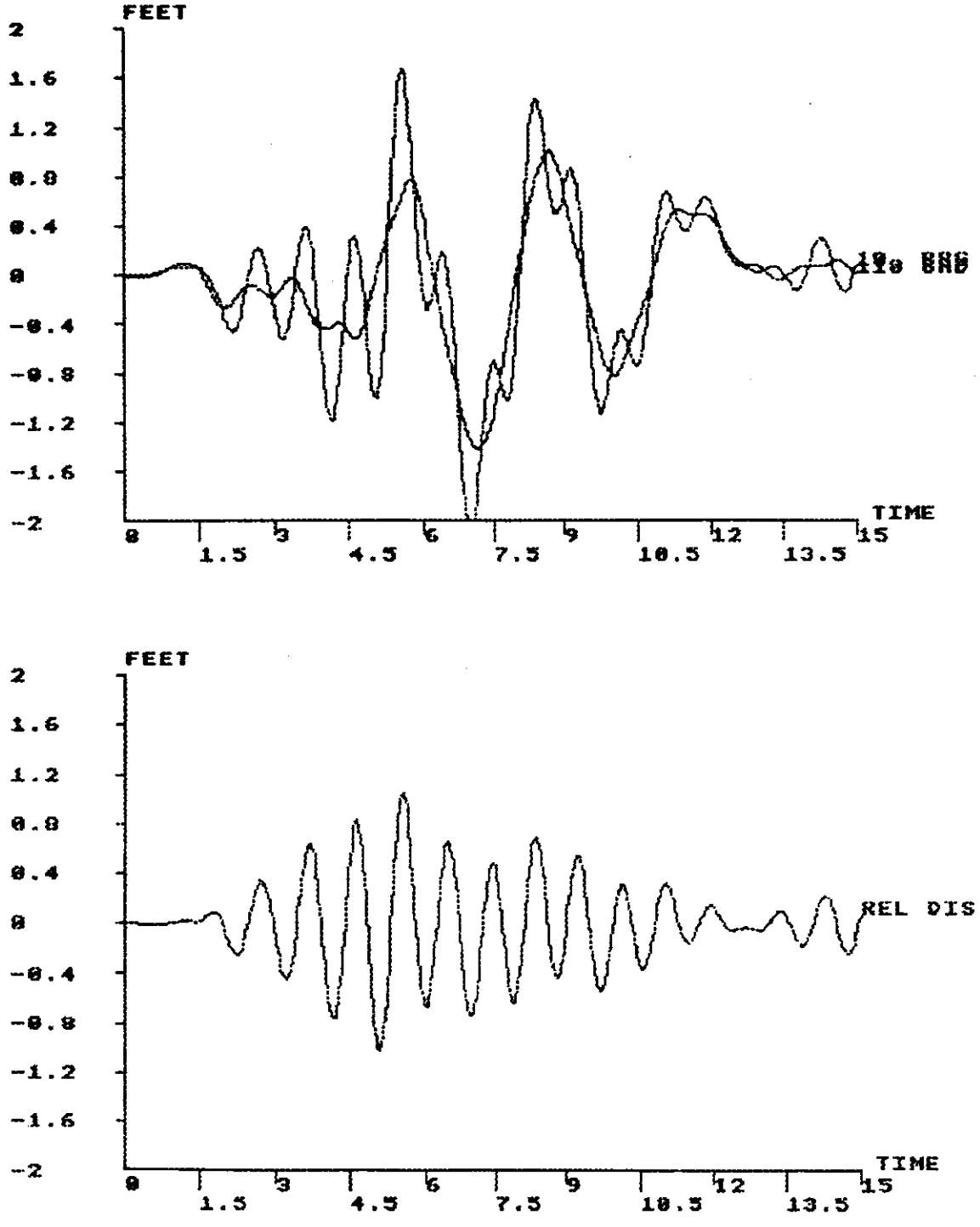

Figure B.2 Transverse Bridge and Ground Nodal Displacements and Relative Transverse Displacement, Lake Hughes Earthquake, Section 2 Soil Profile Twenty-Span Model

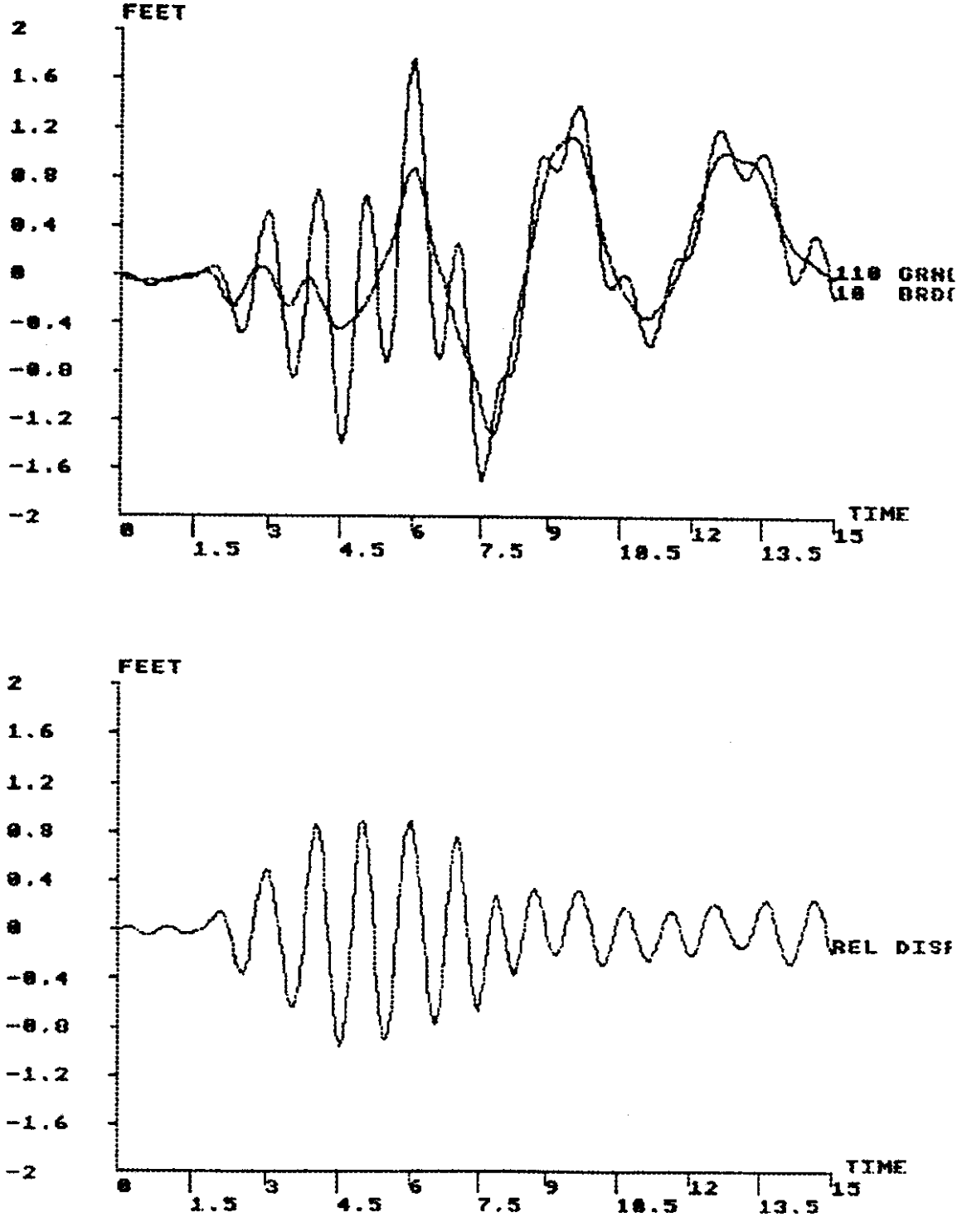

Figure B.3 Transverse Bridge and Ground Nodal Displacements and Relative Transverse Displacement, Lake Hughes Earthquake, Section 3 Soil Profile Twenty-Span Model

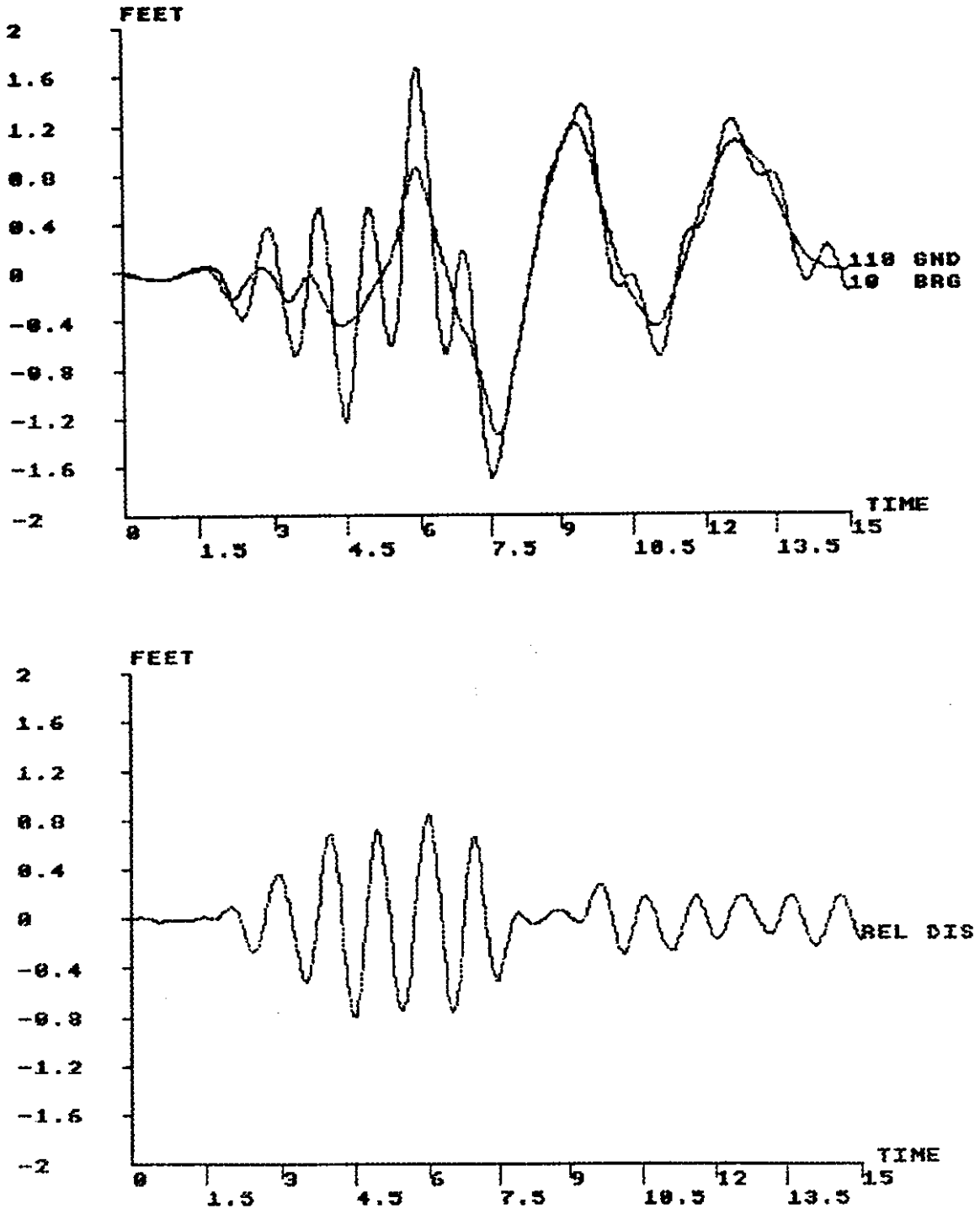

Figure B.4 Transverse Bridge and Ground Nodal Displacements and Relative Transverse Displacement, Lake Hughes Earthquake, Section 4 Soil Profile Twenty-Span Model

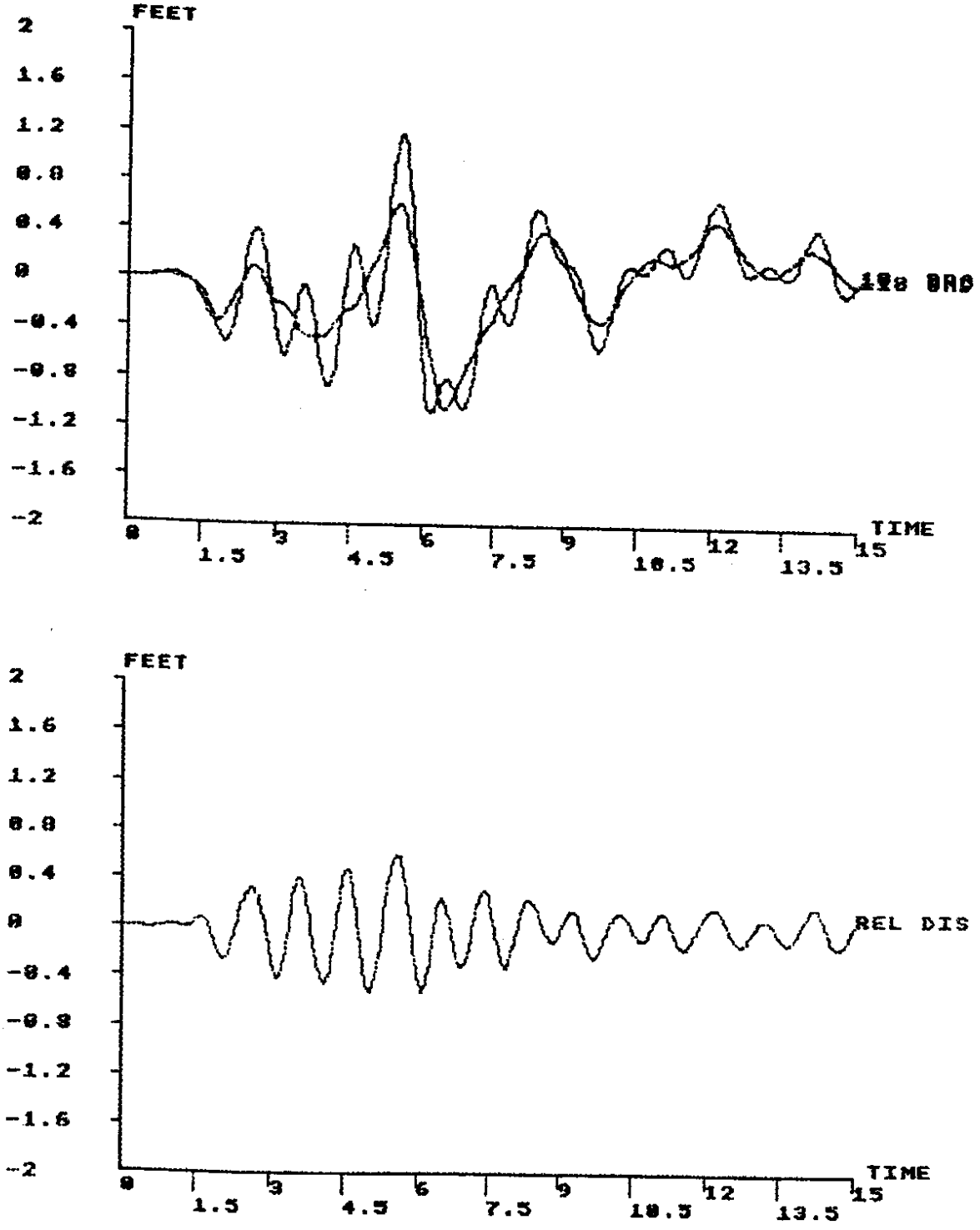

Figure B.5 Transverse Bridge and Ground Nodal Displacements and Relative Transverse Displacement, Lake Hughes Earthquake, Section 5 Soil Profile Twenty-Span Model

APPENDIX C

RESULTS OF SIXTY-FOUR-SPAN ANALYSES WITH DIFFERENT SEISMIC INPUT

Two graphs are shown for each of the five regions of different ground motion input. The first graph shows a time-history plot of the displacement of a point on the bridge and of the corresponding point on the ground surface below. The second is plot of the relative displacement of the two nodes. The bridge node has the lower number and is identified with the BRG label. The ground node has a number 200 larger than the corresponding bridge node and is identified with the GND label. Where the labels are difficult to read, the bridge motion has the larger displacements. Traces are presented for five bridge/ground node pairs. These nodes are each at the center of the area of application of each of the ground motion inputs. Nodes 6 and 206 are at the middle of the first eight spans, where the section 1 Lake Hughes ground motion was applied. Nodes 24 and 224 are at the middle of the second eight spans, where the section 2 ground motion input was applied. Nodes 78 and 278 are at the middle of the sixty-four-span model, where section 3 ground motion was applied. Nodes 114 and 314 are in the middle of the second to last eight spans, where section 4 input was applied. Nodes 132 and 332 are in the middle of the last eight spans, where section 5 input was used.

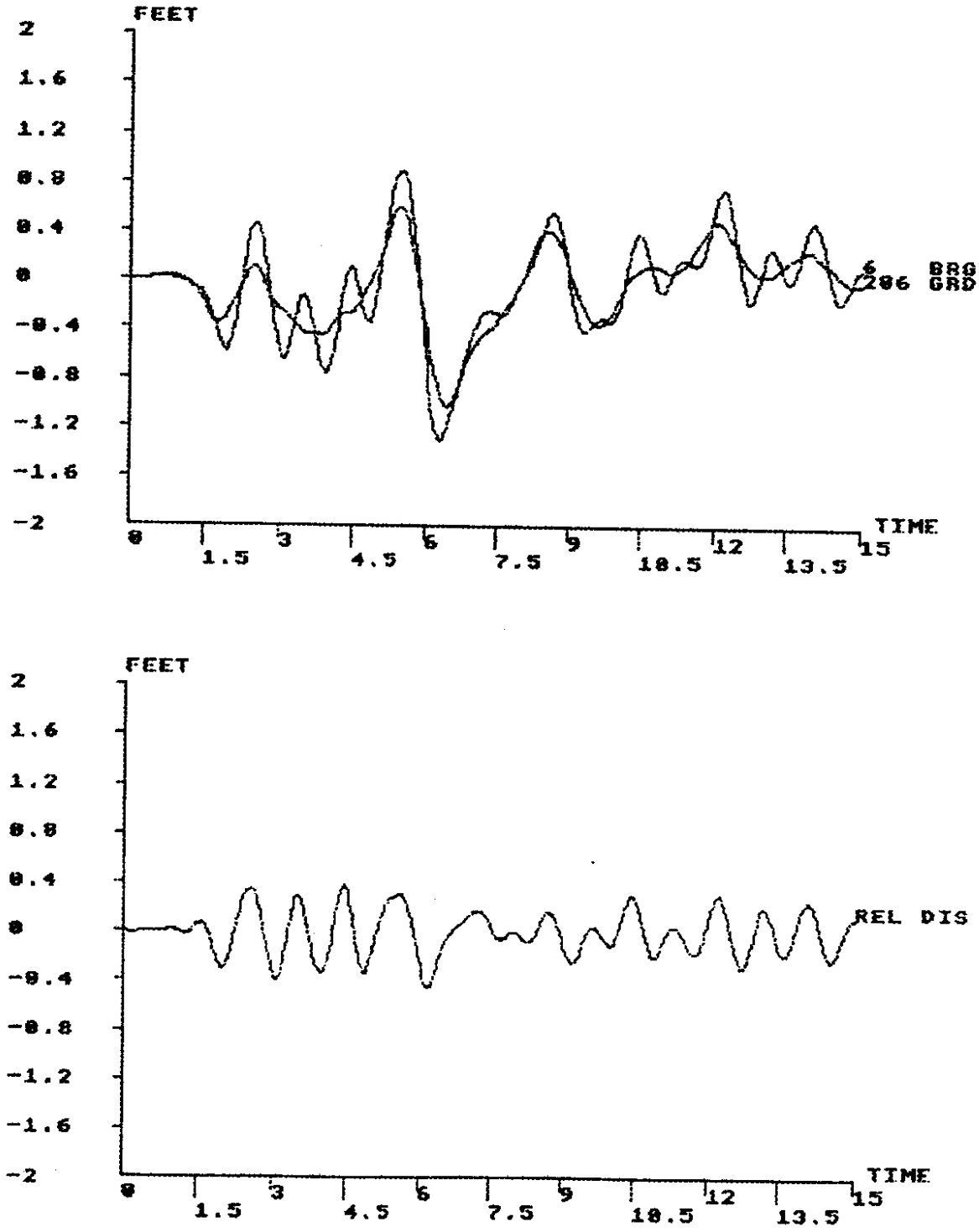

Figure C.1 Transverse Bridge and Ground Nodal Displacements and Relative Transverse Displacement, Lake Hughes Earthquake, Section 1 Sixty-Four-Span Model

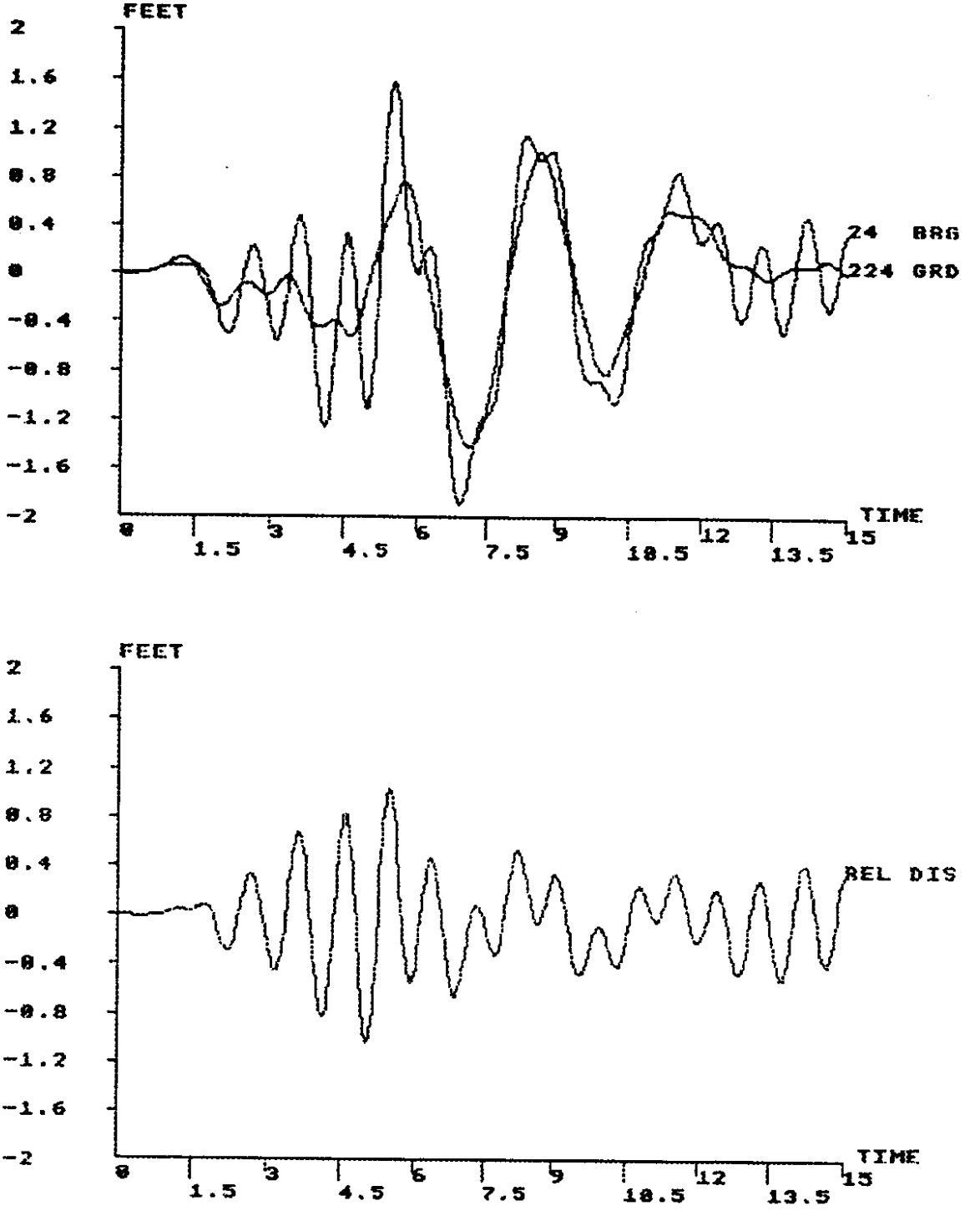

Figure C.2 Transverse Bridge and Ground Nodal Displacements and Relative Transverse Displacement, Lake Hughes Earthquake, Section 2 Sixty-Four-Span Model

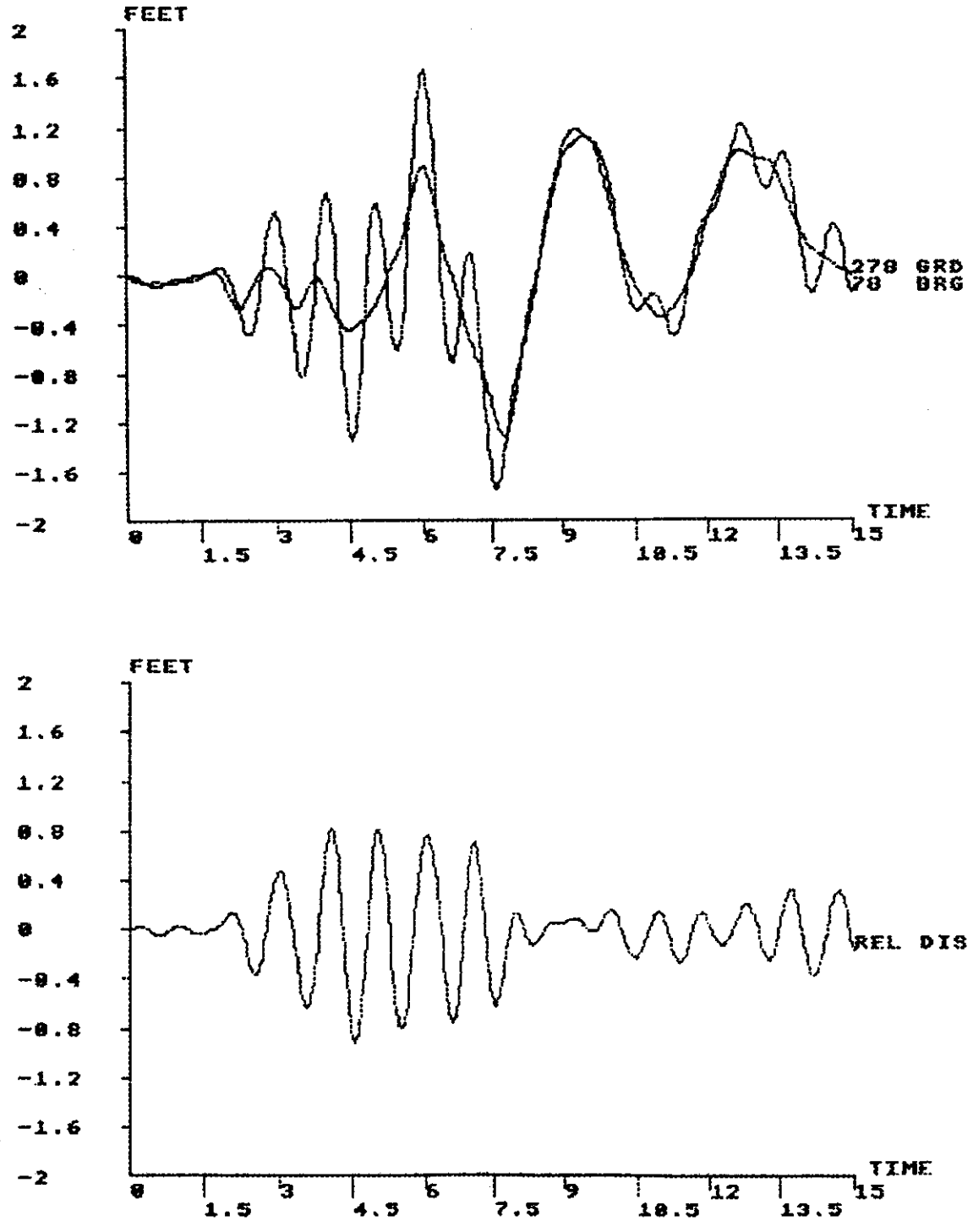

Figure C.3 Transverse Bridge and Ground Nodal Displacements and Relative Transverse Displacement, Lake Hughes Earthquake, Section 3 Sixty-Four-Span Model

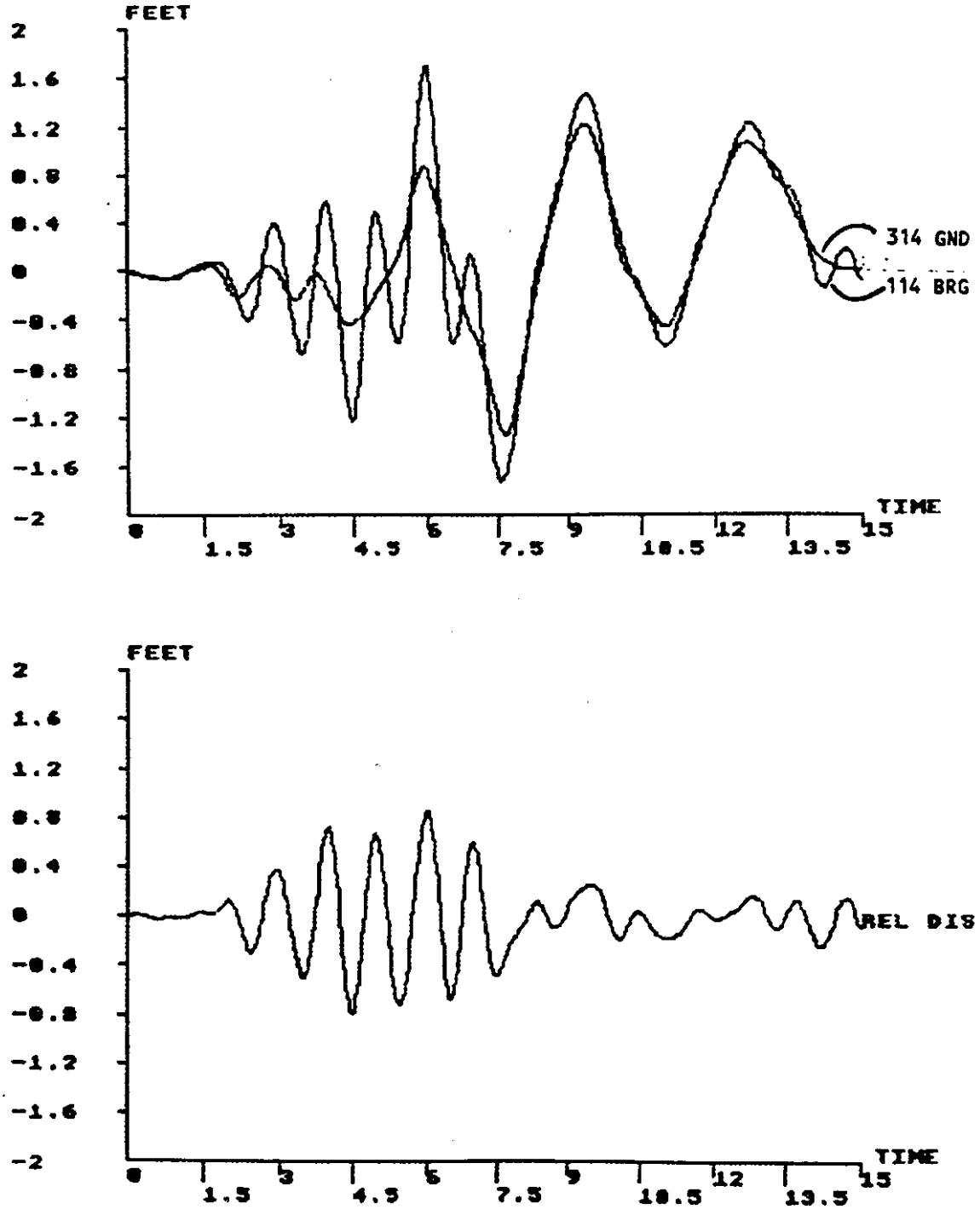

Figure C.4 Transverse Bridge and Ground Nodal Displacements and Relative Transverse Displacement, Lake Hughes Earthquake, Section 4 Sixty-Four-Span Model

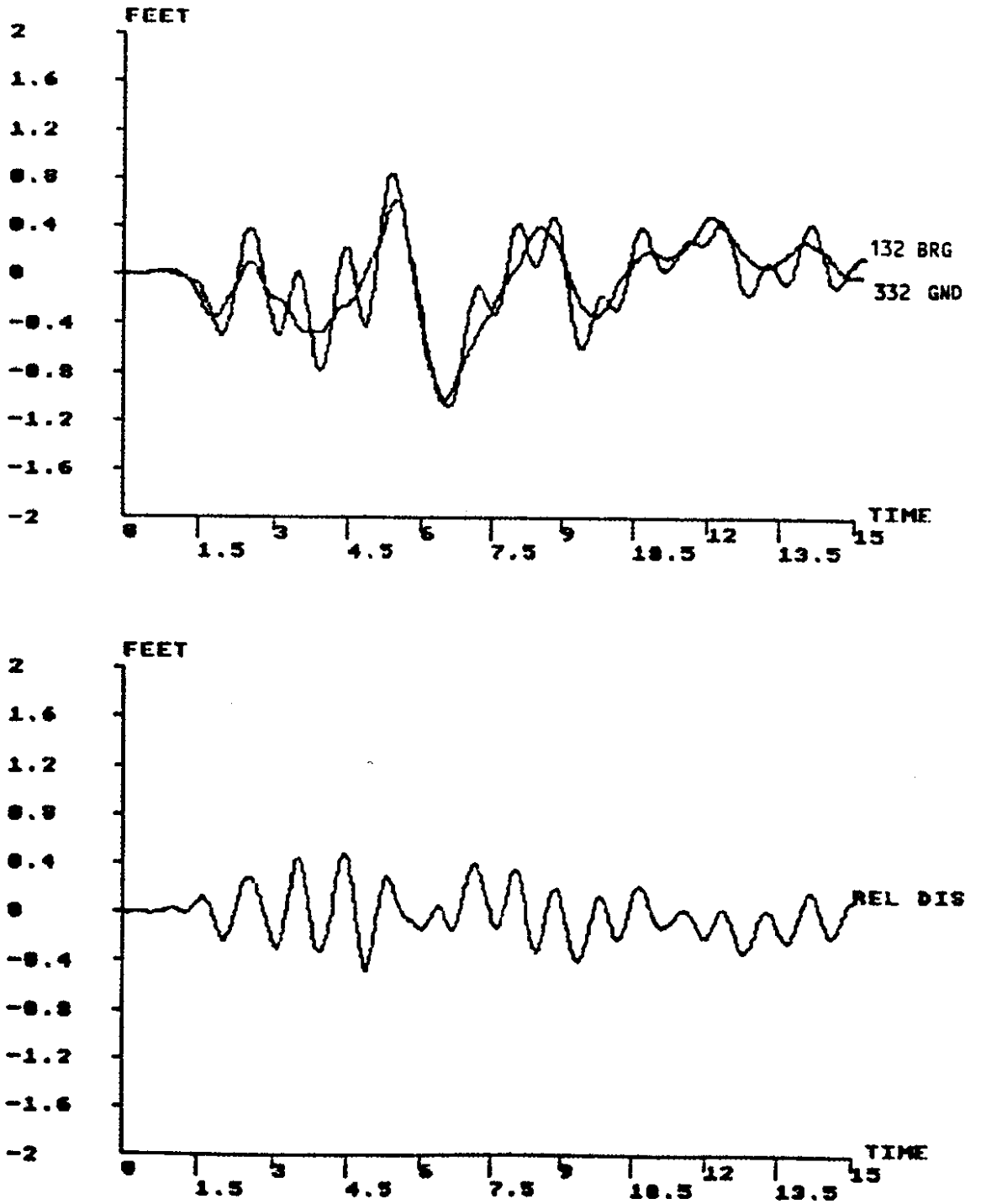

Figure C.5 Transverse Bridge and Ground Nodal Displacements and Relative Transverse Displacement, Lake Hughes Earthquake, Section 5 Sixty-Four-Span Model

APPENDIX D

RESULTS OF SIXTY-FOUR-SPAN ANALYSES

WITH TIME-DELAYED SEISMIC INPUT

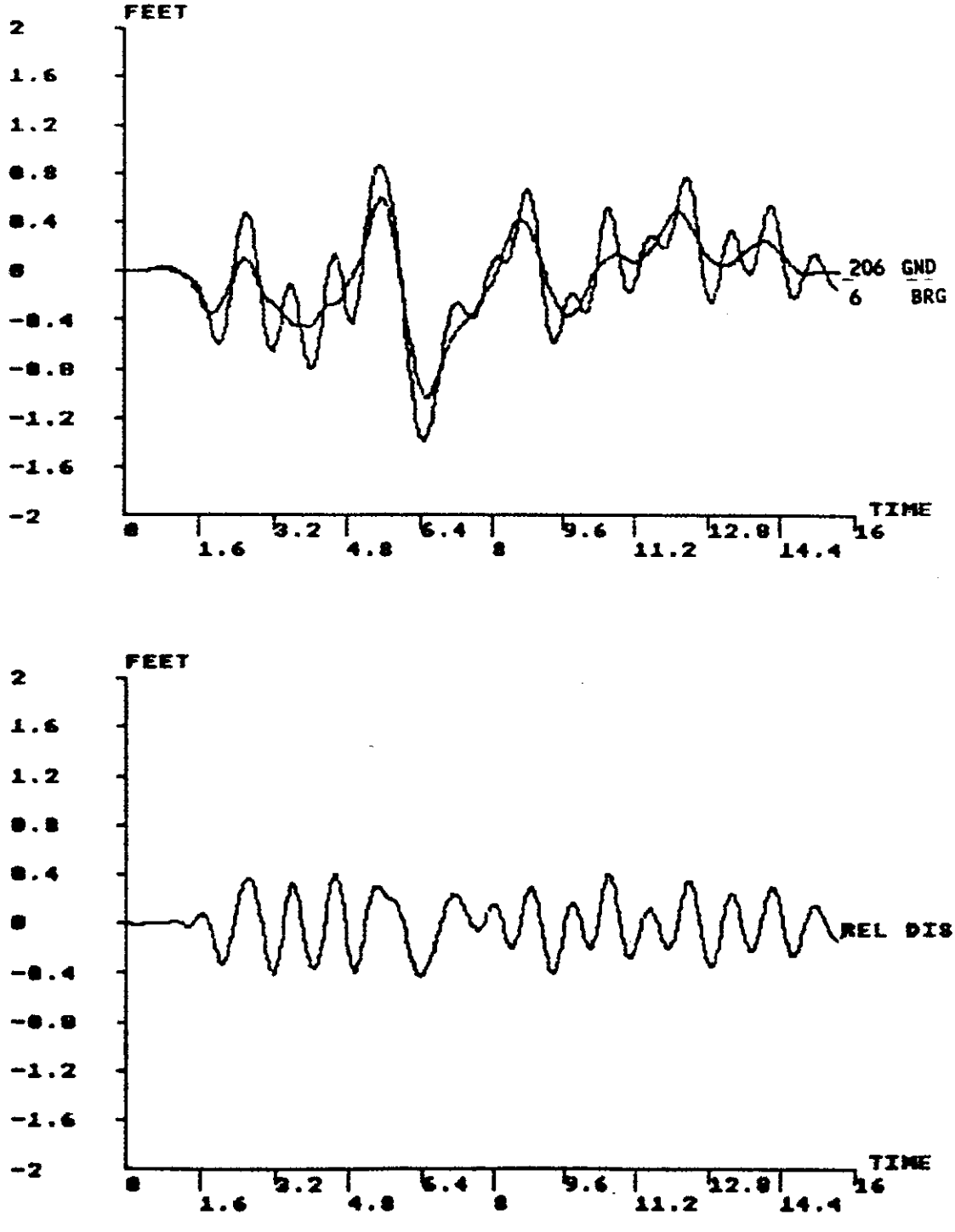

Figure D.1 Transverse Bridge and Ground Nodal Displacements and Relative Transverse Displacement, Lake Hughes Earthquake, Section 1 Sixty-Four-Span Model, Time-Delayed Input

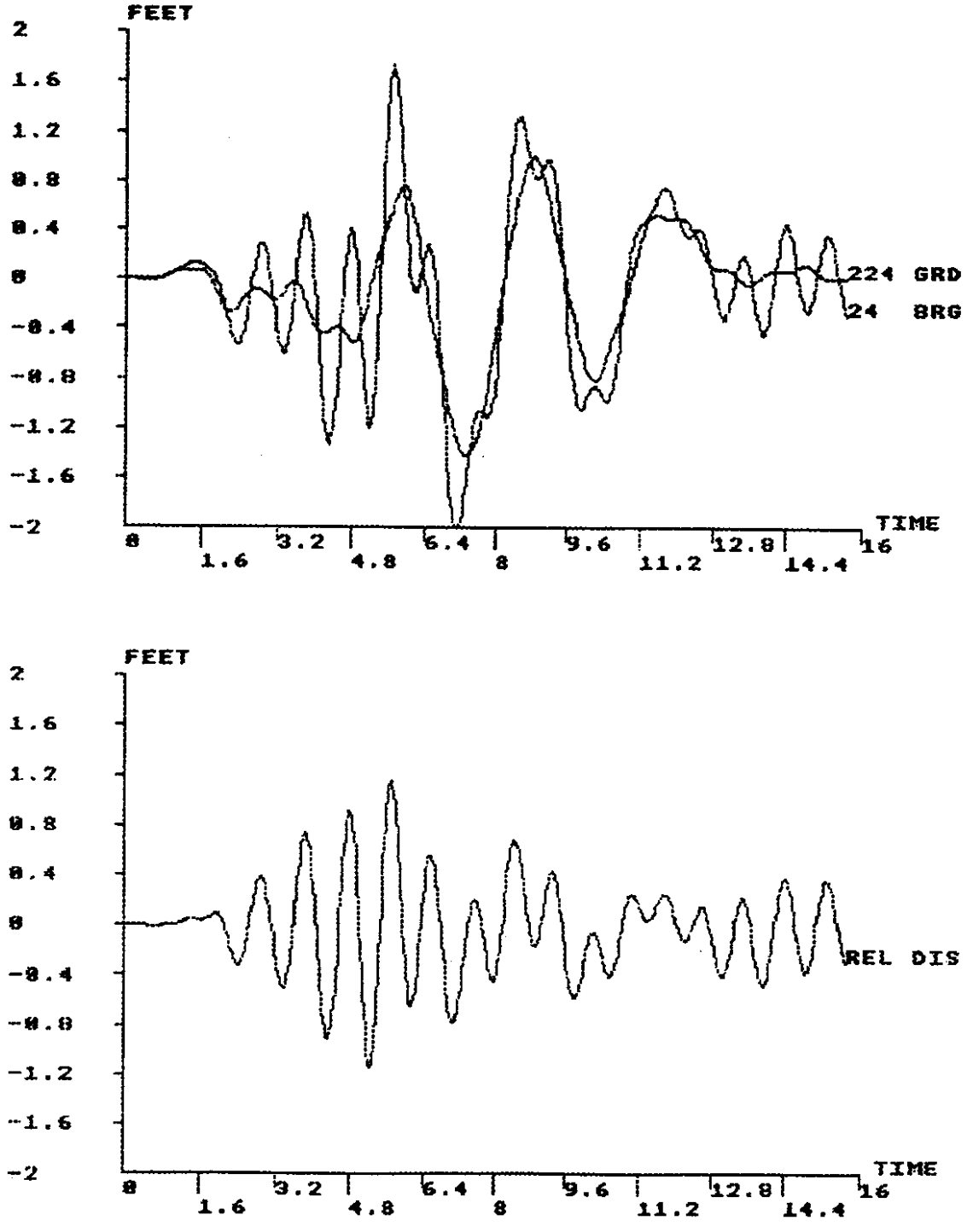

Figure D.2 Transverse Bridge and Ground Nodal Displacements and Relative Transverse Displacement, Lake Hughes Earthquake, Section 2 Sixty-Four-Span Model, Time-Delayed Input

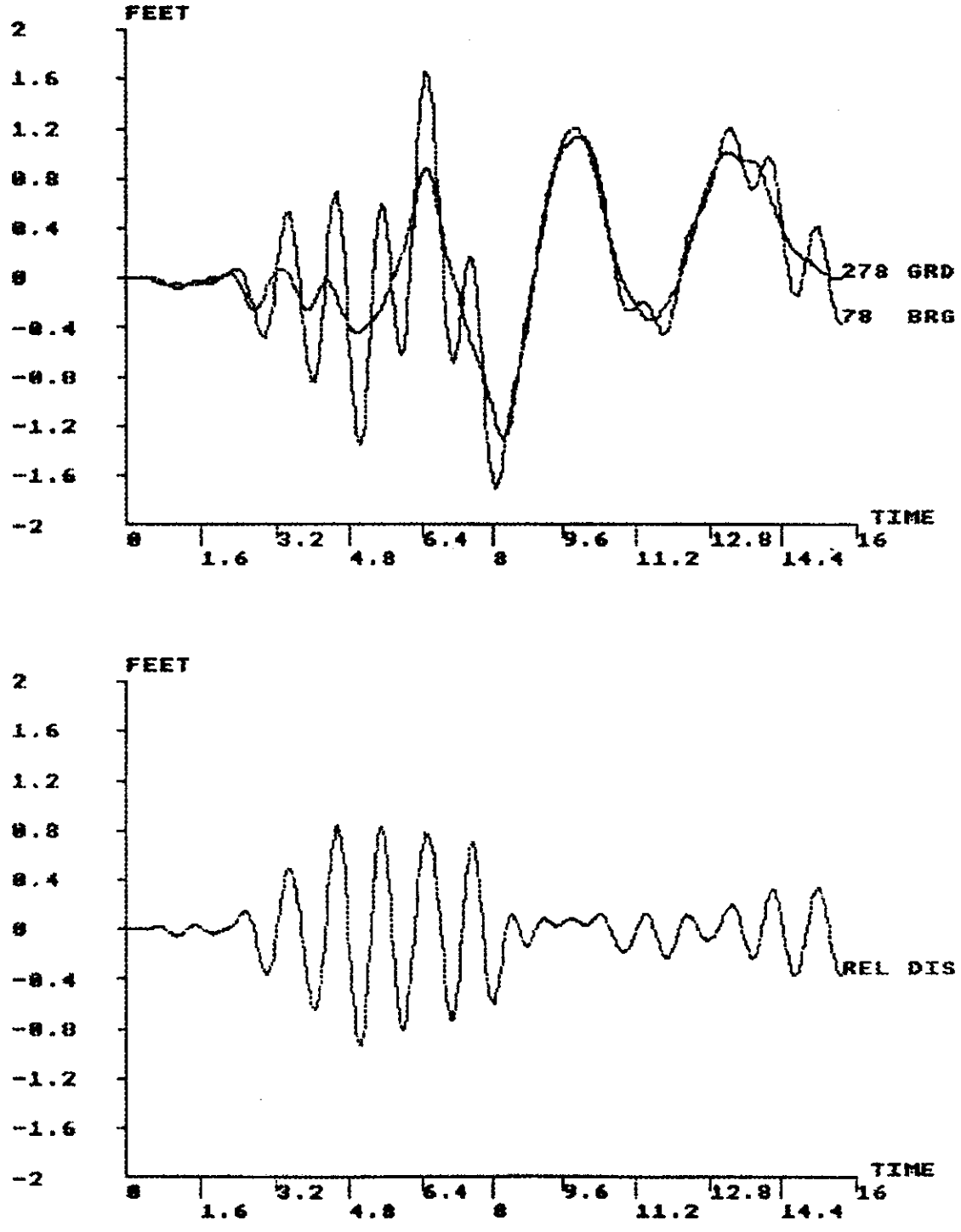

Figure D.3 Transverse Bridge and Ground Nodal Displacements and Relative Transverse Displacement, Lake Hughes Earthquake, Section 3 Sixty-Four-Span Model, Time-Delayed Input

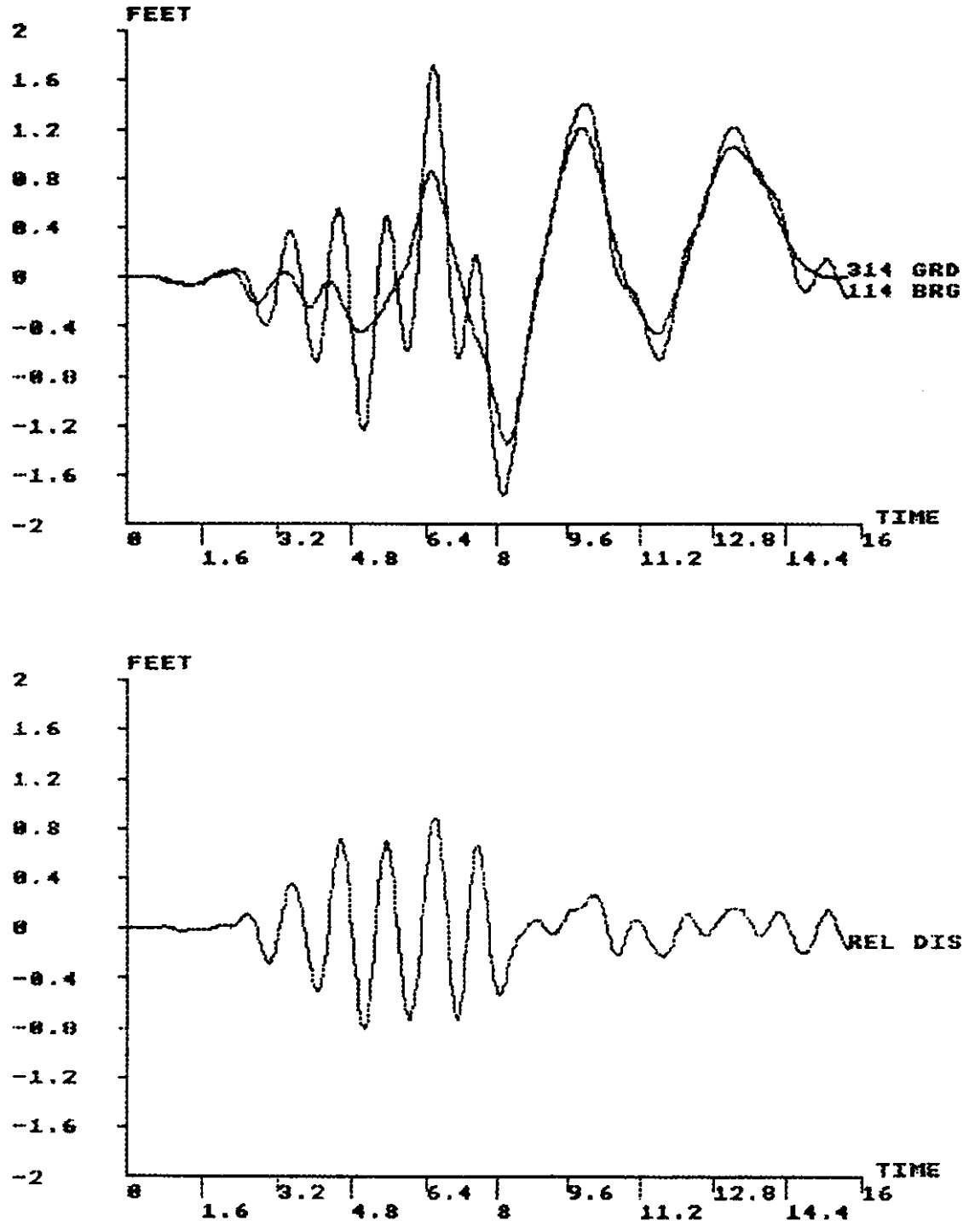

Figure D.4 Transverse Bridge and Ground Nodal Displacements and Relative Transverse Displacement, Lake Hughes Earthquake, Section 4 Sixty-Four-Span Model, Time-Delayed Input

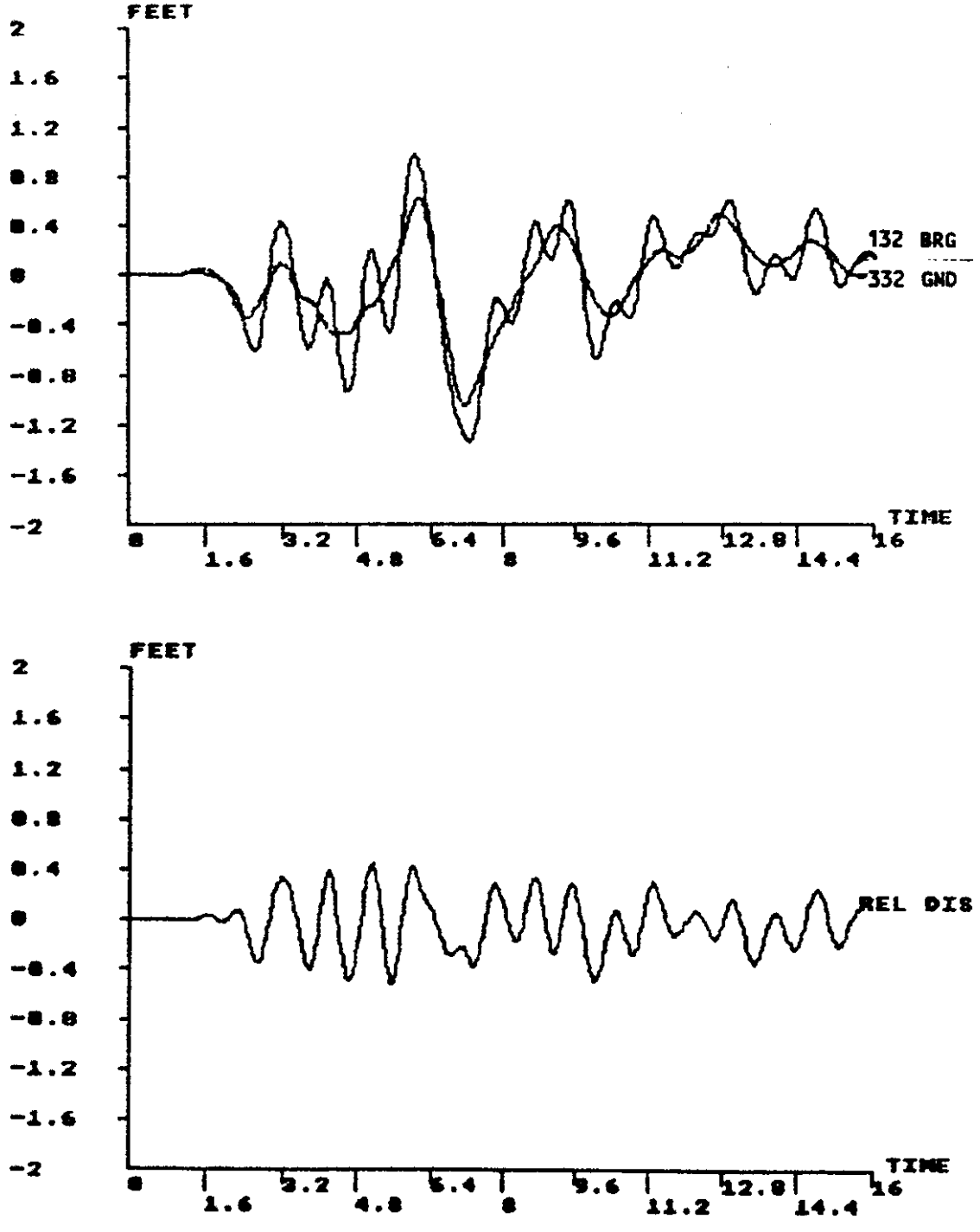

Figure D.5 Transverse Bridge and Ground Nodal Displacements and Relative Transverse Displacement, Lake Hughes Earthquake, Section 5 Sixty-Four-Span Model, Time-Delayed Input

APPENDIX E

RESULTS OF SIXTY-FOUR-SPAN ANALYSES

WITH NONLINEAR JOINTS

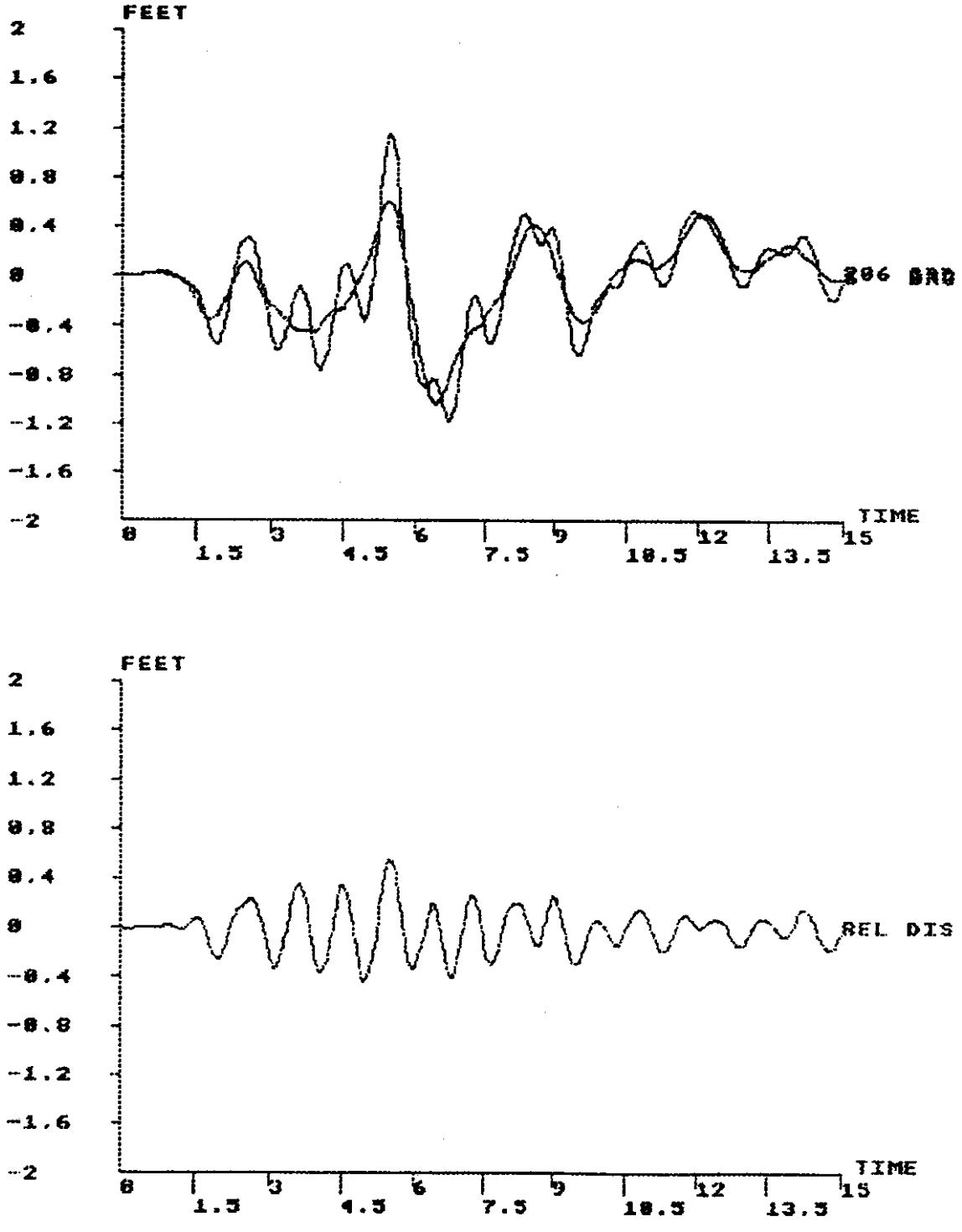

Figure E.1 Transverse Bridge and Ground Nodal Displacements and Relative Transverse Displacement, Lake Hughes Earthquake, Section 1 Sixty-Four-Span Model, Nonlinear Joints

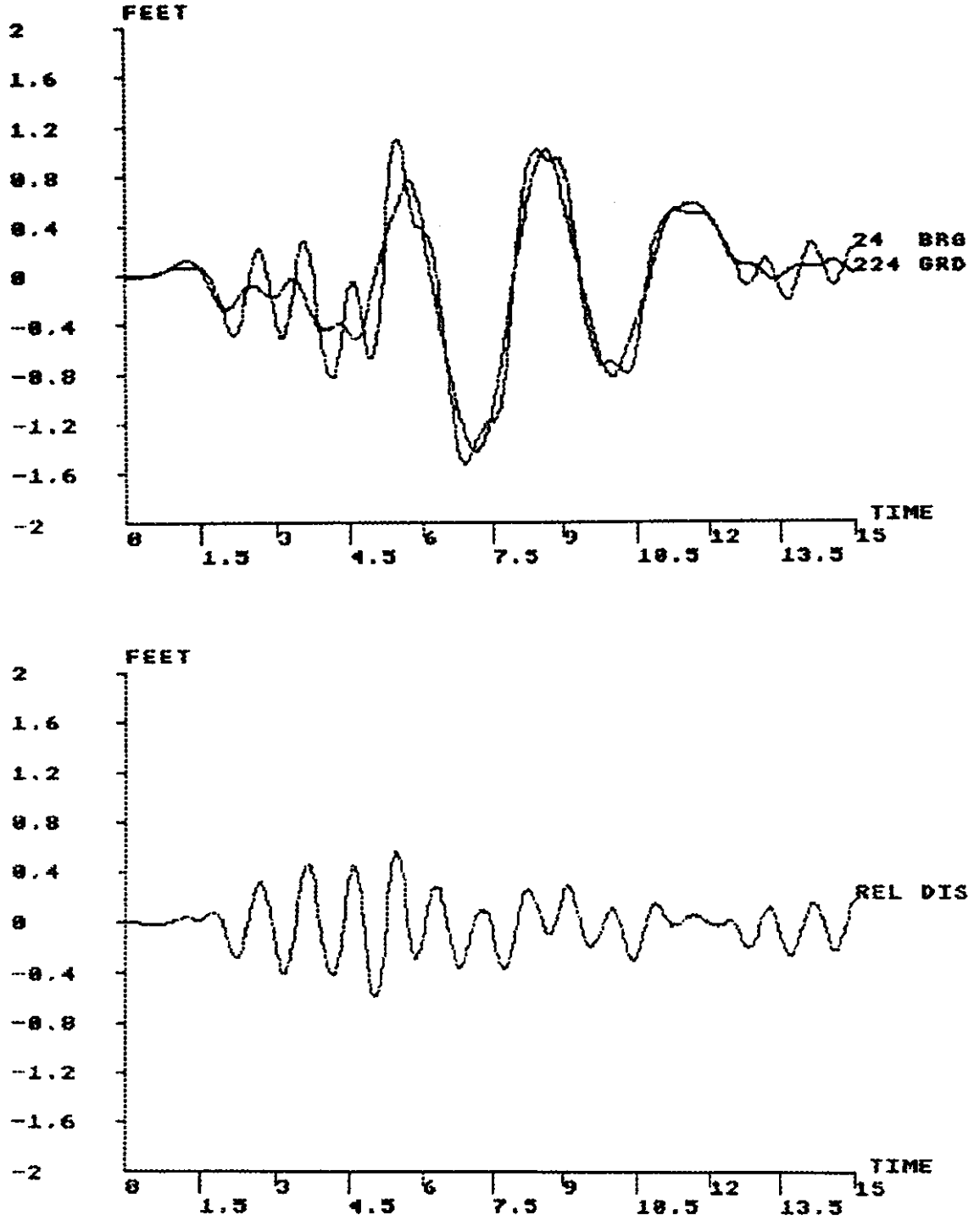

Figure E.2 Transverse Bridge and Ground Nodal Displacements and Relative Transverse Displacement, Lake Hughes Earthquake, Section 2 Sixty-Four-Span Model, Nonlinear Joints

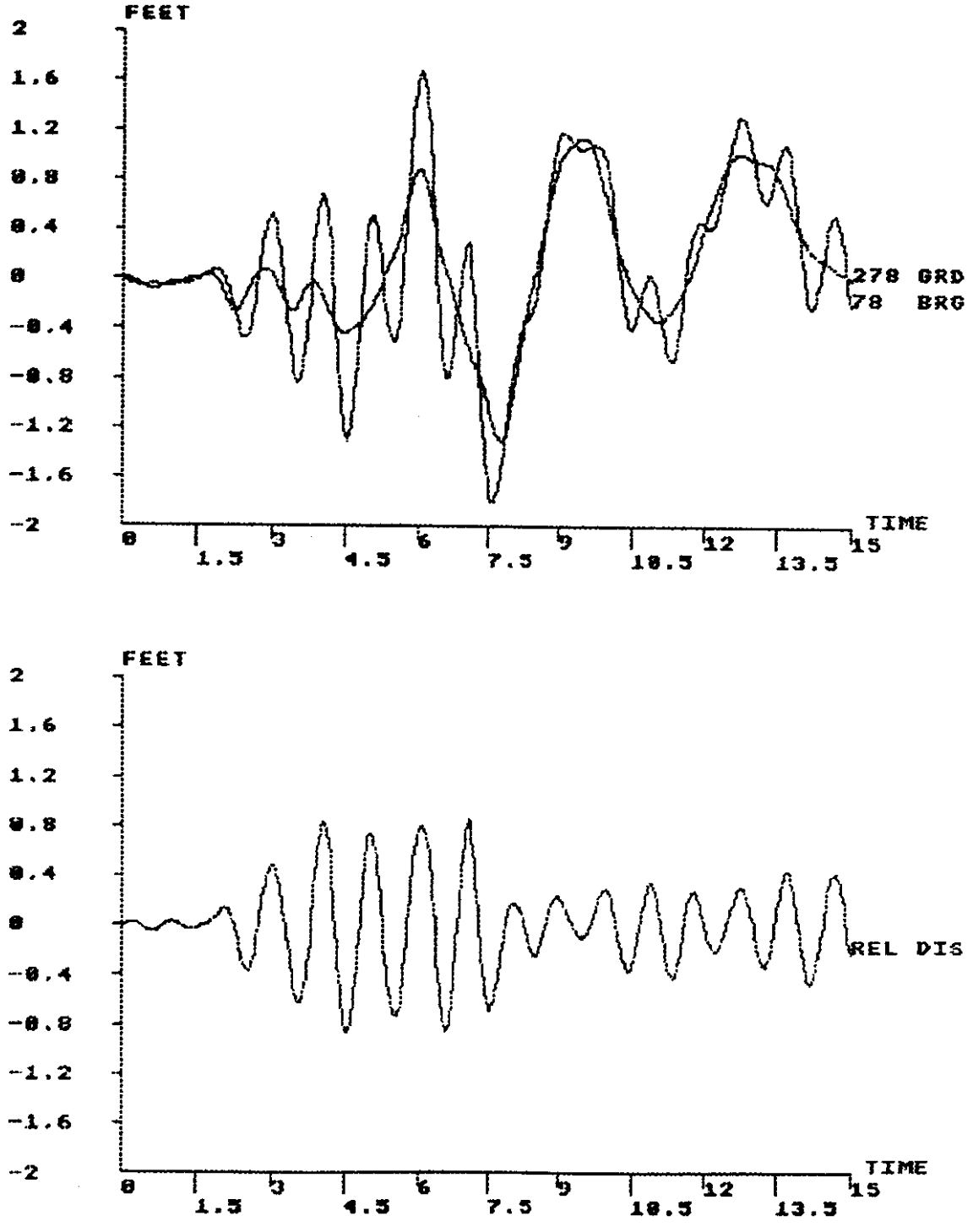

Figure E.3 Transverse Bridge and Ground Nodal Displacements and Relative Transverse Displacement, Lake Hughes Earthquake, Section 3 Sixty-Four-Span Model, Nonlinear Joints

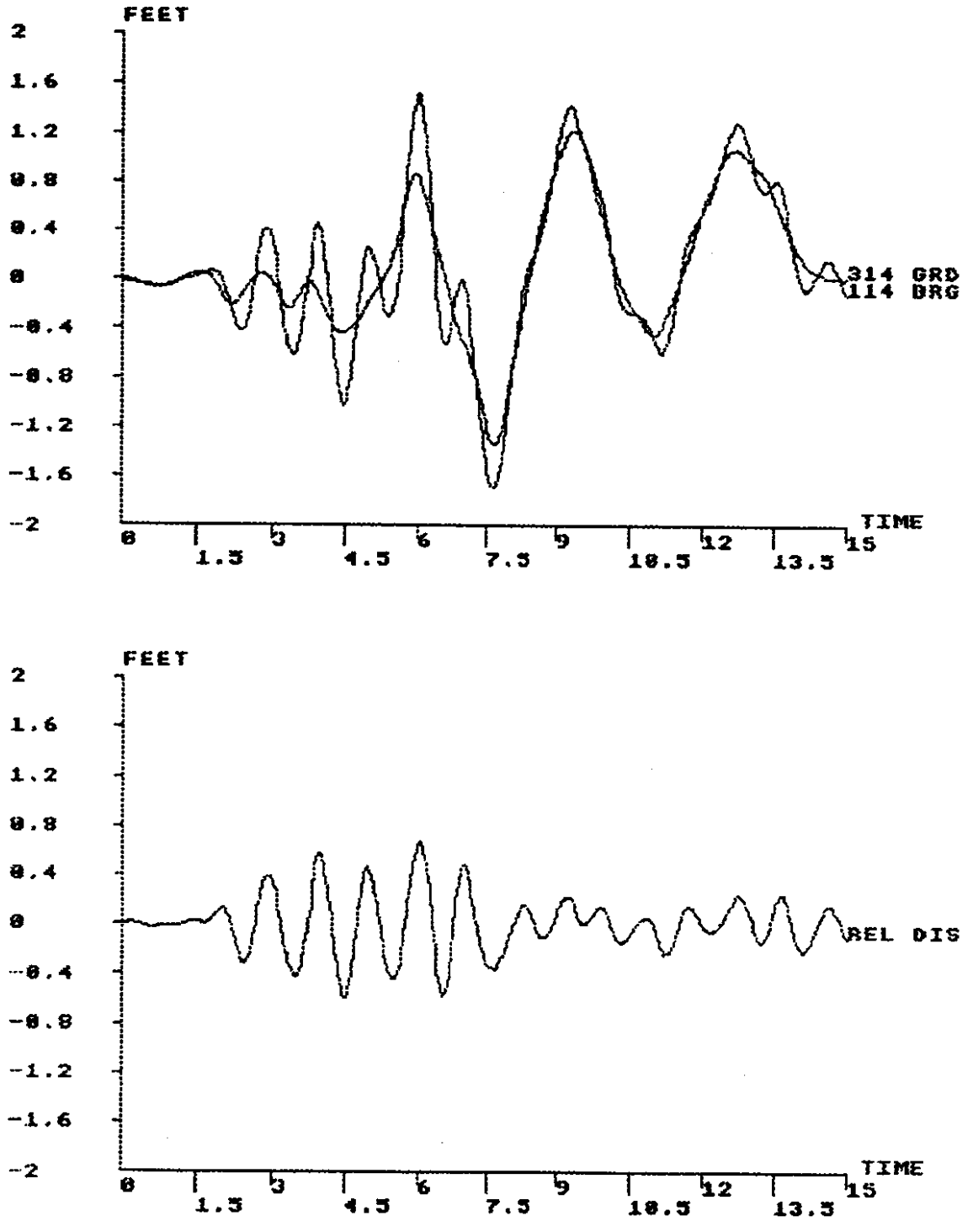

Figure E.4 Transverse Bridge and Ground Nodal Displacements and Relative Transverse Displacement, Lake Hughes Earthquake, Section 4 Sixty-Four-Span Model, Nonlinear Joints

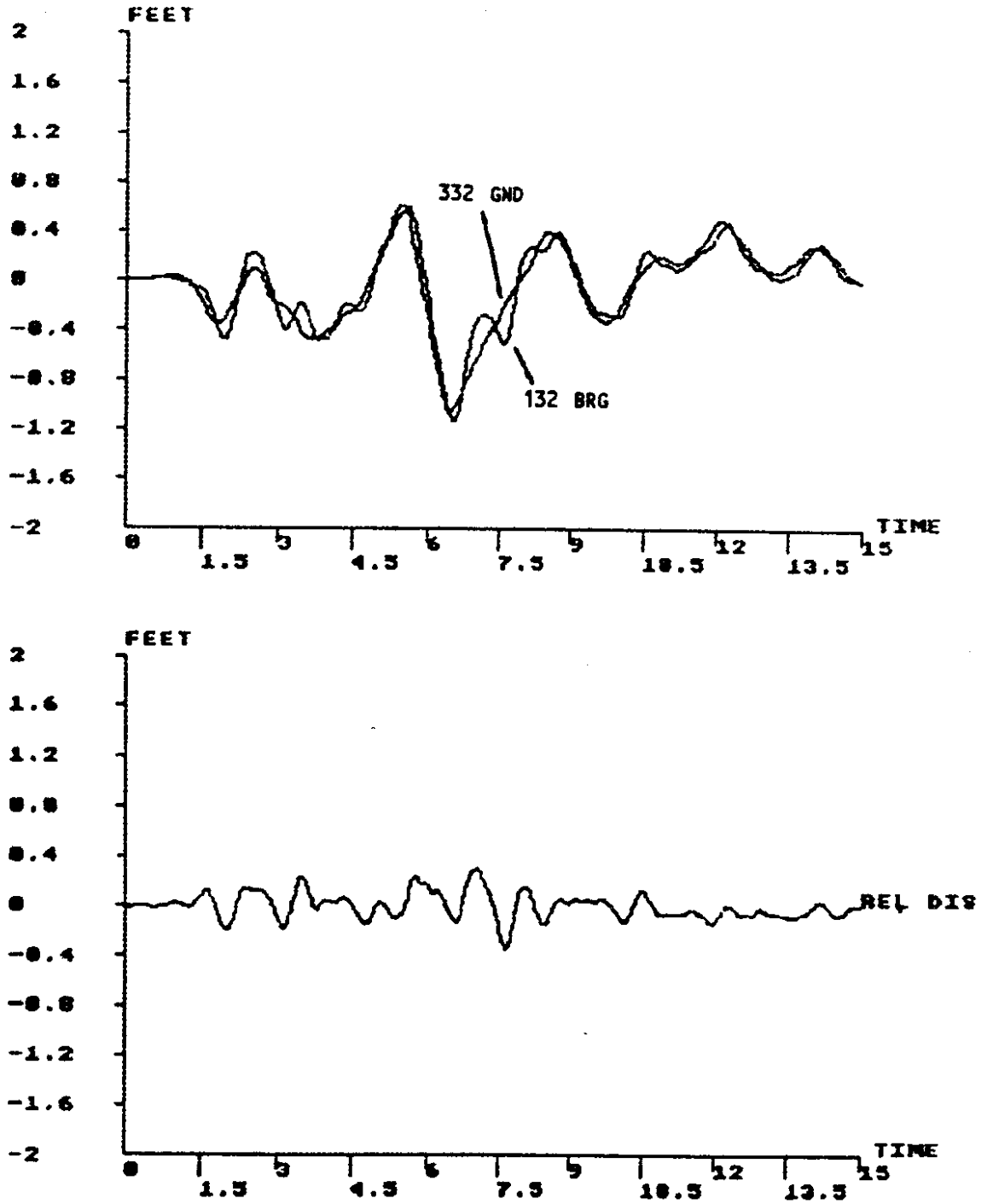

Figure E.5 Transverse Bridge and Ground Nodal Displacements and Relative Transverse Displacement, Lake Hughes Earthquake, Section 5 Sixty-Four-Span Model, Nonlinear Joints

APPENDIX F

EXPANSION JOINT GAP DISPLACEMENTS

Expansion joint displacements are presented from the simple joint model and the nonlinear joint model. The simple joint nodes and the nonlinear nodes from Gap A are on the north side of the bridge, which runs east and west. They are the same nodes in the corresponding models. The nodes in the Gap B traces are from the south side of the bridge. The first set of three figures is for the joint between the section 1 input and the section 2 input. The second set of three figures is for the joint between the section 2 input and section 3 input. The third set of three figures is for the joint at the center of the section 3 input, the center of the sixty-four-span model. The fourth set of three figures is for the joint between the section 3 input and the section 4 input. The final set of three figures is for the joint between the section 4 input and the section 5 input.

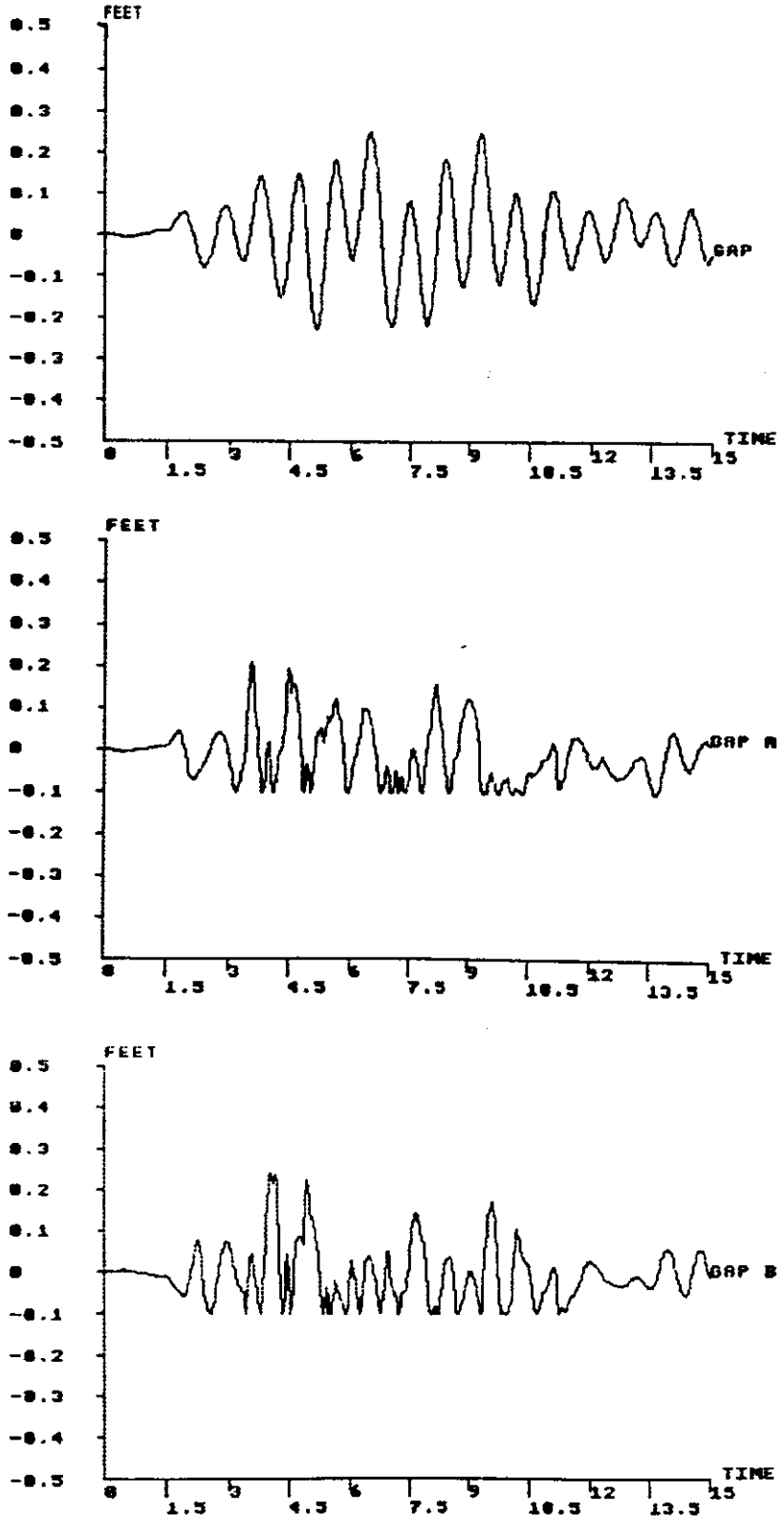

Figure F.1 Relative Longitudinal Gap Displacement for Simple Joint Model (GAP) and Nonlinear Joint Model (GAP A and GAP B), Section 1-2

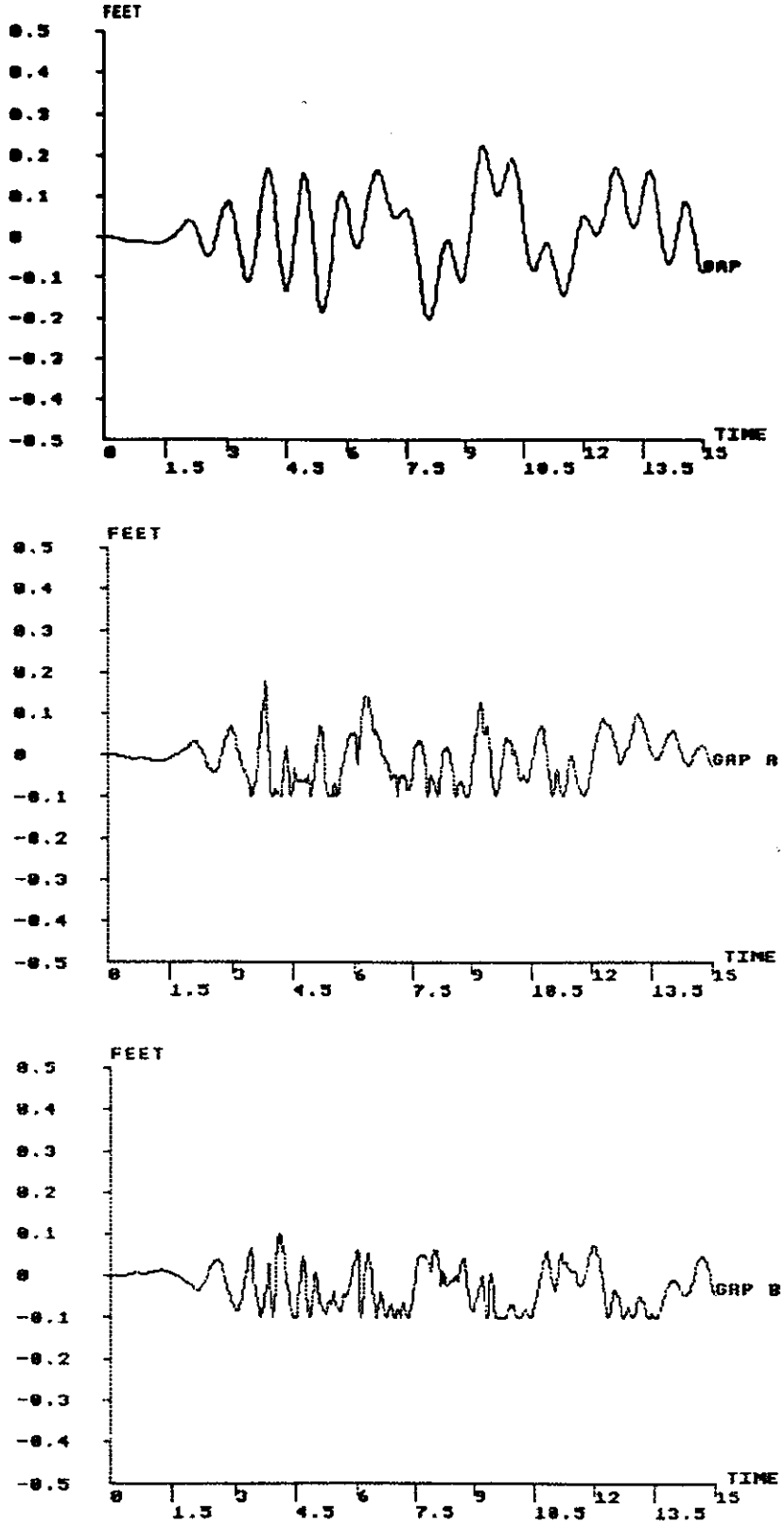

Figure F.2 Relative Longitudinal Gap Displacement for Simple Joint Model (GAP) and Nonlinear Joint Model (GAP A and GAP B), Section 2-3

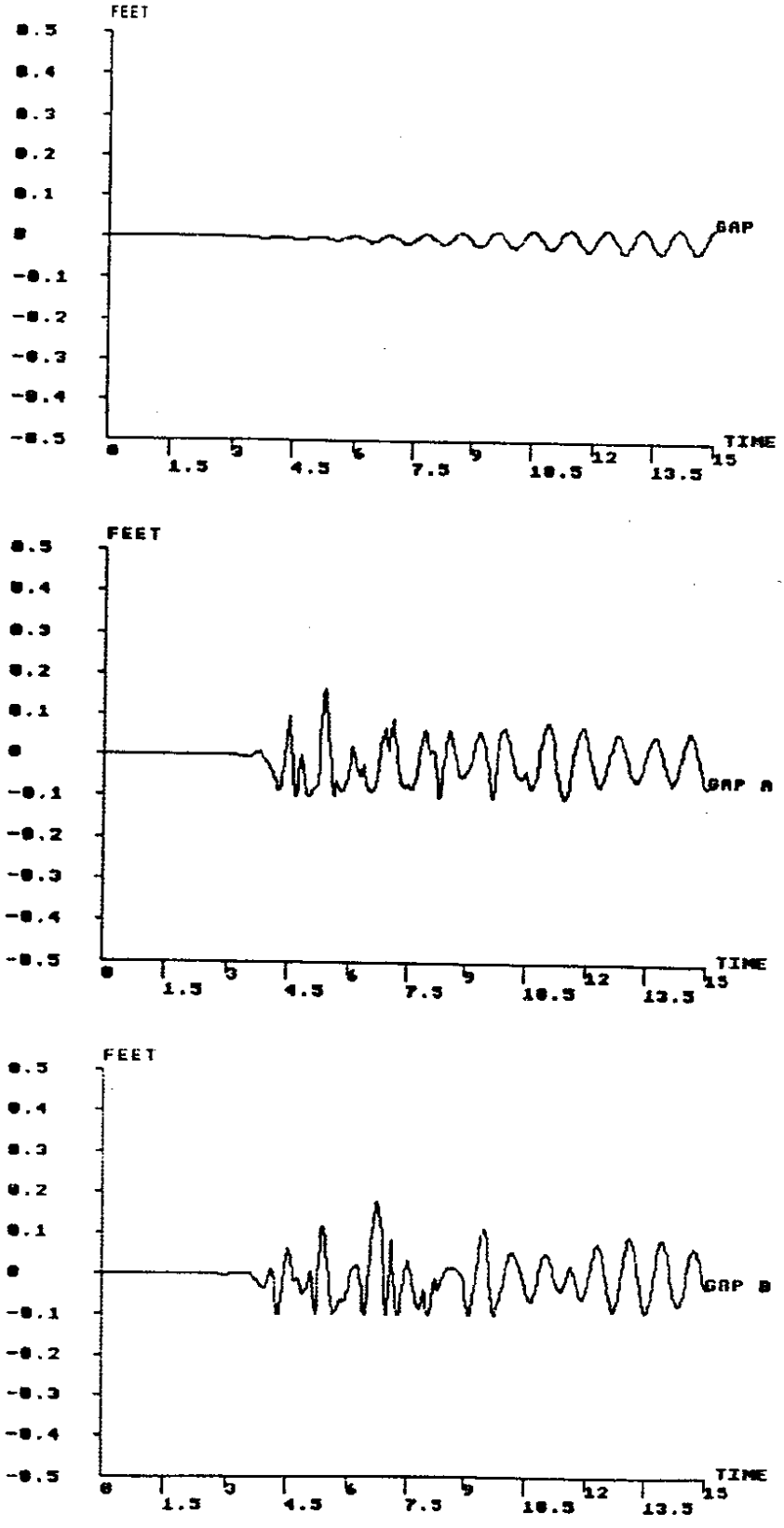

Figure F.3 Relative Longitudinal Gap Displacement for Simple Joint Model (GAP) and Nonlinear Joint Model (GAP A and GAP B), Section 3

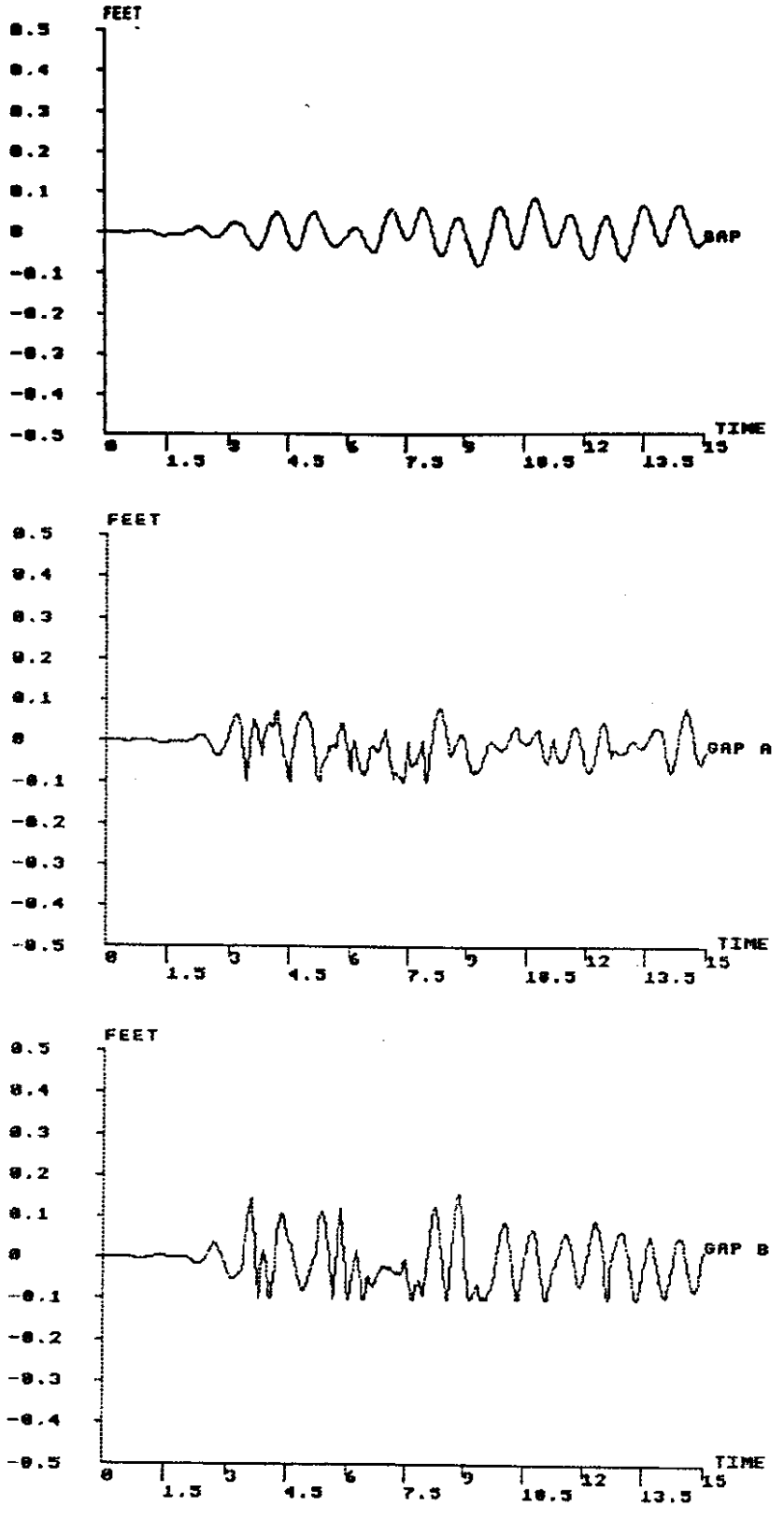

Figure F.4 Relative Longitudinal Gap Displacement for Simple Joint Model (GAP) and Nonlinear Joint Model (GAP A and GAP B), Section 3-4

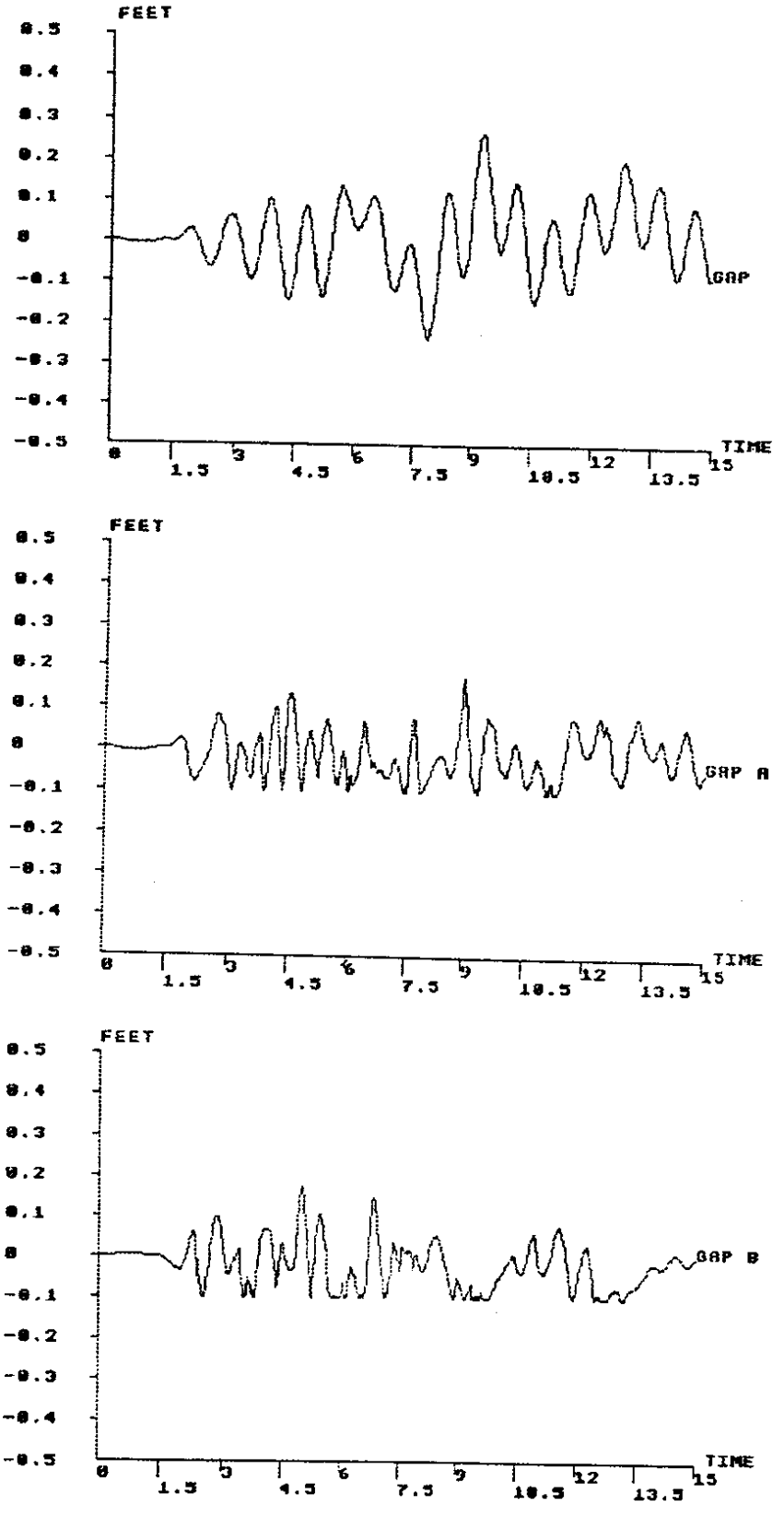

Figure F.5 Relative Longitudinal Gap Displacement for Simple Joint Model (GAP) and Nonlinear Joint Model (GAP A and GAP B), Section 4-5